Search for heavy charged long-lived particles in the ATLAS detector in 36.1 fb^{-1} of proton-proton collision data at $\sqrt{s} = 13$ TeV

M. Aaboud *et al.*[*]
(ATLAS Collaboration)

(Received 6 February 2019; published 28 May 2019)

A search for heavy charged long-lived particles is performed using a data sample of 36.1 fb^{-1} of proton-proton collisions at $\sqrt{s} = 13$ TeV collected by the ATLAS experiment at the Large Hadron Collider. The search is based on observables related to ionization energy loss and time of flight, which are sensitive to the velocity of heavy charged particles traveling significantly slower than the speed of light. Multiple search strategies for a wide range of lifetimes, corresponding to path lengths of a few meters, are defined as model independently as possible, by referencing several representative physics cases that yield long-lived particles within supersymmetric models, such as gluinos/squarks (R-hadrons), charginos and staus. No significant deviations from the expected Standard Model background are observed. Upper limits at 95% confidence level are provided on the production cross sections of long-lived R-hadrons as well as directly pair-produced staus and charginos. These results translate into lower limits on the masses of long-lived gluino, sbottom and stop R-hadrons, as well as staus and charginos of 2000, 1250, 1340, 430, and 1090 GeV, respectively.

DOI: 10.1103/PhysRevD.99.092007

I. INTRODUCTION

The search for heavy charged long-lived particles presented in this paper is based on a data sample of 36.1 fb^{-1} of proton-proton (pp) collisions at $\sqrt{s} = 13$ TeV collected in 2015 and 2016. It utilizes observables related to large ionization energy loss (dE/dx) and time of flight (ToF), which are signatures of heavy charged particles traveling significantly slower than the speed of light. The mass of the particles is estimated using the dE/dx ($m_{dE/dx}$) or ToF (m_{ToF}) measurements together with the reconstructed momentum. The background is estimated in a purely data-driven manner, and multiple signal regions are defined to address the different possible signatures of heavy long-lived particles (LLPs) that reach at least the ATLAS hadronic calorimeter, which corresponds to decay lengths of a few meters. Previous searches for LLPs that are stable within the detector were performed by the CMS Collaboration using 2.5 fb^{-1} of data at 13 TeV [1], as well as by the ATLAS Collaboration using 3.2 fb^{-1} of data at 13 TeV [2] and 19.8 fb^{-1} of data at 8 TeV [3].

LLPs are predicted in a variety of theories that extend the Standard Model (SM) [4]. Theories with supersymmetry (SUSY) [5–10], which either violate [11–13] or conserve [4,14–19] R-parity, allow for the existence of charged long-lived sleptons ($\tilde{\ell}$), squarks ($\tilde{q}$), gluinos ($\tilde{g}$) and charginos ($\tilde{\chi}_1^{\pm}$).

Colored LLPs (e.g., $\tilde{q}$ and $\tilde{g}$) would hadronize forming so-called R-hadrons [14], which are bound states composed of the LLP and light SM quarks or gluons, and may emerge from the collision as charged or neutral states. Through hadronic interactions of the light-quark constituents with the detector material, especially inside the calorimeters, R-hadrons can change to states with a different electric charge. Thus they might not be reconstructed as a consistently charged track in the inner tracking detector (ID) and in the muon spectrometer (MS), even if the lifetime is long enough to traverse the entire detector. Searches for R-hadrons are performed following two different approaches: using all available detector information ("full-detector R-hadron search"), or disregarding all information from the muon spectrometer ("MS-agnostic R-hadron search") to minimize the dependence on the modeling of R-hadron interactions with the material of the detector. Long-lived gluinos are motivated for example by split-SUSY models [18,19], in which high-mass squarks can lead to very long gluino lifetimes. Long-lived squarks, in particular a light top squark (stop) as the next-to-lighest SUSY particle, is motivated for example by electroweak baryogenesis [20,21], where nonuniversal squark mass terms can lead to a small mass difference between the stop and the neutralino as the lightest supersymmetric particle (LSP),

[*]Full author list given at the end of the article.

and the lightest chargino is heavy, leading to suppressed radiative decays and long stop lifetimes.

If the charged LLP does not interact hadronically, it would predominantly lose energy via ionization as it passes through the ATLAS detector. Searches for long-lived charginos and sleptons (focusing on staus, as they are expected in most models to be the lightest) identified in both the ID and MS are therefore performed. The searches for staus are motivated by gauge-mediated SUSY breaking (GMSB) [15,22–27] assuming the LSP to be a gravitino and with the light stau ($\tilde{\tau}$) as an LLP, decaying to a τ-lepton and a gravitino with an unconstrained lifetime. While essentially all events in the GMSB models that include long-lived staus involve cascade decays that end in two LLPs, in this paper direct di-stau production through a Drell-Yan process is taken as a benchmark. Results for pair-produced charginos are motivated by a minimal anomaly-mediated supersymmetry breaking (mAMSB) model, where often the supersymmetric partners of the SM W-boson fields, the wino fermions, are the lightest gaugino states. In this particular case, the lightest of the charged mass eigenstates, a chargino, and the lightest of the neutral mass eigenstates, a neutralino, are both almost pure wino and nearly mass-degenerate, resulting in long-lived charginos (see Refs. [28,29] for details).

This paper is organized as follows. A brief description of the ATLAS detector is given in Sec. II with emphasis on the parts relevant for this analysis, followed by details of the calibration of key observables in Sec. III. The dataset and simulated event samples and the subsequent event selection are described in Secs. IV and V, respectively. Section VI explains the method of background estimation and compares these estimates with data. Section VII details the origin and estimation of systematic uncertainties. The results including upper cross-section limits are shown in Sec. VIII, and finally the conclusions are summarized in Sec. IX.

II. ATLAS DETECTOR

The ATLAS detector [30] is a multipurpose particle detector consisting of the ID immersed in a 2 T solenoidal magnetic field, electromagnetic as well as hadronic calorimeters and a MS based on three large air-core toroid superconducting magnets with eight coils each. The ID comprises a silicon pixel detector, a silicon microstrip detector (SCT) and a transition-radiation tracker. With almost 4π coverage in solid angle,[1] the ATLAS detector is sensitive to the missing transverse momentum associated with each event. Several components are used to determine either dE/dx or ToF in this search and are discussed in more detail below.

The innermost component of the ATLAS detector is the pixel detector, consisting of four radial layers of pixel-sensors in the barrel region and three disks on each side in the end cap region. The pixel detector measures the ionization energy loss of charged particles traversing it via a time-over-threshold (ToT) technique [31].

The ATLAS calorimeter in the central detector region consists of a liquid-argon electromagnetic calorimeter followed by a steel-absorber scintillator-tile sampling calorimeter. The latter serves as hadronic calorimeter covering the region up to $|\eta| = 1.7$. In the ϕ-direction the tile calorimeter is segmented into 64 wedges with a size of $\Delta\phi = 2\pi/64 \approx 0.1$. In the r-z plane it is formed by three radial layers in the central barrel region and three in an extended barrel on each side, where each layer is further segmented into cells. The cells in the first and third layer in the barrel and in all layers in the extended barrel have a rectangular shape, while in the second layer of the barrel they are composed of two shifted rectangles (see Fig. 1). Overall, the tile calorimeter consists of 73 cells in 64 ϕ-segments resulting in 4672 individual cells. The optimal filtering algorithm (OFA) [32] used for the readout provides, besides a precise measurement of the energy deposits of particles and jets, a timing measurement. The resolution of the single-cell timing in the tile calorimeter is 1.3–1.7 ns.

The outermost part of the ATLAS detector is the MS. Immersed in toroidal magnetic fields, the MS provides particle tracking and momentum reconstruction for charged particles with $|\eta| < 2.7$, as well as triggering information in the range $|\eta| < 2.4$. Three layers of muon detectors are arranged in concentric shells at distances between 5 and 10 m from the interaction point (IP) in the barrel region, and in wheels perpendicular to the beam axis at distances between 7.4 and 21.5 m in the end cap regions where $|\eta| > 1.05$. Four different detector technologies are used in the MS. In the barrel region the muon trigger relies on resistive-plate chambers (RPCs), while thin-gap chambers are employed in the end cap wheels. High-precision tracking for the momentum measurements is performed by monitored drift tubes (MDTs), except for the innermost layer in the forward region of $2.0 < |\eta| < 2.7$, where cathode-strip chambers are installed. A muon traversing the detector in the barrel region typically has around 20 hits in the MDTs and 14 hits in the RPCs. Both systems exhibit a sufficiently precise single-hit timing resolution (MDTs 3.2 ns, RPCs 1.8 ns) to distinguish relativistic muons traveling at almost the speed of light from slowly propagating stable massive particles. For the reconstruction of slow particles traversing the full detector, a dedicated tracking algorithm that treats the velocity β as a free parameter is used [33,34].

[1]ATLAS uses a right-handed coordinate system with its origin at the nominal interaction point (IP) in the center of the detector and the z axis coinciding with the axis of the beam pipe. The x axis points from the IP to the center of the LHC ring, and the y axis points upward. Cylindrical coordinates (r, ϕ) are used in the transverse plane, ϕ being the azimuthal angle around the beam pipe. The pseudorapidity is defined in terms of the polar angle θ as $\eta = -\ln\tan(\theta/2)$. Object distances in the η–ϕ plane are given by $\Delta R = \sqrt{(\Delta\eta)^2 + (\Delta\phi)^2}$.

The ATLAS trigger system [35] consists of a hardware-based level-1 trigger followed by a software-based high-level trigger, which runs reconstruction and calibration software similar to the offline reconstruction, and reduces the event rate to about 1 kHz.

III. CALIBRATION OF MAIN OBSERVABLES

To achieve optimal identification performance for heavy, charged, LLPs, measurements of the specific ionization energy loss and ToF have to be calibrated.

The pixel detector provides measurements of specific ionization energy losses. The dE/dx is corrected for η-dependence and on a run-by-run basis, to reduce the effect of the degradation of charge collection in the silicon sensor due to accumulated irradiation. Individual measurements resulting from a particle traversing the detector are combined in a truncated mean to reduce the effects of the Landau tails on the estimate of the most probable value (MPV). Finally, a value of the $\beta\gamma$ of the particle is estimated from the MPV and the momentum, using a three-parameter empirical function, calibrated using protons, kaons and pions with low transverse momentum (p_{T}). The expected resolution for $\beta\gamma$ from the dE/dx and momentum measurement is about 14%, which is taken as the uncertainty in the measured values. A detailed description of the $\beta\gamma$ estimation using the pixel detector can be found in Ref. [31].

The particle velocity, β, is determined via ToF measurements in the tile calorimeter, the MDTs and the RPCs. To ensure an optimal β resolution, a series of custom calibrations is performed. High-p_{T} muons are used for the calibration as, given the timing resolutions, they travel effectively at the speed of light.

For the tile calorimeter, only cells with a minimum energy deposit of 500 MeV are used. The time difference (t_0) relative to a particle traveling at the speed of light from the IP to the cell center (cell distance) is not allowed to be larger than 25 ns to reduce the effect of out-of-time pileup. As the first calibration step, a bias introduced by the OFA is corrected. The signal simulation reproduces the OFA bias reliably. The correction is very small for an in-time signal, while for late-arriving particles it ranges up to 10 ns. This is followed by a correction for the particle path in the cell. An effective spatial position corresponding to the timing measurement is estimated using an extrapolation of the particle track from the production vertex to the respective cell in the tile calorimeter (effective distance). The difference between the effective distance and the cell distance is used as a correction for the timing calibrations, while the effective distance is used for the estimation of the individual measurements of the velocity ($\beta^{\mathrm{HIT}}_{\mathrm{TILE}}$). The corresponding correction is largest (3 ns) for the edge η regions of the largest cells in the tile calorimeter, which are located in the outermost layer of the extended barrel. This is followed by separate η-dependent corrections for data and simulation, which accounts for small remaining η-dependences of the timing for the outer parts of the cells in data, and ensures an η-independent timing measurement in simulation. Furthermore, a calibration of the timing as a function of the energy deposit per ϕ-projected cell (averaging cells of identical geometry over ϕ) is applied, which does not exceed 0.2 ns. Additionally, calibration constants in data are estimated for each cell followed by a run-by-run correction of the overall timing. These calibrations account for differences between single-tile calorimeter cells and for misalignments of the ATLAS and LHC clocks. The cell-wise calibration factors are mostly well below 1 ns, while for some cells they range up to 2 ns. The run-by-run correction constants are between -0.6 and 0.2 ns. A smearing of the timing obtained in simulation is applied to achieve the same resolution as observed in data. The width of a Gaussian parametrization of the t_0 distribution serves as the uncertainty. The uncertainties are estimated as a function of the energy deposit per ϕ-projected cell. Finally, the uncertainties are adjusted to achieve a unit Gaussian width for the pull distribution, which gives a correction of 1% to the uncertainty. The individual measurements of $\beta^{\mathrm{HIT}}_{\mathrm{TILE}}$, with the ϕ-projected resolutions shown in Fig. 1, are combined in a weighted average β_{TILE} using the inverse squared uncertainties as weights. The final resolution achieved for β_{TILE} is $\sigma_{\beta_{\mathrm{TILE}}} = 0.068$.[2]

For the MDTs and RPCs, each of the 323799 drift tubes and 362262 RPC readout strips is calibrated individually by performing a Gaussian parametrization of the timing information, and correcting for the offset to the expected value for a particle traveling at the speed of light. The width of the fitted distribution is taken as the uncertainty for the measurements in the respective tube/strip. The uncertainties are, in a manner similar to the tile calorimeter, adjusted to give a unit Gaussian width for the pull distributions. The corrections to the uncertainties are 16% for the MDTs, less than 1% for the RPC η-strips and 2% for the ϕ-strips. The squared inverse of the uncertainty is used as a weight for the calculation of a weighted-average β. Time-dependent phase-shift variations between the ATLAS and LHC clocks are addressed similarly to the tile calorimeter in a separate correction of timing information for each LHC run, and separately for MDTs, RPC readout strips measuring η and RPC strips measuring ϕ. The calibration results in a β resolution of $\sigma_{\beta_{\mathrm{MDT}}} = 0.026$ for the MDTs and $\sigma_{\beta_{\mathrm{RPC}}} = 0.022$ for the RPCs (with single-hit t_0 resolutions of about 3.2 and 1.8 ns, respectively).

Finally, the ToF-based β measurements in the different subsystems are combined into an overall β_{ToF}, which is estimated as a weighted average of the β measurements from the different subsystems using the inverse squared uncertainties as weights. Furthermore, the combined

[2]The resolutions (σ_{x}) are determined by performing a Gaussian fit to the core of the respective distributions.

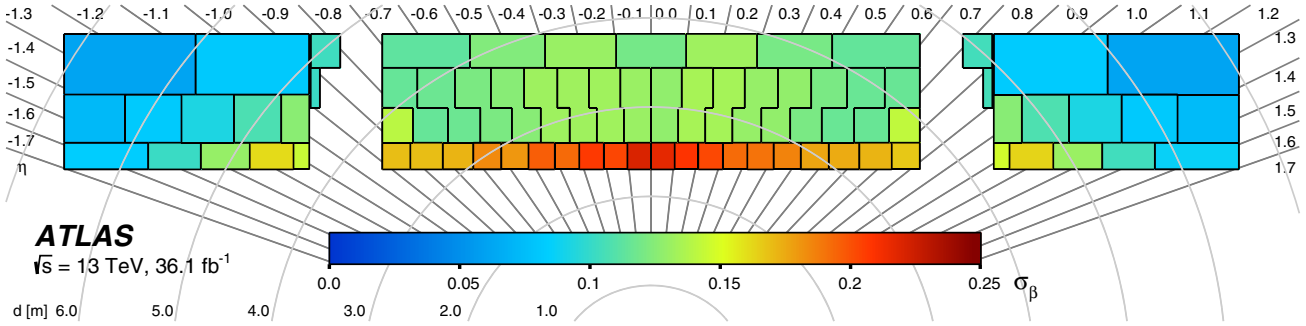

FIG. 1. Resolution (σ_β) of the $\beta^{\mathrm{HIT}}_{\mathrm{TILE}}$ measurement for the different tile-calorimeter cells, which are shown with their actual shape. The gray circles indicate, the distance, d, from the interaction point and the gray straight lines the direction in η.

uncertainty and the probability of compatibility between the measurements from the different subsystems are calculated for each candidate. The final distributions of the β measurements are shown in Fig. 2 for muons from $Z \to \mu\mu$ selected events in data and simulation. The final resolution achieved for β_{ToF} is $\sigma_{\beta_{\mathrm{ToF}}} = 0.021$.

IV. DATA AND SIMULATED EVENTS

The analysis presented in this paper is based on a data sample of 36.1 fb^{-1} of pp collisions at $\sqrt{s} = 13$ TeV collected in 2015 and 2016, with a bunch spacing of 25 ns. Reconstructed $Z \to \mu\mu$ events in data and simulation are used for timing resolution studies. Simulated signal events are used to study the expected signal behavior.

Pair production of gluinos (squarks), with masses between 400 and 3000 GeV (600 and 1400 GeV), was simulated in PYTHIA6 [36] (version 6.427) with the AUET2B [37] tuned set of underlying event and hadronization parameters (tune) and the CTEQ6L1 [38] PDF set, incorporating specialized hadronization routines [39,40] to produce final states containing R-hadrons. The other SUSY particle masses, except that of the lightest neutralino, were set to very high values to ensure negligible effects on gluino or squark pair-production. The fraction of gluino-balls, i.e., bound states of a gluino and gluon, was conservatively set to 10% [4,39], in order to account for the possibility of other (neutral and hence invisible) final states than those searched for. While the search is optimized for R-hadrons long-lived enough to reach at least the hadronic calorimeter, samples with gluino lifetimes of 10, 30 and 50 ns, where a significant fraction of the LLPs will decay before the calorimeter, are also investigated.

PYTHIA6 relies on a parton shower to add additional high-p_{T} partons to the event. To achieve a more accurate description of QCD radiative effects, the PYTHIA6 events were reweighted to match the transverse-momentum distribution of the gluino–gluino or squark–squark system to the distribution obtained in dedicated leading-order MG5_aMC@NLO (version 2.2.3) [41] simulations with one additional parton in the matrix-element calculation.

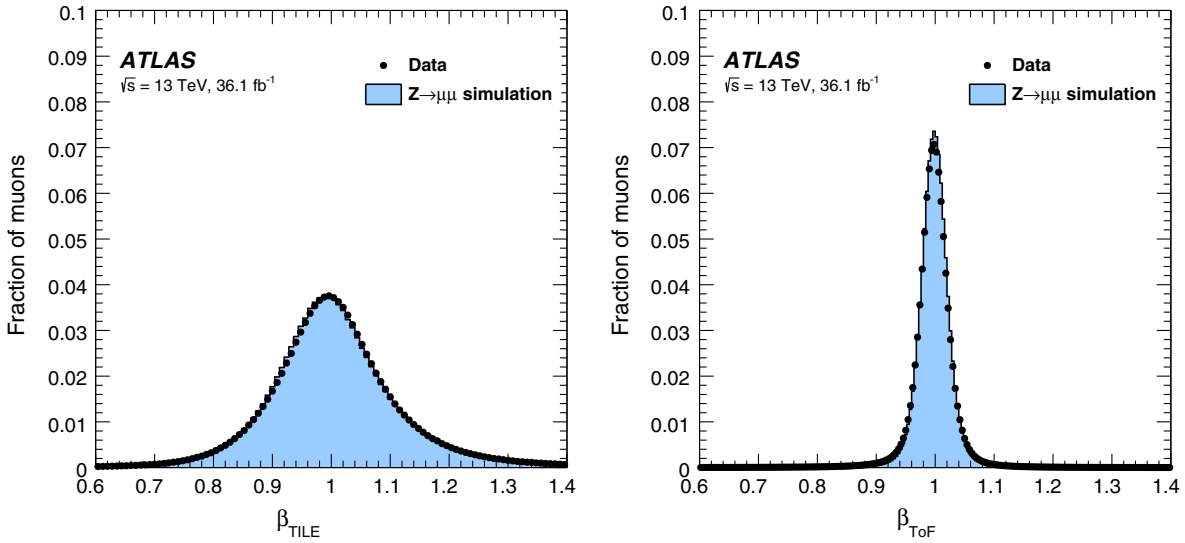

FIG. 2. The β-distributions of muons for a $Z \to \mu\mu$ selection in data and simulation, with β measured solely in the tile calorimeter (β_{TILE}, left), and as a combined measurement from RPCs, MDTs and tile calorimeter (β_{ToF}, right).

Pair production of staus in a GMSB scenario [$m_{\text{Messenger}} = 500$ TeV, $C_{\text{grav}} = 100000$, $\tan\beta = 10$, $\text{sign}(\mu) = 1$] was simulated with two additional partons at leading order, using MG5_aMC@NLO (version 2.3.3) in combination with Pythia8 [42] (version 8.212) and EvtGen [43] (version 1.2.0) with the A14 [44] tune and NNPDF23LO [45] PDF set. The pair-produced lightest stau mass eigenstate is a mixture of the left-handed and right-handed superpartners of the τ-lepton, although it is the partner of the right-handed lepton at the 99% level in the model considered here.

Pair production of charginos in an mAMSB scenario ($m_0 = 5$ TeV, $\tan\beta = 5$) was simulated with two additional partons at leading order, using MG5_aMC@NLO (version 2.3.3) in combination with Pythia8 (version 8.212) and EvtGen (version 1.2.0) with the A14 tune and NNPDF23LO PDF set.

Samples of $Z \to \mu\mu$ events, which are used for general testing, calorimeter and MS timing calibrations as well as the evaluation of systematic uncertainties, were simulated using Powheg-Box [46] (r2856) in combination with Pythia8 (version 8.186) and EvtGen (version 1.2.0) with the AZNLO [47] tune and CTEQ6L1 PDF set.

All events were passed through a full detector simulation [48] based on the Geant4 framework [49]. For the R-hadron simulations, hadronic interactions with matter were handled by dedicated Geant4 [49] routines based on different scattering models: the model used to describe gluino (squark) R-hadron interactions is referred to as the generic (Regge) model [50]. The R-hadrons interact only moderately with the detector material, as most of the R-hadron momentum is carried by the heavy gluino or squark, which has a small interaction cross section. Typically, the energy deposit in the calorimeters is less than 10 GeV.

All simulated events included a modeling of contributions from pileup by overlaying minimum-bias pp interactions from the same (in-time pileup) and nearby (out-of-time pileup) bunch crossings simulated in Pythia8 (version 8.186) and EvtGen (version 1.2.0) with the A2 [51] tune and MSTW2008LO [52] PDF set. The simulated events were reconstructed using the same software used for collision data, and were reweighted so that the distribution of the number of collisions per bunch crossing matched that of the data.

V. EVENT SELECTION

Five dedicated signal regions (SRs), imposing requirements on the entire event and on the individual candidate tracks, are defined in this section, addressing differences in topology and expected interactions with the detector for three different benchmark scenarios: staus, charginos and R-hadrons.

Events are selected by online triggers based on large missing transverse momentum ($\vec{p}_{\text{T}}^{\text{miss}}$, with magnitude denoted by $E_{\text{T}}^{\text{miss}}$) or signatures of single (isolated) high-momentum muons. Large $E_{\text{T}}^{\text{miss}}$ values are produced mainly when QCD initial-state radiation (ISR) boosts the R-hadron system, resulting in an imbalance between ISR and R-hadrons whose momenta are not fully accounted for in the $E_{\text{T}}^{\text{miss}}$ calculation. The adopted triggers impose thresholds from 70 to 110 GeV on $E_{\text{T}}^{\text{miss}}$ and 20 to 26 GeV on single muons, depending on the data-taking period.

The offline event selection requires all relevant detector components to be fully operational, a primary vertex (PV) built from at least two well-reconstructed charged-particle tracks, each with $p_{\text{T}} > 400$ MeV, and at least one candidate track that meets the criteria specified below.

A "common track selection" is implemented for candidates in all SRs and is described below. ID tracks (denoted by the superscript "trk") are required to have a minimum $p_{\text{T}}^{\text{trk}}$ of 50 GeV and a momentum measurement $p^{\text{trk}} < 6.5$ TeV. The candidate track is required to be matched to the PV using 'loose' requirements on the transverse (d_0) and longitudinal (z_0) impact parameters ($|d_0| < 2$ mm, $|z_0 \sin\theta| < 3$ mm).[3] To ensure good track reconstruction, the candidate track must have at least seven silicon clusters[4] ($N_{\text{silicon}}^{\text{clusters}} > 6$), no shared or split clusters in the pixel detector ($N_{\text{pix}}^{\text{shared}} + N_{\text{pix}}^{\text{split}} = 0$) [55], and at least three clusters[5] in the SCT ($N_{\text{SCT}}^{\text{clusters+dead}} > 2$). Mainly to ensure a reliable timing measurement in the calorimeters, it is required that the sum of the track-p_{T} in a cone of $\Delta R = 0.2$ around the candidate track is below 5 GeV. Jets reconstructed in the calorimeter are used to veto electrons and SM hadrons. Jets are reconstructed with the anti-k_t clustering algorithm [56] with radius parameter $R = 0.4$ and using as inputs clusters of energy deposits in the calorimeter, calibrated such that the average response of an electron is unity. The jets are then calibrated using the method described in Ref. [57]. An electron veto is imposed by rejecting any candidate track for which the nearest jet with $p_{\text{T}} > 20$ GeV and within a $\Delta R = 0.05$ cone around the track has at least 95% of its energy deposited in the electromagnetic calorimeter. A veto against SM hadrons is imposed by rejecting any candidate track for which any associated jet within a $\Delta R = 0.05$ cone of the track has an energy larger than the track momentum. Candidate tracks are required to have a cluster in the innermost

[3]The transverse impact parameter is defined as the distance of closest approach between a track and the beam-line in the transverse plane. The longitudinal impact parameter corresponds to the z-coordinate distance between the primary vertex and the point along the track at which the transverse impact parameter is defined.

[4]The charge released by a moving charged particle is rarely contained within just one pixel; neighboring pixels/strips registering hits are joined together using a connected component analysis [53,54] to form clusters.

[5]This count includes the number of nonfunctional/dead modules traversed by the particle/track.

TABLE I. Summary of the five sets of SRs. The trigger as well as the track candidate selection and the number of candidates per event required for the respective SR are given. Also the final selection requirements together with the mass window (one- or two-dimensional) for the final counting are stated. SRs in one block (delimited by horizontal lines) are combined for the statistical interpretation of the results. For SR-Rhad-FullDet, the ID+CALO is used as a fallback only if no LOOSE candidates are found in the event; hence the two SRs are mutually exclusive.

				Final requirements				
Signal region	Trigger	Candidate selection	Candidates per event	$\lvert\eta\rvert$	p [GeV]	β_{ToF}	$(\beta\gamma)_{dE/dx}$	Mass
SR-Rhad-MSagno	$E_{\mathrm{T}}^{\mathrm{miss}}$	ID+CALO	≥1	≤1.65	≥200	≤0.75	≤1.0	ToF & dE/dx
SR-Rhad-FullDet	$E_{\mathrm{T}}^{\mathrm{miss}}/\mu$	LOOSE	≥1	≤1.65	≥200	≤0.75	≤1.3	ToF & dE/dx
SR-Rhad-FullDet	$E_{\mathrm{T}}^{\mathrm{miss}}/\mu$	ID+CALO	≥1	≤1.65	≥200	≤0.75	≤1.0	ToF & dE/dx
SR-2Cand-FullDet	$E_{\mathrm{T}}^{\mathrm{miss}}/\mu$	LOOSE	=2	≤2.00	≥100	≤0.95	···	ToF
SR-1Cand-FullDet	$E_{\mathrm{T}}^{\mathrm{miss}}/\mu$	TIGHT	=1	≤1.65	≥200	≤0.80	···	ToF

pixel-detector layer (if expected) or a cluster in the second layer (if the innermost is not expected, but the second layer is). A "cosmics veto" rejects candidate tracks that have an opposite-sign track/muon on the other side of the detector, satisfying $\Delta R_{\mathrm{cosmics}} < 0.04$.[6] A "$Z$ veto" rejects each candidate track that together with the highest-p_{T} muon in the event forms an invariant mass within 10 GeV of the Z-boson mass.

Three different selection criteria for each track in an event, hereafter referred to as ID+CALO, LOOSE and TIGHT, are defined. The ID+CALO selection, which does not use MS information, is designed for the R-hadron searches. The LOOSE and TIGHT criteria are applied to ID–MS combined tracks in the search using the full detector information, with TIGHT providing stricter requirements.

An ID+CALO candidate selection starts from an ID track that fulfills the requirements of the above-mentioned common track selection, and which has at least one timing measurement in the tile calorimeter. In addition, the candidate tracks need to have $|\eta| < 1.65$, to ensure a minimal sensitivity in the tile calorimeter. To obtain a reliable dE/dx measurement in the pixel detector, the tracks are required to have at least two clusters used in the respective estimation ($N^{\mathrm{clusters}}_{\mathrm{good}\ dE/dx} > 1$), a dE/dx value between 0 and 20 MeV g^{-1} cm^2, as well as an estimate of $\beta\gamma$ ($0.2 < (\beta\gamma)_{dE/dx} < 10$). To ensure a reliable ToF measurement in the calorimeter, individual $\beta^{\mathrm{HIT}}_{\mathrm{TILE}}$ estimates and their individual uncertainties from calorimeter cells associated with the track are combined using a χ^2, and the resulting weighted average β_{TILE} is required to be between 0.2 and 2, with an uncertainty $\sigma_{\beta_{\mathrm{TILE}}} < 0.06$ and a χ^2 probability $P(\chi^2, \mathrm{NDF}) > 0.01$.

A LOOSE candidate selection starts from a combined ID–MS track with at least one timing measurement in the tile calorimeter or MS, and fulfilling the requirements of the above-mentioned common track selection for its ID track. In addition, the candidate tracks need to have a large combined transverse momentum ($p_{\mathrm{T}}^{\mathrm{cand}} > 70$ GeV), a combined momentum $p^{\mathrm{cand}} < 6.5$ TeV, $|\eta| < 2$, and hits in at least two MS stations. All ToF -based β measurements must be consistent, i.e., for candidates with β measurements in more than one ToF system ($N_{\mathrm{systems}} > 1$), the weighted means of all systems have to be consistent to within 5σ; and for candidates with only one system ($N_{\mathrm{systems}} = 1$) the respective internal measurements have to be consistent to within 5σ. In cases where a dE/dx measurement from the pixel detector exists, the β estimates based on dE/dx and ToF have to be consistent to within 5σ. The uncertainty in the final β, whether from a single system or a weighted average of several systems, has to be below 0.025 ($\sigma_{\beta_{\mathrm{ToF}}} < 0.025$) for the candidate to be accepted. At least one system has to yield a β measurement and a final value for β_{ToF} between 0.2 and 2 is required.

A TIGHT candidate selection is identical to the LOOSE selection, except for a tighter pseudorapidity requirement ($|\eta| < 1.65$), an additional requirement on the pixel dE/dx measurement ($1 < dE/dx < 20\,\mathrm{MeV\,g^{-1}\,cm^2}$), and requiring at least two systems to yield a β measurement.

To target the three different benchmark scenarios this analysis uses five distinct selections, as shown in Table I. Signal regions are defined by imposing requirements on estimated masses, in addition to the criteria in Table I. The signal regions that are combined are designed to be orthogonal to allow for a combination in the statistical interpretation of the results.

The search for stable R-hadrons is performed in both an MS-agnostic SR (SR-Rhad-MSagno) and a full-detector SR (SR-Rhad-FullDet) approach. The former is much less dependent on the hadronic-interaction model for R-hadrons. It is based on events solely selected through $E_{\mathrm{T}}^{\mathrm{miss}}$ triggers and candidates stemming from ID tracks fulfilling the ID+CALO selection plus the final selection requirements

[6] $\Delta R_{\mathrm{cosmics}} = \sqrt{(\eta_1 + \eta_2)^2 + (\Delta\phi - \pi)^2}$, with $\eta_{1/2}$ being the pseudorapidity of and $\Delta\phi$ the azimuthal angle between the particles in question.

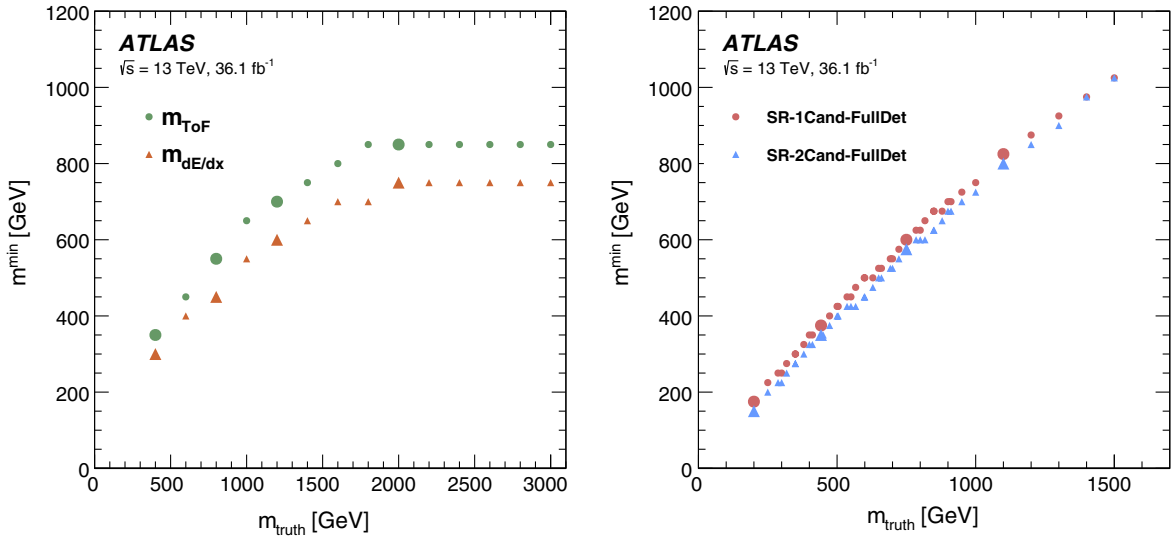

FIG. 3. The lower mass requirement (m_{min}) defining the final counting regions in the m_{ToF}–$m_{dE/dx}$ plane used in the R-hadron searches (left) and the m_{ToF} -distribution used in the chargino and stau searches (right) for the respective simulated mass of the signal at particle level (m_{truth}). The larger markers indicate the lower mass requirements for the "discovery regions."

stated in Table I. The full-detector search, on the other hand, takes full advantage of the MS, both in terms of triggering events and in using additional ToF measurements in the MDTs and RPCs.

Candidates originate from combined ID–MS tracks fulfilling the LOOSE selection and passing the final requirements states in Table I. If no LOOSE candidate is found in the event, then it is checked whether there is any candidate satisfying the ID+CALO requirements with the additional selections of Table I. The two selections are therefore mutually exclusive. In the rare case of events with more than one candidate, the candidate with the highest p_{T} is chosen to improve background suppression.

The masses are derived from $m = p/\beta\gamma$ using momentum and ToF measurements to give m_{ToF}, and, where applicable, ionization measurements to give $m_{dE/dx}$. The final selection requirements on the masses are then obtained by fitting the reconstructed mass distribution in signal events for each simulated mass hypothesis with a Gaussian function, and taking the mean minus twice the width as the lower requirement on the respective mass hypothesis. The upper requirement on the mass is left open, and hence is constrained only by kinematics to be < 6.5 TeV. For the R-hadron SRs the lower requirements are evaluated in the two-dimensional m_{ToF}–$m_{dE/dx}$ -plane, while for SRs SR-2Cand-FullDet and SR-1Cand-FullDet only the m_{ToF} distribution is used. This choice is based on the fact that especially for low-mass candidates a significant fraction of candidates have $dE/dx < 0.945$ MeV g^{-1} cm^2, at which point there is essentially no separation power between the various mass hypotheses. The final lower requirements on the masses are shown in Fig. 3.

The searches for pair-produced stable staus and charginos are performed using two orthogonal SRs. The region SR-2Cand-FullDet contains events with exactly two candidates fulfilling the LOOSE selection and the corresponding final selection requirements stated in Table I, while SR-1Cand-FullDet contains events with exactly one candidate, which in this case must satisfy the TIGHT selection and the corresponding final selection requirements stated in Table I. For the region SR-2Cand-FullDet, which has precedence over SR-1Cand-FullDet in the event categorization, the candidate with the lower m_{ToF} is used to derive limits.

A set of 16 discovery regions (DRs) is defined for setting model-independent upper limits on cross sections and stating p_0 values. These DRs are indicated by larger markers in Fig. 3. The resulting DRs are: four for SR-Rhad-MSagno, four for SR-Rhad-FullDet (combined ID+CALO + LOOSE), as well as four each for exclusive SR-2Cand-FullDet and SR-1Cand-FullDet regions.

VI. BACKGROUND ESTIMATION

The background is estimated with a fully data-driven method. First, the probability density functions (pdfs) of the key variables are determined from data, using sideband regions where possible. The key variables are momentum, β_{ToF} and $(\beta\gamma)_{dE/dx}$ for the R-hadron SRs, and momentum and β_{ToF} for the chargino and stau SRs. Distributions of expected background in m_{ToF} (and $m_{dE/dx}$) are obtained by randomly sampling the pdfs and using the equation $m = p/\beta\gamma$.

For this procedure to be valid, β_{ToF} and $(\beta\gamma)_{dE/dx}$ must not be correlated with momentum. In principle this is true,

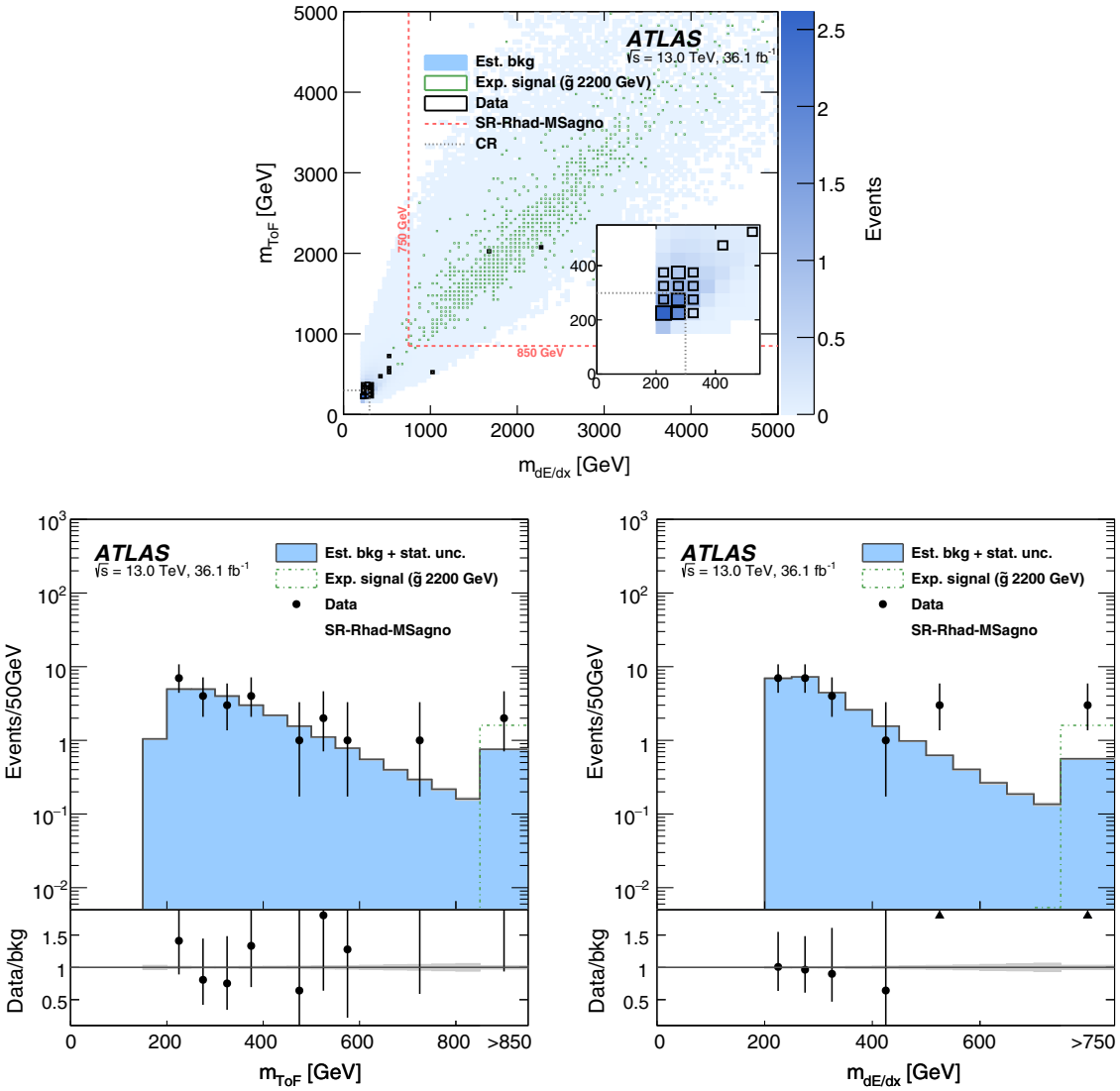

FIG. 4. Background estimate for the MS-agnostic analysis targeting gluino R-hadrons [SR-Rhad-MSagno (ID+CALO)] in the m_{ToF}–$m_{dE/dx}$ plane (top), the m_{ToF} -projection (bottom left) and the $m_{dE/dx}$ -projection (bottom right). The last bin of each distribution includes the overflow. The dashed red lines in the upper figure indicate the lower bounds of the signal region for a representative signal choice, while the dotted gray lines illustrate the upper bound for the control region. The signal (2200 GeV gluino R-hadron) is indicated by green markers in the upper and green dash-dotted lines in the lower plots. The lower panels show the ratio of observed data to estimated background. The shaded gray area shows the statistical uncertainty of the background estimate.

as the primary background contribution is from high-momentum muons with mismeasured β_{ToF} and $(\beta\gamma)_{dE/dx}$, but there can be an implicit correlation via η, in particular as the p_{T} requirement for reconstructing candidates translates into a momentum requirement $p_{\mathrm{req}} > 200$ GeV even for $|\eta| < 2.0$. This means that momentum is correlated with η for $|\eta| > 1.75$ due to the lack of low-momentum tracks. As β_{ToF} and $(\beta\gamma)_{dE/dx}$ are correlated with η due to the different resolutions in different detector regions, the result is some correlation of β_{ToF} and $(\beta\gamma)_{dE/dx}$ with momentum. To remove the effect of these correlations, the pdfs are estimated in five (SR-Rhad-MSagno, SR-Rhad-FullDet, SR-1Cand-FullDet) or six (SR-2Cand-FullDet) $|\eta|$ bins. A variable binning is used to account for the different regions of the subsystems used. For the sampling of the background, η from the candidate is used to get the corresponding pdfs. This is a safe procedure as effects from signal contamination are negligible.

To derive the SR-Rhad-MSagno and SR-Rhad-FullDet momentum pdfs, the final requirements on β_{ToF} and $(\beta\gamma)_{dE/dx}$ are inverted, while for the β_{ToF} and $(\beta\gamma)_{dE/dx}$ pdfs the final requirement on the momentum is inverted and a minimum momentum of 50 GeV is required. For the SR-2Cand-FullDet, the momentum pdf can be estimated from a sideband in β_{ToF}, but not the β_{ToF} pdf, because in the high-$|\eta|$ region no candidates with

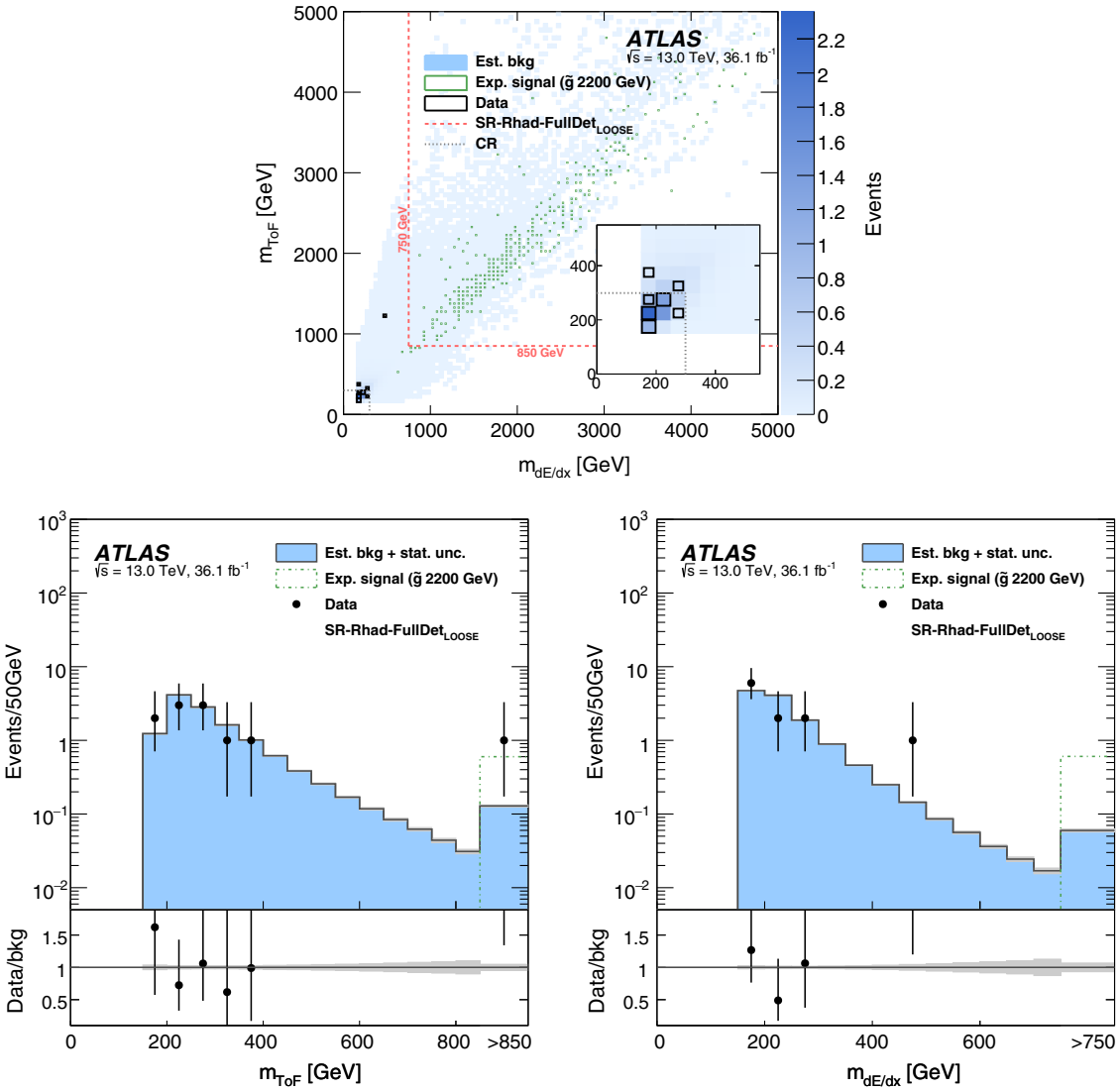

FIG. 5. Background estimate for the full-detector analysis (LOOSE part) targeting gluino R-hadrons (SR-Rhad-FullDet) in the m_{ToF}–$m_{dE/dx}$ plane (top), the m_{ToF} -projection (bottom left) and the $m_{dE/dx}$ -projection (bottom right). The last bin of each distribution includes the overflow. The dashed red lines in the upper figure indicate the lower bounds of the signal region for a representative signal choice, while the dotted gray lines illustrate the upper bound for the control region. The signal (2200 GeV gluino R-hadron) is indicated by green markers in the upper and green dash-dotted lines in the lower plots. The lower panels show the ratio of observed data to estimated background. The shaded gray area shows the statistical uncertainty of the background estimate.

$p < 100$ GeV are left. SR-1Cand-FullDet instead uses sidebands for the momentum pdfs, since for the tight candidates $|\eta| < 1.65$ is required and hence tracks with $p < 200$ GeV for the full range are available. For the β pdf in SR-1Cand-FullDet and SR-2Cand-FullDet, a minimum momentum of 70 GeV is required. The final requirements are summarized in Table I.

The background yield is normalized to data using low-mass control regions (CRs). The number of estimated events is scaled, so that the number of events in the CR matches the number observed in data. In the R-hadron searches, the CR is identical to the SR except that the minimum mass requirement is replaced by an upper limit on $m_{dE/dx}$ and m_{ToF}, which both have to be below 300 GeV. Similarly, in the chargino/stau search, the minimum mass requirement on m_{ToF} is replaced by an upper limit of 150 GeV and 200 GeV for SR-2Cand-FullDet and SR-1Cand-FullDet, respectively.

The background estimates overlaid with MC signal events at the expected mass limit are shown in Figs. 4–7. The statistical uncertainty from the pdfs is propagated to the background estimate and shown as gray bands. For all SRs, agreement between data and estimated background in the low-mass regions is found.

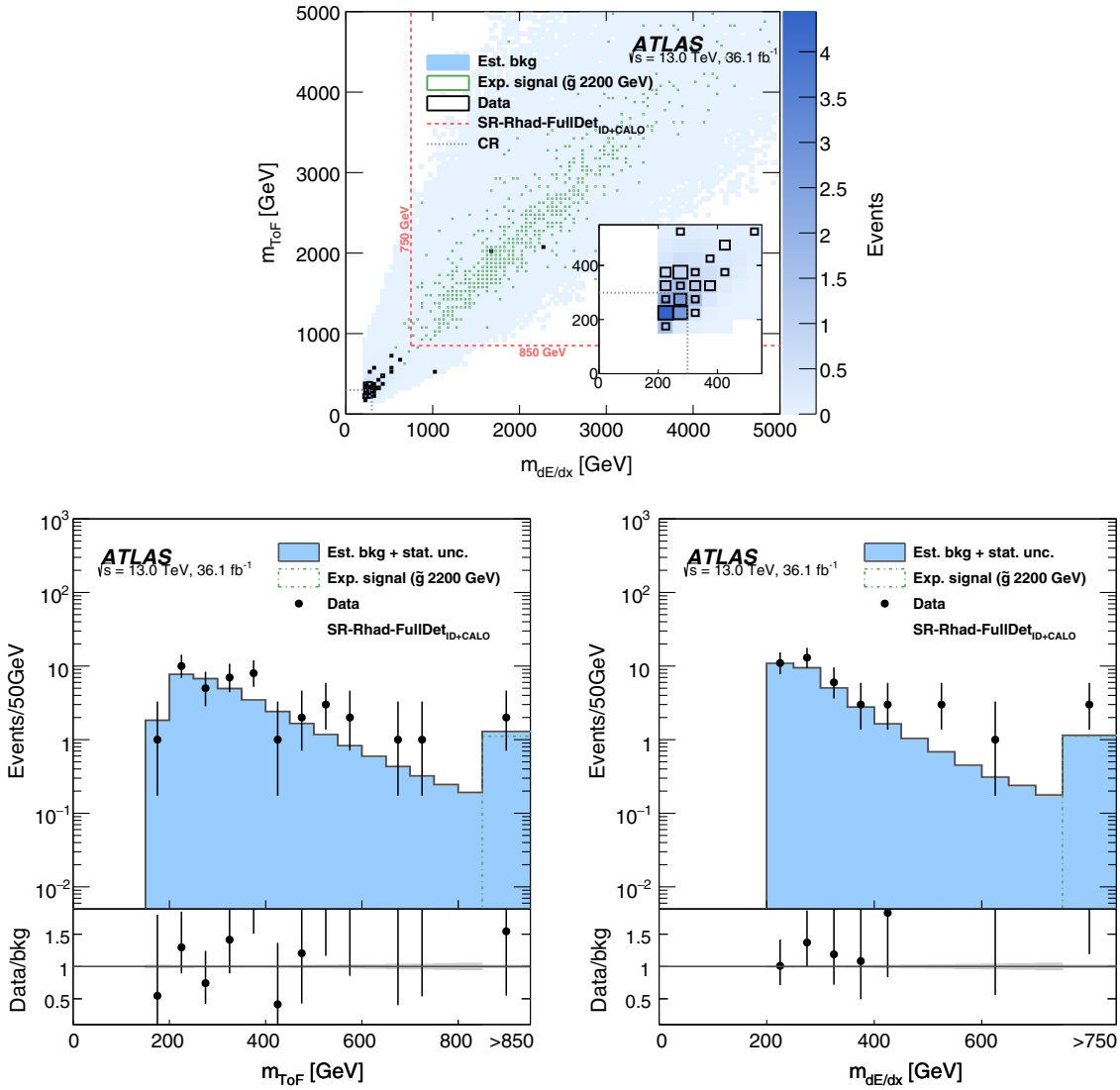

FIG. 6. Background estimate for the full-detector analysis (ID+CALO part) targeting gluino *R*-hadrons (SR-Rhad-FullDet) in the m_{ToF}–$m_{dE/dx}$ plane (top), the m_{ToF} -projection (bottom left) and the $m_{dE/dx}$ -projection (bottom right). The last bin of each distribution includes the overflow. The dashed red lines in the upper figure indicate the lower bounds of the signal region for a representative signal choice, while the dotted gray lines illustrate the upper bound for the control region. The signal (2200 GeV gluino *R*-hadron) is indicated by green markers in the upper and green dash-dotted lines in the lower plots. The lower panels show the ratio of observed data to estimated background. The shaded gray area shows the statistical uncertainty of the background estimate.

VII. SYSTEMATIC UNCERTAINTIES

The two major uncertainties in the signal yields are from the theoretical cross section and the modeling of ISR, as well as the dedicated full-detector track reconstruction and the ToF-based β measurement in the MS in some cases. All individual contributions are outlined below and summarized in Table II.

A. Theoretical cross sections

R-hadron production cross sections are calculated to next-to-leading order (NLO) in the strong coupling constant, adding the resummation of soft-gluon emission at next-to-leading-logarithm accuracy (NLO+NLL) [58–62]. Stau and chargino signal cross sections are calculated to NLO in the strong coupling constant (NLO) using Prospino2 [63]. The nominal cross section and the uncertainty is taken from an envelope of cross-section predictions using different PDF sets and factorization and renormalization scales, as described in Ref. [64]. This prescription results in an uncertainty in the cross section of between 14% (at 600 GeV) and 57% (at 3000 GeV) for gluino *R*-hadrons, and between 14% (at 600 GeV) and 23% (at 1400 GeV) for squark *R*-hadrons. For direct pair-production of staus and chargino pair-production the uncertainty is between 6% (at 290 GeV) and 10%

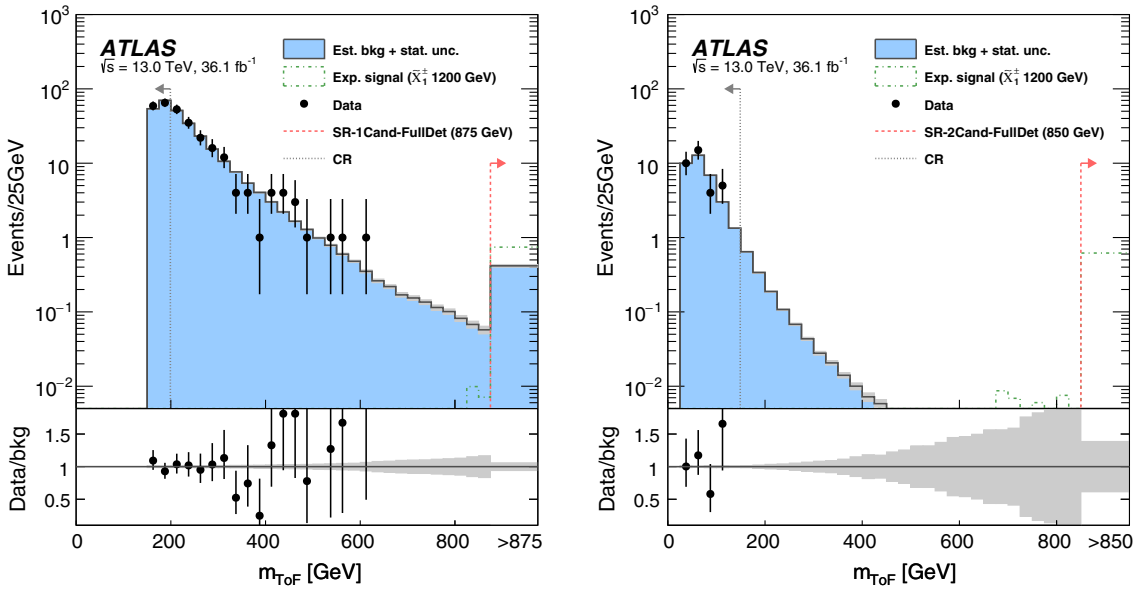

FIG. 7. Background estimate for the analysis targeting pair-produced staus and charginos in the one-TIGHT-candidate SR (left) and the two-LOOSE-candidates SR (right). The last bin of each distribution includes the overflow. The dashed red lines indicate the lower bound of the signal region for a representative signal choice, while the dotted gray lines illustrate the upper bound for the control region. The signal (1200 GeV chargino) is indicated by green dash-dotted lines. The lower panels show the ratio of observed data to estimated background. The shaded gray area shows the statistical uncertainty of the background estimate.

(at 910 GeV) and between 4% (at 200 GeV) and 10% (at 1500 GeV), respectively.

B. Signal efficiency

Missing-transverse-momentum triggers used in these searches rely solely on calorimeter-energy deposits to calculate the transverse energy, and are thus largely blind to muons, which can therefore be used for calibration and systematic uncertainties. To evaluate the trigger efficiency, the trigger turn-on curve is obtained by fitting the measured efficiency as a function of $E_{\mathrm{T}}^{\mathrm{miss}}$ in $Z \to \mu\mu$ events, in both data and simulation. These efficiency turn-on curves are then applied to the $E_{\mathrm{T}}^{\mathrm{miss}}$ spectrum from simulated events. The total uncertainty is estimated from four contributions: the relative difference between the efficiencies obtained using the fitted threshold curves from $Z \to \mu\mu$ in data and

TABLE II. Summary of systematic uncertainties. Ranges indicate a dependence on the mass hypothesis.

	Relative uncertainty [%]			
Source	MS-agnostic R-hadrons	Full-detector R-hadrons	Staus	Charginos
Theoretical inclusive cross section	14–57	14–57	6–10	4–10
Total uncertainty in signal efficiency	17–19	18–30	7–15	9–18
Trigger efficiency	1.6	1.9	4.5	3.9
$E_{\mathrm{T}}^{\mathrm{miss}}$	1.6	1.6	2.0	2.5
Single-muon		1.0	4.0	3.0
Theoretical uncertainty (ISR/FSR)	15	15	4	7
Pileup	0.2–3.8	0.3–5.5	0.1–3.1	0.2–4.4
Full-detector track reconstruction	⋯	1.7–14.8	0.2–12.8	0.8–13.0
Track hit requirements	2	2	2	2
Pixel $\beta\gamma$ measurement	6.0–11.6	6.0–13.0	0.5	0.5
ToF β measurement	0.5–3.6	9.8–21.9	1.0–3.6	2.0–12.0
Calorimeter β measurement	0.1–0.5	0.1–1.1	0.1–0.5	0.1–0.5
Calorimeter OFA correction	0.4–3.6	1.2–3.1	0.1–0.4	0.1–1.3
MS β measurement	⋯	9.7–21.7	1.0–3.5	2.0–12.0
Luminosity	2.1	2.1	2.1	2.1
Uncertainty in background estimate	33–34	27–53	9–31	9–34

simulation, the differences in efficiency obtained from independent $\pm 1\sigma$ variations in fit parameters relative to the unchanged turn-on-curve fit for both $Z \to \mu\mu$ data and simulation, and a 10% variation of the $E_{\mathrm{T}}^{\mathrm{miss}}$ to assess the scale uncertainty. The $E_{\mathrm{T}}^{\mathrm{miss}}$ trigger is estimated to contribute a total uncertainty of 1.6% and 2% to the signal efficiency for *R*-hadrons and staus/charginos, respectively.

To account for a possible mismodeling of the single-muon trigger timing in simulation, all simulated events were reweighted, depending on the β and $|\eta|$ of the candidate, to match the data and to compute systematic uncertainties. Systematic uncertainties of 1%, 4% and 3% are assigned to *R*-hadrons, staus and charginos, respectively, by taking the difference in signal trigger efficiency between unweighted and reweighted events.

To address a possible mismodeling of ISR, and hence $E_{\mathrm{T}}^{\mathrm{miss}}$ in the signal events, half of the difference between the selection efficiency for the nominal PYTHIA6 events and those reweighted to match MG5_aMC@NLO predictions is taken as an uncertainty in the expected signal yield, and found to be below 15% in all cases. For staus and charginos, the uncertainties in the amount of ISR (and FSR) are evaluated by varying generator parameters in the simulation. The uncertainty from the choice of renormalizaton/factorization scale is evaluated by changing the default scale by a factor of two in MG5_aMC@NLO. The uncertainty from the choice of CKKW-L merging [65,66] scale is evaluated by taking the maximum deviation from the nominal MC sample when varying it by a factor of two. The uncertainty from the parton-shower generator tuning is evaluated using PYTHIA8 tune variations. The systematic uncertainty on the ISR/FSR is calculated by adding all three components in quadrature. The uncertainties are evaluated for three mass points of staus and charginos and are estimated to be 4% and 5%, respectively. The latter procedure was also implemented for the MG5_aMC@NLO gluino–gluino and squark–squark samples, and the resulting uncertainties are similar to the nominal-vs-reweighted ones.

The uncertainty in the pileup modeling in simulation is found to affect the signal efficiency by between 0.1% and 5.5%, typically decreasing as a function of the simulated LLP mass and varying with benchmark model.

An additional systematic uncertainty in the signal efficiency is estimated for the dedicated tracking algorithm to cover all discrepancies between data and simulation, by randomly rejecting 10% of the reconstructed objects. The effect on the final signal efficiency is found to be between 0.2% and 14.8%.

TABLE III. Expected signal yield (N_{exp}) and acceptance (a) × efficiency (ε), estimated background (N_{est}) and observed number of events in data (N_{obs}) for the full range of simulated masses in the MS-agnostic *R*-hadron search.

		SR-Rhad-MSagno (ID+CALO)			
R-hadron	Simulated mass [GeV]	$N_{\mathrm{exp}} \pm \sigma_{N_{\mathrm{exp}}}$	$a \times \varepsilon \pm \sigma_{a\times\varepsilon}$	$N_{\mathrm{est}} \pm \sigma_{N_{\mathrm{est}}}$	N_{obs}
Gluino	400	160000 ± 30000	0.044 ± 0.003	8.0 ± 3.0	8
	600	28000 ± 5000	0.086 ± 0.004	3.0 ± 1.0	7
	800	6000 ± 1000	0.106 ± 0.005	1.8 ± 0.6	4
	1000	1300 ± 200	0.114 ± 0.005	1.0 ± 0.3	2
	1200	400 ± 70	0.129 ± 0.006	0.7 ± 0.3	2
	1400	140 ± 30	0.148 ± 0.007	0.6 ± 0.2	2
	1600	42 ± 7	0.143 ± 0.007	0.5 ± 0.2	2
	1800	13 ± 2	0.134 ± 0.007	0.4 ± 0.1	2
	2000	4.4 ± 0.8	0.126 ± 0.006	0.4 ± 0.1	2
	2200	1.5 ± 0.3	0.114 ± 0.004	0.4 ± 0.1	2
	2400	0.51 ± 0.09	0.106 ± 0.004	0.4 ± 0.1	2
	2600	0.18 ± 0.03	0.101 ± 0.004	0.4 ± 0.1	2
	2800	0.06 ± 0.01	0.090 ± 0.004	0.4 ± 0.1	2
	3000	0.023 ± 0.004	0.090 ± 0.004	0.4 ± 0.1	2
Sbottom	600	400 ± 80	0.063 ± 0.003	3.0 ± 1.0	7
	800	80 ± 20	0.083 ± 0.004	1.8 ± 0.6	4
	1000	19 ± 3	0.087 ± 0.004	1.0 ± 0.3	2
	1200	5.4 ± 0.9	0.093 ± 0.004	0.7 ± 0.3	2
	1400	1.5 ± 0.3	0.093 ± 0.004	0.6 ± 0.2	2
Stop	600	600 ± 100	0.095 ± 0.005	3.0 ± 1.0	7
	800	120 ± 200	0.117 ± 0.005	1.8 ± 0.6	4
	1000	28 ± 5	0.128 ± 0.005	1.0 ± 0.3	2
	1200	8 ± 1	0.139 ± 0.005	0.7 ± 0.3	2
	1400	2.4 ± 0.4	0.146 ± 0.005	0.6 ± 0.2	2

TABLE IV. Expected signal yield (N_{exp}) and acceptance (a) × efficiency (ε), estimated background (N_{est}) and observed number of events in data (N_{obs}) for the full range of simulated masses in the full-detector R-hadron search.

		SR-Rhad-FullDet (LOOSE)				SR-Rhad-FullDet (ID+CALO)			
R-hadron	Simulated mass [GeV]	$N_{\text{exp}} \pm \sigma_{N_{\text{exp}}}$	$a \times \varepsilon \pm \sigma_{a\times\varepsilon}$	$N_{\text{est}} \pm \sigma_{N_{\text{est}}}$	N_{obs}	$N_{\text{exp}} \pm \sigma_{N_{\text{exp}}}$	$a \times \varepsilon \pm \sigma_{a\times\varepsilon}$	$N_{\text{est}} \pm \sigma_{N_{\text{est}}}$	N_{obs}
Gluino	400	60000 ± 20000	0.016 ± 0.002	1.5 ± 0.5	1	160000 ± 3000	0.044 ± 0.003	9.0 ± 2.0	13
	600	11000 ± 4000	0.033 ± 0.003	0.5 ± 0.2	1	24000 ± 4000	0.071 ± 0.004	4.0 ± 1.0	9
	800	2400 ± 600	0.044 ± 0.003	0.3 ± 0.1	1	4500 ± 800	0.083 ± 0.004	2.5 ± 0.7	5
	1000	500 ± 100	0.045 ± 0.003	0.14 ± 0.05	0	1100 ± 200	0.091 ± 0.005	1.6 ± 0.4	3
	1200	160 ± 40	0.053 ± 0.004	0.10 ± 0.04	0	300 ± 50	0.096 ± 0.005	1.3 ± 0.4	2
	1400	60 ± 10	0.063 ± 0.005	0.07 ± 0.03	0	100 ± 20	0.104 ± 0.006	1.1 ± 0.3	2
	1600	17 ± 4	0.057 ± 0.004	0.06 ± 0.03	0	30 ± 6	0.104 ± 0.006	1.0 ± 0.3	2
	1800	5 ± 1	0.052 ± 0.004	0.05 ± 0.03	0	10 ± 2	0.099 ± 0.006	0.9 ± 0.3	2
	2000	1.9 ± 0.4	0.053 ± 0.003	0.05 ± 0.02	0	2.9 ± 0.6	0.083 ± 0.004	0.9 ± 0.2	2
	2200	0.6 ± 0.1	0.043 ± 0.003	0.05 ± 0.02	0	1.0 ± 0.2	0.079 ± 0.003	0.9 ± 0.2	2
	2400	0.18 ± 0.04	0.037 ± 0.002	0.05 ± 0.02	0	0.38 ± 0.07	0.079 ± 0.004	0.9 ± 0.2	2
	2600	0.07 ± 0.01	0.036 ± 0.002	0.05 ± 0.02	0	0.13 ± 0.02	0.074 ± 0.003	0.9 ± 0.2	2
	2800	0.019 ± 0.004	0.027 ± 0.002	0.05 ± 0.02	0	0.049 ± 0.009	0.071 ± 0.003	0.9 ± 0.2	2
	3000	0.007 ± 0.002	0.028 ± 0.002	0.05 ± 0.02	0	0.017 ± 0.003	0.066 ± 0.003	0.9 ± 0.2	2
Sbottom	600	200 ± 50	0.032 ± 0.002	0.5 ± 0.2	1	300 ± 60	0.047 ± 0.003	4.0 ± 1.0	9
	800	38 ± 8	0.037 ± 0.003	0.3 ± 0.1	1	60 ± 10	0.061 ± 0.003	2.5 ± 0.7	5
	1000	9 ± 2	0.040 ± 0.003	0.14 ± 0.05	0	14 ± 3	0.064 ± 0.003	1.6 ± 0.4	3
	1200	2.5 ± 0.5	0.043 ± 0.003	0.10 ± 0.04	0	3.9 ± 0.7	0.068 ± 0.003	1.3 ± 0.4	2
	1400	0.7 ± 0.1	0.042 ± 0.003	0.07 ± 0.03	0	1.1 ± 0.2	0.069 ± 0.003	1.1 ± 0.3	2
Stop	600	390 ± 70	0.062 ± 0.004	0.5 ± 0.2	1	370 ± 70	0.059 ± 0.004	4 ± 1	9
	800	80 ± 20	0.075 ± 0.004	0.3 ± 0.1	1	80 ± 20	0.077 ± 0.004	2.5 ± 0.7	5
	1000	18 ± 4	0.083 ± 0.004	0.14 ± 0.05	0	18 ± 3	0.081 ± 0.004	1.6 ± 0.4	3
	1200	5 ± 1	0.088 ± 0.004	0.10 ± 0.04	0	4.9 ± 0.9	0.085 ± 0.004	1.3 ± 0.4	2
	1400	1.6 ± 0.3	0.093 ± 0.005	0.07 ± 0.03	0	1.5 ± 0.3	0.089 ± 0.004	1.1 ± 0.3	2

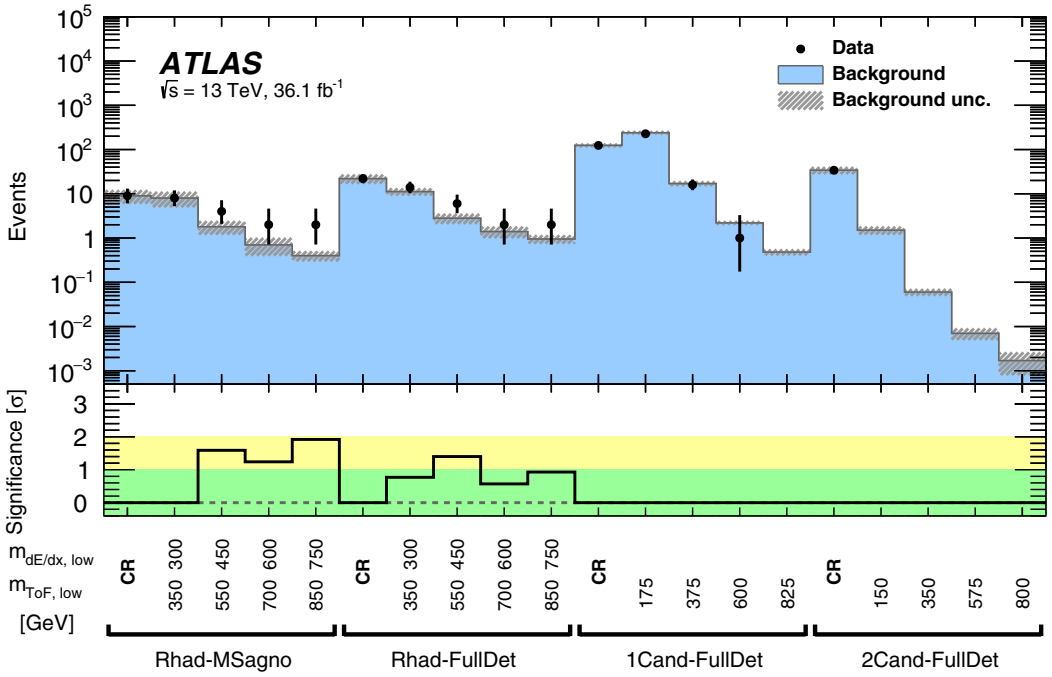

FIG. 8. Expected and observed events in the 16 discovery regions introduced in Sec. V and for the respective CRs, including the systematic uncertainties. For data the Poisson error is shown. The lower plot shows the significance for SRs with a surplus of events between observed and estimated. The bin contents of SRs with inclusive mass ranges are correlated.

TABLE V. p_0 values and model-independent upper limits on cross section (σ) × acceptance (a) × efficiency (ε) for the 16 discovery regions.

	Lower mass requirements						
Selection	$m_{\mathrm{ToF}}^{\mathrm{min}}$ [GeV]	$m_{dE/dx}^{\mathrm{min}}$ [GeV]	$N_{\mathrm{est}} \pm \sigma_{N_{\mathrm{est}}}$	N_{obs}	p_0	Significance [σ]	95% C.L. upper limit $\sigma \times a \times \varepsilon$ [fb]
SR-Rhad-MSagno	350	300	8.0 ± 3.0	8	0.5		0.25
	550	450	1.8 ± 0.6	4	0.056	1.59	0.20
	700	600	0.7 ± 0.3	2	0.11	1.24	0.17
	850	750	0.4 ± 0.1	2	0.028	1.92	0.17
SR-Rhad-FullDet	350	300	11 ± 2	14	0.22	0.77	0.42
	550	450	2.8 ± 0.7	6	0.081	1.40	0.25
	700	600	1.4 ± 0.4	2	0.28	0.57	0.14
	850	750	0.95 ± 0.2	2	0.18	0.93	0.14
SR-1Cand-FullDet	175		240 ± 20	227	0.5		1.26
	375		17 ± 2	16	0.5		0.24
	600		2.2 ± 0.2	1	0.5		0.10
	825		0.48 ± 0.07	0	0.5		0.08
SR-2Cand-FullDet	150		1.5 ± 0.3	0	0.5		0.09
	350		0.06 ± 0.01	0	0.5		0.08
	575		0.007 ± 0.002	0	0.5		0.08
	800		0.0017 ± 0.0009	0	0.5		0.08

Uncertainties in the measurement of dE/dx in the pixel detector result in uncertainties in the signal yield ranging from 6% to 13% for R-hadrons and less than 0.5% for staus and charginos. They account for both the shape difference between the ionization distribution in data and simulation, and the scale shift in data due to radiation damage.

The systematic uncertainty in the calorimeter-based β estimation is assessed by scaling the calorimeter-cell-time smearing of simulated events by ±5% and by varying the cell-time correction introduced to correct for the bias due to the OFA by ±50%, and is found to be below 2% in all cases.

The systematic uncertainty in the MS-based β estimation is derived by varying the MDT smearing constants by ±10% to bracket the distribution seen in data. By comparing the signal efficiency with and without the correction for incorrectly modeled timing behavior in the RPCs, the overall uncertainty is found to be between 1.0% and 21.7%.

C. Integrated luminosity

The uncertainty in the combined 2015 + 2016 integrated luminosity is 2.1%. It is derived, following a methodology similar to that detailed in Ref. [67], from a calibration of the luminosity scale using x-y beam-separation scans performed in August 2015 and May 2016.

D. Background estimation

To estimate the systematic uncertainty of the background estimate, three main contributions are considered: the

TABLE VI. Expected signal yield (N_{exp}) and acceptance (a) × efficiency (ε), estimated background (N_{est}) and observed number of events in data (N_{obs}) for the full range of simulated masses in the MS-agnostic search for metastable gluino R-hadrons.

Gluino R-hadron	SR-Rhad-MSagno (ID+CALO)							
Lifetime	10 ns		30 ns		50 ns			
Simulated mass [GeV]	$N_{\mathrm{exp}} \pm \sigma_{N_{\mathrm{exp}}}$	$a \times \varepsilon \pm \sigma_{a\times\varepsilon}$	$N_{\mathrm{exp}} \pm \sigma_{N_{\mathrm{exp}}}$	$a \times \varepsilon \pm \sigma_{a\times\varepsilon}$	$N_{\mathrm{exp}} \pm \sigma_{N_{\mathrm{exp}}}$	$a \times \varepsilon \pm \sigma_{a\times\varepsilon}$	$N_{\mathrm{est}} \pm \sigma_{N_{\mathrm{est}}}$	N_{obs}
1000	800 ± 100	0.065 ± 0.004	1400 ± 300	0.121 ± 0.006	1500 ± 300	0.125 ± 0.005	1.0 ± 0.3	2
1200	220 ± 40	0.072 ± 0.004	400 ± 70	0.129 ± 0.006	410 ± 70	0.133 ± 0.005	0.7 ± 0.3	2
1400	70 ± 10	0.079 ± 0.004	120 ± 20	0.132 ± 0.005	140 ± 30	0.149 ± 0.006	0.6 ± 0.2	2
1600	22 ± 4	0.074 ± 0.003	41 ± 7	0.140 ± 0.005	41 ± 7	0.142 ± 0.005	0.5 ± 0.2	2
1800	8 ± 1	0.077 ± 0.003	14 ± 2	0.139 ± 0.005	14 ± 2	0.142 ± 0.005	0.4 ± 0.1	2
2000	2.8 ± 0.5	0.080 ± 0.005	4.7 ± 0.8	0.132 ± 0.007	5.2 ± 0.9	0.146 ± 0.005	0.4 ± 0.1	2
2200	1.0 ± 0.2	0.075 ± 0.004	1.7 ± 0.3	0.132 ± 0.005	1.7 ± 0.3	0.130 ± 0.004	0.4 ± 0.1	2
2400	0.35 ± 0.06	0.073 ± 0.004	0.58 ± 0.10	0.120 ± 0.004	0.6 ± 0.1	0.122 ± 0.004	0.4 ± 0.1	2

TABLE VII. Expected signal yield (N_{exp}) and acceptance (a) × efficiency (ε), estimated background (N_{est}) and observed number of events in data (N_{obs}) for the full range of simulated masses in the full-detector direct-stau search.

Simulated mass [GeV]	SR-2Cand-FullDet				SR-1Cand-FullDet			
	$N_{\text{exp}} \pm \sigma_{N_{\text{exp}}}$	$a \times \varepsilon \pm \sigma_{a\times\varepsilon}$	$N_{\text{exp}} \pm \sigma_{N_{\text{exp}}}$	N_{obs}	$N_{\text{exp}} \pm \sigma_{N_{\text{exp}}}$	$a \times \varepsilon \pm \sigma_{a\times\varepsilon}$	$N_{\text{est}} \pm \sigma_{N_{\text{est}}}$	N_{obs}
287	13 ± 1	0.167 ± 0.005	0.33 ± 0.06	0	5.1 ± 0.6	0.068 ± 0.003	80.0 ± 7.0	74
318	9 ± 1	0.179 ± 0.007	0.22 ± 0.04	0	3.6 ± 0.4	0.073 ± 0.004	56.0 ± 5.0	52
349	6.1 ± 0.7	0.181 ± 0.005	0.15 ± 0.03	0	2.5 ± 0.2	0.076 ± 0.003	41.0 ± 4.0	36
380	4.3 ± 0.6	0.184 ± 0.006	0.11 ± 0.02	0	2.1 ± 0.2	0.089 ± 0.005	30.0 ± 3.0	24
411	3.2 ± 0.4	0.196 ± 0.005	0.08 ± 0.02	0	1.5 ± 0.1	0.093 ± 0.004	23.0 ± 2.0	20
442	2.4 ± 0.3	0.198 ± 0.007	0.06 ± 0.01	0	1.2 ± 0.2	0.096 ± 0.005	17.0 ± 2.0	16
473	1.8 ± 0.3	0.204 ± 0.005	0.045 ± 0.009	0	0.92 ± 0.09	0.105 ± 0.004	13.0 ± 1.0	15
504	1.4 ± 0.2	0.210 ± 0.005	0.035 ± 0.007	0	0.68 ± 0.06	0.105 ± 0.004	10.1 ± 1.0	11
536	1.0 ± 0.1	0.208 ± 0.005	0.027 ± 0.006	0	0.55 ± 0.06	0.111 ± 0.004	7.9 ± 0.8	7
567	0.84 ± 0.10	0.224 ± 0.006	0.027 ± 0.006	0	0.43 ± 0.04	0.113 ± 0.004	6.3 ± 0.6	4
598	0.65 ± 0.09	0.227 ± 0.006	0.022 ± 0.005	0	0.34 ± 0.03	0.118 ± 0.004	5.0 ± 0.5	3
629	0.50 ± 0.07	0.227 ± 0.006	0.017 ± 0.004	0	0.27 ± 0.02	0.124 ± 0.004	5.0 ± 0.5	3
660	0.40 ± 0.05	0.234 ± 0.006	0.014 ± 0.003	0	0.22 ± 0.02	0.125 ± 0.005	4.0 ± 0.4	3
692	0.30 ± 0.05	0.224 ± 0.008	0.011 ± 0.003	0	0.17 ± 0.02	0.125 ± 0.005	3.2 ± 0.3	2
723	0.24 ± 0.03	0.229 ± 0.007	0.009 ± 0.002	0	0.13 ± 0.01	0.120 ± 0.005	2.6 ± 0.3	1
754	0.19 ± 0.02	0.224 ± 0.006	0.008 ± 0.002	0	0.112 ± 0.009	0.132 ± 0.004	2.2 ± 0.2	1
785	0.15 ± 0.02	0.222 ± 0.006	0.007 ± 0.002	0	0.091 ± 0.007	0.135 ± 0.005	1.8 ± 0.2	0
817	0.12 ± 0.01	0.219 ± 0.006	0.007 ± 0.002	0	0.073 ± 0.006	0.134 ± 0.004	1.5 ± 0.1	0
848	0.09 ± 0.01	0.215 ± 0.005	0.006 ± 0.001	0	0.061 ± 0.005	0.138 ± 0.004	1.3 ± 0.1	0
879	0.08 ± 0.01	0.212 ± 0.005	0.005 ± 0.001	0	0.052 ± 0.005	0.146 ± 0.005	1.3 ± 0.1	0
911	0.065 ± 0.007	0.225 ± 0.006	0.004 ± 0.001	0	0.041 ± 0.003	0.144 ± 0.005	1.1 ± 0.1	0

TABLE VIII. Expected signal yield (N_{exp}) and acceptance (a) × efficiency (ε), estimated background (N_{est}) and observed number of events in data (N_{obs}) for the full range of simulated masses in the full-detector chargino search.

Simulated mass [GeV]	SR-2Cand-FullDet				SR-1Cand-FullDet			
	$N_{\text{exp}} \pm \sigma_{N_{\text{exp}}}$	$a \times \varepsilon \pm \sigma_{a\times\varepsilon}$	$N_{\text{est}} \pm \sigma_{N_{\text{exp}}}$	N_{obs}	$N_{\text{exp}} \pm \sigma_{N_{\text{exp}}}$	$a \times \varepsilon \pm \sigma_{a\times\varepsilon}$	$N_{\text{est}} \pm \sigma_{N_{\text{est}}}$	N_{obs}
200	2600 ± 400	0.083 ± 0.003	1.5 ± 0.3	0	1200 ± 200	0.038 ± 0.002	230 ± 20	227
250	1200 ± 200	0.091 ± 0.003	0.51 ± 0.10	0	800 ± 100	0.062 ± 0.003	110 ± 10	109
300	690 ± 100	0.102 ± 0.004	0.33 ± 0.06	0	490 ± 50	0.073 ± 0.003	79 ± 7	74
350	360 ± 50	0.101 ± 0.004	0.15 ± 0.03	0	280 ± 30	0.078 ± 0.003	41 ± 4	36
400	220 ± 30	0.107 ± 0.004	0.08 ± 0.02	0	180 ± 20	0.089 ± 0.004	23 ± 2	20
450	140 ± 20	0.113 ± 0.004	0.06 ± 0.01	0	120 ± 10	0.100 ± 0.004	17 ± 2	16
500	90 ± 10	0.115 ± 0.004	0.034 ± 0.007	0	77 ± 8	0.100 ± 0.004	10 ± 1	11
550	59 ± 8	0.119 ± 0.004	0.027 ± 0.006	0	52 ± 5	0.105 ± 0.004	7.9 ± 0.8	7
600	42 ± 6	0.129 ± 0.004	0.021 ± 0.004	0	36 ± 4	0.110 ± 0.004	5.0 ± 0.5	3
650	27 ± 4	0.123 ± 0.004	0.014 ± 0.003	0	24 ± 2	0.107 ± 0.004	4.0 ± 0.4	3
700	18 ± 3	0.122 ± 0.004	0.011 ± 0.003	0	17 ± 2	0.113 ± 0.004	3.2 ± 0.3	2
750	12 ± 2	0.113 ± 0.004	0.008 ± 0.002	0	13 ± 1	0.118 ± 0.004	2.1 ± 0.2	1
800	9 ± 1	0.120 ± 0.004	0.007 ± 0.002	0	9.2 ± 0.9	0.123 ± 0.004	1.8 ± 0.2	0
850	6.0 ± 0.8	0.112 ± 0.005	0.006 ± 0.001	0	6.1 ± 0.6	0.114 ± 0.005	1.3 ± 0.1	0
900	4.2 ± 0.6	0.108 ± 0.004	0.004 ± 0.001	0	4.7 ± 0.5	0.121 ± 0.004	1.1 ± 0.1	0
950	3.2 ± 0.5	0.112 ± 0.004	0.003 ± 0.001	0	3.3 ± 0.3	0.118 ± 0.004	1.0 ± 0.1	0
1000	2.2 ± 0.4	0.106 ± 0.005	0.0029 ± 0.0009	0	2.5 ± 0.2	0.120 ± 0.006	0.84 ± 0.10	0
1100	1.2 ± 0.2	0.105 ± 0.004	0.0019 ± 0.0007	0	1.5 ± 0.2	0.131 ± 0.004	0.54 ± 0.07	0
1200	0.62 ± 0.09	0.096 ± 0.004	0.0015 ± 0.0006	0	0.74 ± 0.07	0.115 ± 0.004	0.42 ± 0.06	0
1300	0.32 ± 0.04	0.087 ± 0.003	0.0012 ± 0.0006	0	0.44 ± 0.05	0.118 ± 0.004	0.33 ± 0.05	0
1400	0.19 ± 0.03	0.087 ± 0.004	0.0009 ± 0.0005	0	0.26 ± 0.03	0.120 ± 0.004	0.27 ± 0.04	0
1500	0.10 ± 0.02	0.077 ± 0.003	0.0007 ± 0.0005	0	0.16 ± 0.01	0.121 ± 0.004	0.21 ± 0.04	0

systematic uncertainty of the normalization as well as the influence of the $|\eta|$ binning and the definition of the sidebands. The normalization uncertainty, derived by applying the relative statistical uncertainty in the number of data events in the CR to the estimated number of background events in the SR, is the dominant contribution for most SRs. Only at very high masses do the other contributions become significant and eventually take over. To test the stability of the choice of $|\eta|$ binning, the number of $|\eta|$ bins in the pdfs is varied from nominal five (six) to three (four) and six (nine) for `SR-Rhad-MSagno`, `SR-Rhad-FullDet` and `SR-1Cand-FullDet` (`SR-2Cand-FullDet`). For each pdf, the background is estimated and half the maximal difference in the number of background events in the SR is taken as a systematic uncertainty. To check for an influence of the sideband definition, the selection requirements are varied, the pdfs re-evaluated correspondingly, and half the maximal difference of background counts in the SR, using the nominal and varied pdfs, is taken as the systematic uncertainty.

VIII. RESULTS

Mass distributions observed in data together with the background estimate, its statistical uncertainty and a representative expected signal are shown in Figs. 4–7 for

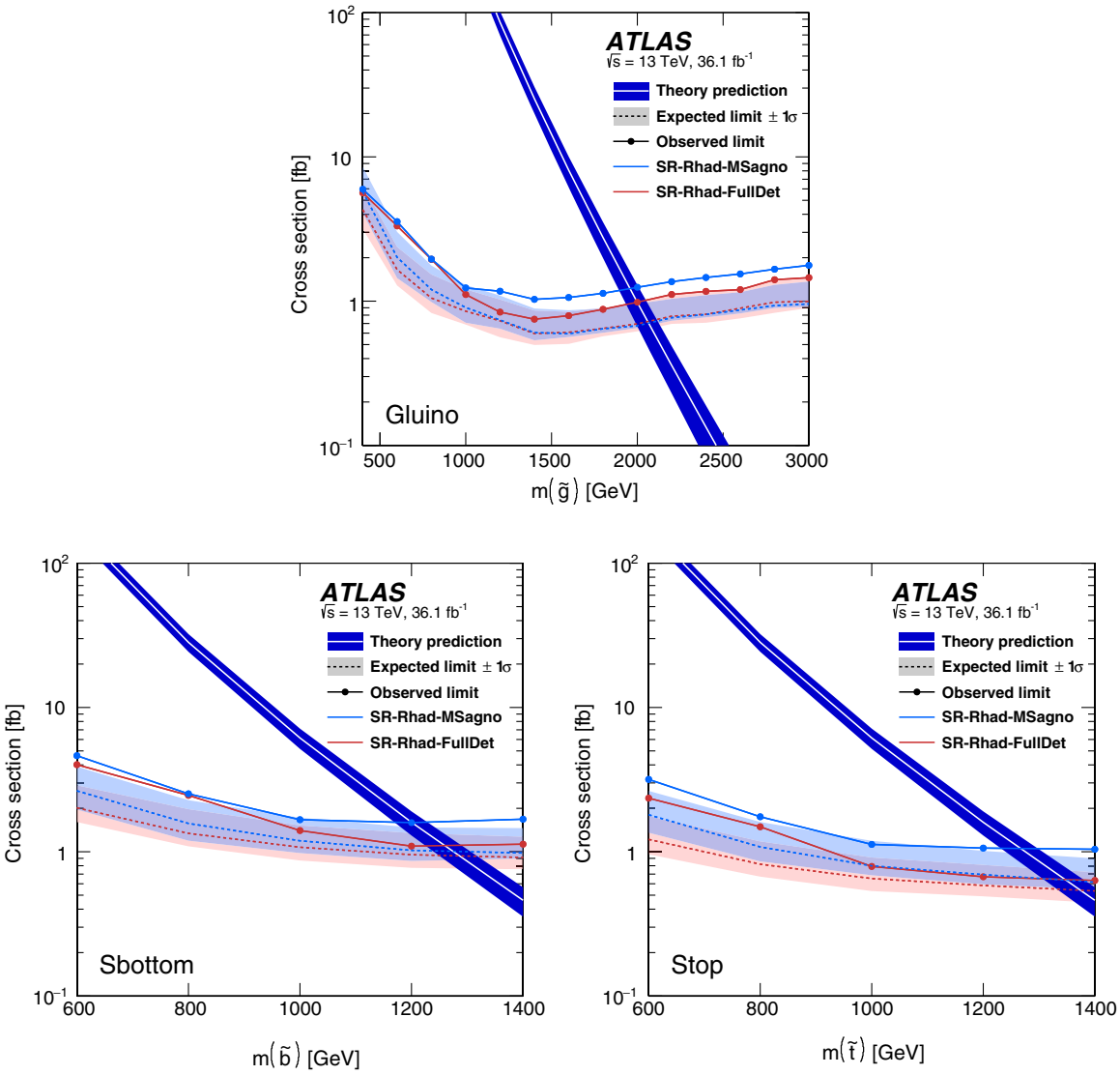

FIG. 9. Expected (dashed lines) and observed (marked solid lines) upper cross-section limits in the gluino (top), sbottom (bottom left) and stop (bottom right) R-hadron searches, respectively, using two independent and not to be combined approaches based on SRs `SR-Rhad-MSagno` (light blue) and `SR-Rhad-FullDet` (red). The shaded light-blue/light-red bands represent the $\pm 1\sigma$ uncertainties in the expected limits. The result obtained using the former SR has a much reduced dependence on the modeling of R-hadron interaction with matter with respect to the other, therefore the two results must not combined. The theory prediction along with its $\pm 1\sigma$ uncertainty is shown as a white line and a dark-blue band, respectively.

the MS-agnostic and full-detector R-hadron, stau and chargino searches, respectively.

As can be seen in Tables III–VIII, no significant excess of observed data events above the expected background is found in the examined mass ranges and signal regions. The yields are summarized for a subset of discovery regions (see Sec. V) in Fig. 8 and Table V, the latter also showing the p_0 values.

Upper limits at 95% confidence level (C.L.) are placed on the production cross sections for various benchmark models, as shown in Figs. 9 and 10. These limits are obtained from the expected signal and the estimated background in signal region `SR-Rhad-MSagno` (`SR-Rhad-FullDet` or `SR-1Cand-FullDet/SR-2Cand-FullDet`) using a one-bin (two-bin) counting experiment applying the CL_s prescription [68]. Model-independent upper limits defined as cross section × acceptance × efficiency for the above-mentioned discovery regions are shown in Table V. Given the predicted theoretical cross sections, also shown in Figs. 9 and 10, the cross-section limits are translated into lower limits on masses for the various benchmark models.

The MS-agnostic search yields expected lower limits at 95% C.L. on the R-hadron masses of 2060, 1270 and 1345 GeV for the production of long-lived gluino, sbottom and stop R-hadrons, respectively. The corresponding observed lower limits on the masses are 1950, 1190 and 1265 GeV. The expected signal yield (N_{exp}) and efficiency, estimated background (N_{est}) and observed number of events in data (N_{obs}) for the full range of simulated masses can be found in Table III. The sensitivity first increases and then decreases with increasing R-hadron mass. The same effect is visible in the total efficiency of the $E_{\text{T}}^{\text{miss}}$ trigger, and is due to the change in production channel for gluino R-hadrons from gluon-initiated to quark-initiated with increasing mass.

For metastable gluino R-hadrons, the MS-agnostic search yields expected lower limits on mass of 1980, 2080 and 2090 GeV for lifetimes of 10, 30 and 50 ns, respectively. The corresponding observed lower limits are 1860, 1960 and 1980 GeV. The expected signal yield (N_{exp}) and efficiency, estimated background (N_{est}) and observed number of events in data (N_{obs}) for the full range of simulated masses can be found in Table VI. As additional $E_{\text{T}}^{\text{miss}}$ can arise from one of the gluino R-hadrons decaying before the calorimeters, the sensitivity increases for mass regions that have limited trigger efficiency (low and high masses). With decreasing lifetime, and thereby increasing probability for both gluino R-hadrons to decay before the calorimeters, the signal efficiency drops, as does the sensitivity of the search optimized for R-hadrons long-lived enough to exit the detector. However, the expected lower limits on mass at lifetimes of 50 and 30 ns remain more stringent than those of the search targeting low-lifetime metastable gluino R-hadrons [31]. Expected and observed lower limits on mass as a function of lifetime for both the MS-agnostic and full-detector searches for gluino R-hadrons are shown in Fig. 11.

Using the full-detector search, the expected (observed) lower limits on the mass are 2050 GeV (2000 GeV), 1280 GeV (1250 GeV) and 1370 GeV (1340 GeV) for the production of long-lived gluino, sbottom and stop R-hadrons, respectively. The expected signal yield (N_{exp}) and efficiency, estimated background (N_{est}) and observed number of events in data (N_{obs}) for the full range of

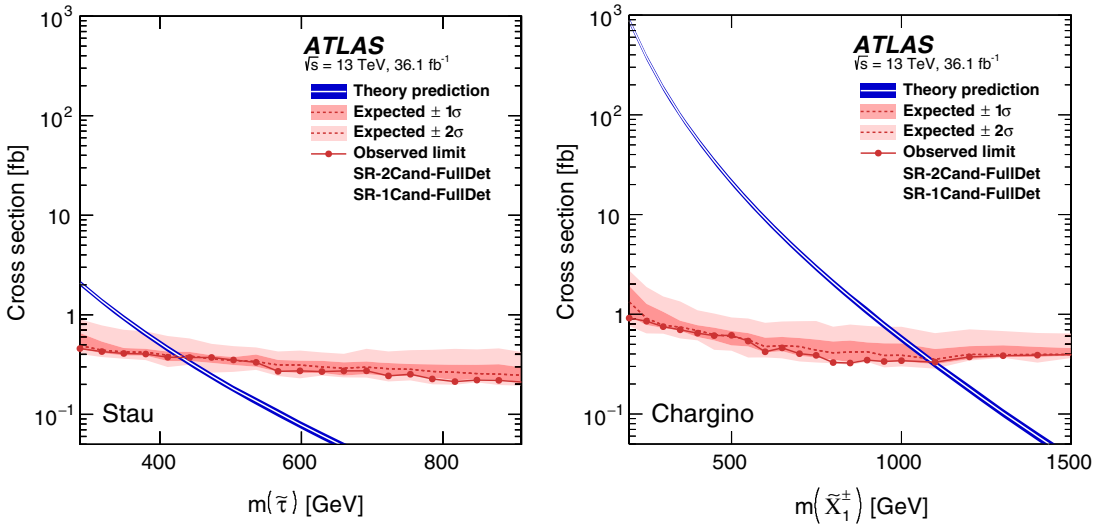

FIG. 10. Expected (dashed red line) and observed (marked solid red line) upper cross-section limits using combined two- and one-candidate SRs for stau pair production (left) and chargino pair production (right). The shaded dark-red (light-red) bands represent the $\pm 1\sigma$ ($\pm 2\sigma$) uncertainties in the expected limits. The theory prediction along with its $\pm 1\sigma$ uncertainty is shown as a white line and a blue band, respectively.

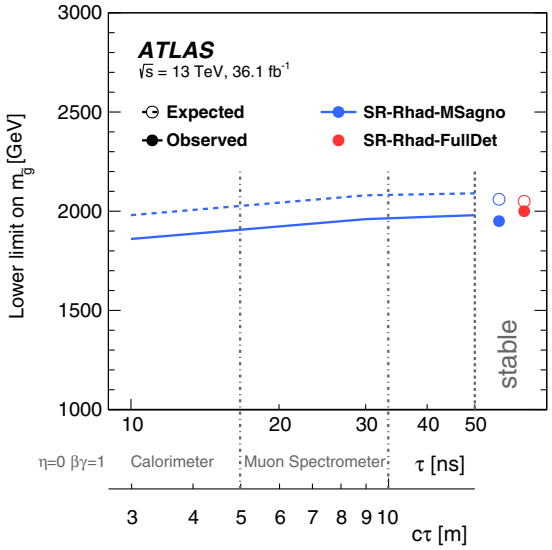

FIG. 11. Expected (dashed blue line) and observed (solid blue line) lower mass limits at the 95% C.L. level for gluino *R*-hadrons with different mean lifetimes derived using the MS-agnostic analysis (`SR-Rhad-MSagno`). Expected (empty circles) and observed (filled circles) limits on stable gluino *R*-hadrons are shown for both the MS-agnostic (`SR-Rhad-MSagno`) and the full-detector analysis (`SR-Rhad-FullDet`).

simulated masses can be found in Table IV. The sensitivity of the *R*-hadron full-detector search in mass regions with noticeable background yields is slightly better than that of the MS-agnostic search, due mainly to the increased signal efficiency when including the single-muon trigger and an improved β-resolution when using full-detector candidates. However, this specific search is consequently slightly more model-dependent, especially on the modeling of hadronic interactions.

Expected (observed) lower limits on mass for direct production of staus and charginos are set at 420 GeV (430 GeV) and 1070 GeV (1090 GeV), respectively. The expected signal yield (N_{exp}) and efficiency, estimated background (N_{est}) and observed number of events in data (N_{obs}) for the full range of simulated masses can be found in Tables VII and VIII.

IX. CONCLUSION

A search for heavy, charged, long-lived particles is performed using a data sample of 36.1 fb^{-1} of proton-proton collisions at $\sqrt{s} = 13$ TeV collected by the ATLAS experiment at the Large Hadron Collider at CERN. The search is based on observables related to large ionization losses, measured in the innermost tracking detector, and slow propagation velocities, measured in the tile calorimeter and muon spectrometer. Both observables are signatures of heavy charged particles traveling significantly slower than the speed of light. No significant deviations from the expected background are observed. Upper limits at 95% confidence level are provided on the production cross sections of long-lived *R*-hadrons, as well as directly pair-produced staus and charginos. These results translate into lower limits on the masses of long-lived gluino, sbottom and stop *R*-hadrons, as well as staus and charginos of 2000, 1250, 1340, 430 and 1090 GeV, respectively.

ACKNOWLEDGMENTS

We thank CERN for the very successful operation of the LHC, as well as the support staff from our institutions without whom ATLAS could not be operated efficiently. We acknowledge the support of ANPCyT, Argentina; YerPhI, Armenia; ARC, Australia; BMWFW and FWF, Austria; ANAS, Azerbaijan; SSTC, Belarus; CNPq and FAPESP, Brazil; NSERC, NRC and CFI, Canada; CERN; CONICYT, Chile; CAS, MOST and NSFC, China; COLCIENCIAS, Colombia; MSMT CR, MPO CR and VSC CR, Czech Republic; DNRF and DNSRC, Denmark; IN2P3-CNRS, CEA-DRF/IRFU, France; SRNSFG, Georgia; BMBF, HGF, and MPG, Germany; GSRT, Greece; RGC, Hong Kong SAR, China; ISF and Benoziyo Center, Israel; INFN, Italy; MEXT and JSPS, Japan; CNRST, Morocco; NWO, Netherlands; RCN, Norway; MNiSW and NCN, Poland; FCT, Portugal; MNE/IFA, Romania; MES of Russia and NRC KI, Russian Federation; JINR; MESTD, Serbia; MSSR, Slovakia; ARRS and MIZŠ, Slovenia; DST/NRF, South Africa; MINECO, Spain; SRC and Wallenberg Foundation, Sweden; SERI, SNSF and Cantons of Bern and Geneva, Switzerland; MOST, Taiwan; TAEK, Turkey; STFC, United Kingdom; DOE and NSF, United States of America. In addition, individual groups and members have received support from BCKDF, CANARIE, CRC and Compute Canada, Canada; COST, ERC, ERDF, Horizon 2020, and Marie Skłodowska-Curie Actions, European Union; Investissements d' Avenir Labex and Idex, ANR, France; DFG and AvH Foundation, Germany; Herakleitos, Thales and Aristeia programmes co-financed by EU-ESF and the Greek NSRF, Greece; BSF-NSF and GIF, Israel; CERCA Programme Generalitat de Catalunya, Spain; The Royal Society and Leverhulme Trust, United Kingdom. The crucial computing support from all WLCG partners is acknowledged gratefully, in particular from CERN, the ATLAS Tier-1 facilities at TRIUMF (Canada), NDGF (Denmark, Norway, Sweden), CC-IN2P3 (France), KIT/GridKA (Germany), INFN-CNAF (Italy), NL-T1 (Netherlands), PIC (Spain), ASGC (Taiwan), RAL (UK) and BNL (USA), the Tier-2 facilities worldwide and large non-WLCG resource providers. Major contributors of computing resources are listed in Ref. [69].

[1] CMS Collaboration, Search for long-lived charged particles in proton-proton collisions at $\sqrt{s} = 13$ TeV, Phys. Rev. D **94**, 112004 (2016).

[2] ATLAS Collaboration, Search for heavy long-lived charged R-hadrons with the ATLAS detector in 3.2 fb^{-1} of proton-proton collision data at $\sqrt{s} = 13$ TeV, Phys. Lett. B **760**, 647 (2016).

[3] ATLAS Collaboration, Searches for heavy long-lived charged particles with the ATLAS detector in proton-proton collisions at $\sqrt{s} = 8$ TeV, J. High Energy Phys. 01 (2015) 068.

[4] M. Fairbairn, A. C. Kraan, D. A. Milstead, T. Sjöstrand, P. Skands, and T. Sloan, Stable massive particles at colliders, Phys. Rep. **438**, 1 (2007).

[5] Y. A. Gol'fand and E. P. Likhtman, Extension of the algebra of Poincare group generators and violation of p invariance, Pis'ma Zh. Eksp. Teor. Fiz. **13**, 452 (1971) [JETP Lett. **13**, 323 (1971)].

[6] D. V. Volkov and V. P. Akulov, Is the neutrino a goldstone particle, Phys. Lett. B **46**, 109 (1973).

[7] J. Wess and B. Zumino, Supergauge transformations in four-dimensions, Nucl. Phys. **B70**, 39 (1974).

[8] J. Wess and B. Zumino, Supergauge invariant extension of quantum electrodynamics, Nucl. Phys. **B78**, 1 (1974).

[9] S. Ferrara and B. Zumino, Supergauge invariant Yang-Mills theories, Nucl. Phys. **B79**, 413 (1974).

[10] A. Salam and J. A. Strathdee, Supersymmetry and non-abelian gauges, Phys. Lett. B **51**, 353 (1974).

[11] H. K. Dreiner, An introduction to explicit R-parity violation, Adv. Ser. Dir. High Energy Phys. **21**, 565 (2010).

[12] E. L. Berger and Z. Sullivan, Lower Limits on R-Parity-Violating Couplings in Supersymmetric Models with Light Squarks, Phys. Rev. Lett. **92**, 201801 (2004).

[13] R. Barbier, C. Berat, M. Besancon, M. Chemtob, A. Deandrea *et al.*, R-parity violating supersymmetry, Phys. Rep. **420**, 1 (2005).

[14] G. R. Farrar and P. Fayet, Phenomenology of the production, decay, and detection of new hadronic states associated with supersymmetry, Phys. Lett. **76B**, 575 (1978).

[15] C. F. Kolda, Gauge-mediated supersymmetry breaking: Introduction, review and update, Nucl. Phys. B, Proc. Suppl. **62**, 266 (1998).

[16] H. Baer, K. Cheung, and J. F. Gunion, A heavy gluino as the lightest supersymmetric particle, Phys. Rev. D **59**, 075002 (1999).

[17] S. J. Gates, Jr. and O. Lebedev, Searching for supersymmetry in hadrons, Phys. Lett. B **477**, 216 (2000).

[18] G. F. Giudice and A. Romanino, Split supersymmetry, Nucl. Phys. **B699**, 65 (2004); Erratum, Nucl. Phys. **B706**, 65(E) (2005).

[19] N. Arkani-Hamed, S. Dimopoulos, G. F. Giudice, and A. Romanino, Aspects of split supersymmetry, Nucl. Phys. **B709**, 3 (2005).

[20] M. Carena, D. Choudhury, R. A. Diaz, H. E. Logan, and C. E. M. Wagner, Top squark searches at the Tevatron in models of low-energy supersymmetry breaking, Phys. Rev. D **66**, 115010 (2002).

[21] C. Balazs, M. Carena, and C. E. M. Wagner, Dark matter, light stops and electroweak baryogenesis, Phys. Rev. D **70**, 015007 (2004).

[22] M. Dine and W. Fischler, A phenomenological model of particle physics based on supersymmetry, Phys. Lett. **110B**, 227 (1982).

[23] L. Alvarez-Gaume, M. Claudson, and M. B. Wise, Low-energy supersymmetry, Nucl. Phys. **B207**, 96 (1982).

[24] C. R. Nappi and B. A. Ovrut, Supersymmetric extension of the $SU(3) \times SU(2) \times U(1)$ model, Phys. Lett. **113B**, 175 (1982).

[25] M. Dine and A. E. Nelson, Dynamical supersymmetry breaking at low-energies, Phys. Rev. D **48**, 1277 (1993).

[26] M. Dine, A. E. Nelson, and Y. Shirman, Low-energy dynamical supersymmetry breaking simplified, Phys. Rev. D **51**, 1362 (1995).

[27] M. Dine, A. E. Nelson, Y. Nir, and Y. Shirman, New tools for low-energy dynamical supersymmetry breaking, Phys. Rev. D **53**, 2658 (1996).

[28] L. Randall and R. Sundrum, Out of this world supersymmetry breaking, Nucl. Phys. **B557**, 79 (1999).

[29] G. F. Giudice, M. A. Luty, H. Murayama, and R. Rattazzi, Gaugino mass without singlets, J. High Energy Phys. 12 (1998) 027.

[30] ATLAS Collaboration, The ATLAS experiment at the CERN Large Hadron Collider, J. Instrum. **3**, S08003 (2008).

[31] ATLAS Collaboration, Search for heavy charged long-lived particles in proton-proton collisions at $\sqrt{s} = 13$ TeV using an ionisation measurement with the ATLAS detector, Phys. Lett. B **788**, 96 (2019).

[32] E. Fullana *et al.*, Optimal filtering in the ATLAS hadronic tile calorimeter, Report No. ATL-TILECAL-2005-001, 2005, http://cds.cern.ch/record/816152.

[33] S. Tarem, S. Bressler, H. Nomoto, and A. Di Mattia, Trigger and reconstruction for heavy long-lived charged particles with the ATLAS detector, Eur. Phys. J. C **62**, 281 (2009).

[34] S. Tarem, Reconstruction and identification of heavy long-lived particles at the ATLAS detector at the LHC, AIP Conf. Proc. **1200**, 762 (2010).

[35] ATLAS Collaboration, Performance of the ATLAS trigger system in 2015, Eur. Phys. J. C **77**, 317 (2017).

[36] T. Sjöstrand, S. Mrenna, and P. Skands, PYTHIA 6.4 physics and manual, J. High Energy Phys. 05 (2006) 026.

[37] ATLAS Collaboration, Further ATLAS tunes of PYTHIA6 and Pythia 8, Report No. ATL-PHYS-PUB-2011-014, 2011, http://cds.cern.ch/record/1400677.

[38] J. Pumplin, D. Robert Stump, J. Huston, H.-L. Lai, P. Nadolsky, and W.-K. Tung, New generation of parton distributions with uncertainties from global QCD analysis, J. High Energy Phys. 07 (2002) 012.

[39] R. Mackeprang, Stable heavy hadrons in ATLAS, Ph.D. thesis, University of Copenhagen, 2007.

[40] A. C. Kraan, Interactions of heavy stable hadronizing particles, Eur. Phys. J. C **37**, 91 (2004).

[41] J. Alwall, R. Frederix, S. Frixione, V. Hirschi, F. Maltoni, O. Mattelaer, H.-S. Shao, T. Stelzer, P. Torrielli, and M. Zaro, The automated computation of tree-level and next-to-leading order differential cross sections, and their matching to parton shower simulations, J. High Energy Phys. 07 (2014) 079.

[42] T. Sjöstrand, S. Mrenna, and P. Z. Skands, A brief introduction to PYTHIA 8.1, Comput. Phys. Commun. **178**, 852 (2008).

[43] D. J. Lange, The EvtGen particle decay simulation package, Nucl. Instrum. Methods Phys. Res., Sect. A **462**, 152 (2001).
[44] ATLAS Collaboration, ATLAS Run 1 Pythia8 tunes, Report No. ATL-PHYS-PUB-2014-021, 2014, https://cds.cern.ch/record/1966419.
[45] R. D. Ball *et al.*, Parton distributions with LHC data, Nucl. Phys. **B867**, 244 (2013).
[46] S. Alioli, P. Nason, C. Oleari, and E. Re, A general framework for implementing NLO calculations in shower Monte Carlo programs: The POWHEG BOX, J. High Energy Phys. 06 (2010) 043.
[47] ATLAS Collaboration, Measurement of the Z/γ^* boson transverse momentum distribution in pp collisions at $\sqrt{s} = 7$ TeV with the ATLAS detector, J. High Energy Phys. 09 (2014) 145.
[48] ATLAS Collaboration, The ATLAS simulation infrastructure, Eur. Phys. J. C **70**, 823 (2010).
[49] S. Agostinelli *et al.*, GEANT4: A simulation toolkit, Nucl. Instrum. Methods Phys. Res., Sect. A **506**, 250 (2003).
[50] R. Mackeprang and D. Milstead, An updated description of heavy-hadron interactions in GEANT-4, Eur. Phys. J. C **66**, 493 (2010).
[51] ATLAS Collaboration, Summary of ATLAS Pythia 8 tunes, Report No. ATL-PHYS-PUB-2012-003, 2012, https://cds.cern.ch/record/1474107.
[52] A. D. Martin, W. J. Stirling, R. S. Thorne, and G. Watt, Parton distributions for the LHC, Eur. Phys. J. C **63**, 189 (2009).
[53] A. Rosenfeld and J. L. Pfaltz, Sequential operations in digital picture processing, J. ACM **13**, 471 (1966).
[54] ATLAS Collaboration, A neural network clustering algorithm for the ATLAS silicon pixel detector, J. Instrum. **9**, P09009 (2014).
[55] ATLAS Collaboration, Performance of the ATLAS track reconstruction algorithms in dense environments in LHC Run 2, Eur. Phys. J. C **77**, 673 (2017).
[56] M. Cacciari, G. P. Salam, and G. Soyez, The anti-kt jet clustering algorithm, J. High Energy Phys. 04 (2008) 063.
[57] ATLAS Collaboration, Jet energy scale measurements and their systematic uncertainties in proton-proton collisions at $\sqrt{s} = 13$ TeV with the ATLAS detector, Phys. Rev. D **96**, 072002 (2017).
[58] W. Beenakker, R. Hopker, M. Spira, and P. Zerwas, Squark and gluino production at hadron colliders, Nucl. Phys. **B492**, 51 (1997).
[59] A. Kulesza and L. Motyka, Threshold Resummation for Squark-Antisquark and Gluino-Pair Production at the LHC, Phys. Rev. Lett. **102**, 111802 (2009).
[60] A. Kulesza and L. Motyka, Soft gluon resummation for the production of gluino-gluino and squark-antisquark pairs at the LHC, Phys. Rev. D **80**, 095004 (2009).
[61] W. Beenakker, S. Brensing, M. Kramer, A. Kulesza, E. Laenen, and I. Niessen, Soft-gluon resummation for squark and gluino hadroproduction, J. High Energy Phys. 12 (2009) 041.
[62] W. Beenakker, S. Brensing, M. Kramer, A. Kulesza, E. Laenen, L. Motyka, and I. Niessen, Squark and gluino hadroproduction, Int. J. Mod. Phys. A **26**, 2637 (2011).
[63] W. Beenakker, R. Hopker, and M. Spira, PROSPINO: A Program for the production of supersymmetric particles in next-to-leading order QCD, arXiv:hep-ph/9611232.
[64] C. Borschensky, M. Krämer, A. Kulesza, M. Mangano, S. Padhi, T. Plehn, and X. Portell, Squark and gluino production cross sections in pp collisions at $\sqrt{s} = 13$, 14, 33 and 100 TeV, Eur. Phys. J. C **74**, 3174 (2014).
[65] S. Catani, F. Krauss, B. R. Webber, and R. Kuhn, QCD matrix elements + parton showers, J. High Energy Phys. 11 (2001) 063.
[66] L. Lonnblad and S. Prestel, Matching tree-level matrix elements with interleaved showers, J. High Energy Phys. 03 (2012) 019.
[67] ATLAS Collaboration, Luminosity determination in pp collisions at $\sqrt{s} = 8$ TeV using the ATLAS detector at the LHC, Eur. Phys. J. C **76**, 653 (2016).
[68] A. L. Read, Presentation of search results: The CLs technique, J. Phys. G **28**, 2693 (2002).
[69] ATLAS Collaboration, ATLAS computing acknowledgements, Report No. ATL-GEN-PUB-2016-002, https://cds.cern.ch/record/2202407.

M. Aaboud,[34d] G. Aad,[99] B. Abbott,[125] D. C. Abbott,[100] O. Abdinov,[13,a] B. Abeloos,[129] D. K. Abhayasinghe,[91] S. H. Abidi,[164] O. S. AbouZeid,[39] N. L. Abraham,[153] H. Abramowicz,[158] H. Abreu,[157] Y. Abulaiti,[6] B. S. Acharya,[64a,64b,b] S. Adachi,[160] L. Adam,[97] L. Adamczyk,[81a] L. Adamek,[164] J. Adelman,[119] M. Adersberger,[112] A. Adiguzel,[12c,c] T. Adye,[141] A. A. Affolder,[143] Y. Afik,[157] C. Agheorghiesei,[27c] J. A. Aguilar-Saavedra,[137f,137a,d] F. Ahmadov,[77,e] G. Aielli,[71a,71b] S. Akatsuka,[83] T. P. A. Åkesson,[94] E. Akilli,[52] A. V. Akimov,[108] G. L. Alberghi,[23b,23a] J. Albert,[173] P. Albicocco,[49] M. J. Alconada Verzini,[86] S. Alderweireldt,[117] M. Aleksa,[35] I. N. Aleksandrov,[77] C. Alexa,[27b] D. Alexandre,[19] T. Alexopoulos,[10] M. Alhroob,[125] B. Ali,[139] G. Alimonti,[66a] J. Alison,[36] S. P. Alkire,[145] C. Allaire,[129] B. M. M. Allbrooke,[153] B. W. Allen,[128] P. P. Allport,[21] A. Aloisio,[67a,67b] A. Alonso,[39] F. Alonso,[86] C. Alpigiani,[145] A. A. Alshehri,[55] M. I. Alstaty,[99] B. Alvarez Gonzalez,[35] D. Álvarez Piqueras,[171] M. G. Alviggi,[67a,67b] B. T. Amadio,[18] Y. Amaral Coutinho,[78b] A. Ambler,[101] L. Ambroz,[132] C. Amelung,[26] D. Amidei,[103] S. P. Amor Dos Santos,[137a,137c] S. Amoroso,[44] C. S. Amrouche,[52] F. An,[76] C. Anastopoulos,[146] L. S. Ancu,[52] N. Andari,[142] T. Andeen,[11] C. F. Anders,[59b] J. K. Anders,[20] K. J. Anderson,[36] A. Andreazza,[66a,66b] V. Andrei,[59a] C. R. Anelli,[173] S. Angelidakis,[37] I. Angelozzi,[118] A. Angerami,[38] A. V. Anisenkov,[120b,120a] A. Annovi,[69a] C. Antel,[59a] M. T. Anthony,[146] M. Antonelli,[49] D. J. A. Antrim,[168] F. Anulli,[70a] M. Aoki,[79]

J. A. Aparisi Pozo,[171] L. Aperio Bella,[35] G. Arabidze,[104] J. P. Araque,[137a] V. Araujo Ferraz,[78b] R. Araujo Pereira,[78b] A. T. H. Arce,[47] R. E. Ardell,[91] F. A. Arduh,[86] J-F. Arguin,[107] S. Argyropoulos,[75] J.-H. Arling,[44] A. J. Armbruster,[35] L. J. Armitage,[90] A. Armstrong,[168] O. Arnaez,[164] H. Arnold,[118] M. Arratia,[31] O. Arslan,[24] A. Artamonov,[109,a] G. Artoni,[132] S. Artz,[97] S. Asai,[160] N. Asbah,[57] E. M. Asimakopoulou,[169] L. Asquith,[153] K. Assamagan,[29] R. Astalos,[28a] R. J. Atkin,[32a] M. Atkinson,[170] N. B. Atlay,[148] K. Augsten,[139] G. Avolio,[35] R. Avramidou,[58a] M. K. Ayoub,[15a] A. M. Azoulay,[165b] G. Azuelos,[107,f] A. E. Baas,[59a] M. J. Baca,[21] H. Bachacou,[142] K. Bachas,[65a,65b] M. Backes,[132] P. Bagnaia,[70a,70b] M. Bahmani,[82] H. Bahrasemani,[149] A. J. Bailey,[171] V. R. Bailey,[170] J. T. Baines,[141] M. Bajic,[39] C. Bakalis,[10] O. K. Baker,[180] P. J. Bakker,[118] D. Bakshi Gupta,[8] S. Balaji,[154] E. M. Baldin,[120b,120a] P. Balek,[177] F. Balli,[142] W. K. Balunas,[134] J. Balz,[97] E. Banas,[82] A. Bandyopadhyay,[24] S. Banerjee,[178,g] A. A. E. Bannoura,[179] L. Barak,[158] W. M. Barbe,[37] E. L. Barberio,[102] D. Barberis,[53b,53a] M. Barbero,[99] T. Barillari,[113] M-S. Barisits,[35] J. Barkeloo,[128] T. Barklow,[150] R. Barnea,[157] S. L. Barnes,[58c] B. M. Barnett,[141] R. M. Barnett,[18] Z. Barnovska-Blenessy,[58a] A. Baroncelli,[72a] G. Barone,[29] A. J. Barr,[132] L. Barranco Navarro,[171] F. Barreiro,[96] J. Barreiro Guimarães da Costa,[15a] R. Bartoldus,[150] A. E. Barton,[87] P. Bartos,[28a] A. Basalaev,[135] A. Bassalat,[129] R. L. Bates,[55] S. J. Batista,[164] S. Batlamous,[34e] J. R. Batley,[31] M. Battaglia,[143] M. Bauce,[70a,70b] F. Bauer,[142] K. T. Bauer,[168] H. S. Bawa,[150] J. B. Beacham,[123] T. Beau,[133] P. H. Beauchemin,[167] P. Bechtle,[24] H. C. Beck,[51] H. P. Beck,[20,h] K. Becker,[50] M. Becker,[97] C. Becot,[44] A. Beddall,[12d] A. J. Beddall,[12a] V. A. Bednyakov,[77] M. Bedognetti,[118] C. P. Bee,[152] T. A. Beermann,[74] M. Begalli,[78b] M. Begel,[29] A. Behera,[152] J. K. Behr,[44] F. Beisiegel,[24] A. S. Bell,[92] G. Bella,[158] L. Bellagamba,[23b] A. Bellerive,[33] M. Bellomo,[157] P. Bellos,[9] K. Belotskiy,[110] N. L. Belyaev,[110] O. Benary,[158,a] D. Benchekroun,[34a] M. Bender,[112] N. Benekos,[10] Y. Benhammou,[158] E. Benhar Noccioli,[180] J. Benitez,[75] D. P. Benjamin,[6] M. Benoit,[52] J. R. Bensinger,[26] S. Bentvelsen,[118] L. Beresford,[132] M. Beretta,[49] D. Berge,[44] E. Bergeaas Kuutmann,[169] N. Berger,[5] B. Bergmann,[139] L. J. Bergsten,[26] J. Beringer,[18] S. Berlendis,[7] N. R. Bernard,[100] G. Bernardi,[133] C. Bernius,[150] F. U. Bernlochner,[24] T. Berry,[91] P. Berta,[97] C. Bertella,[15a] G. Bertoli,[43a,43b] I. A. Bertram,[87] G. J. Besjes,[39] O. Bessidskaia Bylund,[179] M. Bessner,[44] N. Besson,[142] A. Bethani,[98] S. Bethke,[113] A. Betti,[24] A. J. Bevan,[90] J. Beyer,[113] R. Bi,[136] R. M. Bianchi,[136] O. Biebel,[112] D. Biedermann,[19] R. Bielski,[35] K. Bierwagen,[97] N. V. Biesuz,[69a,69b] M. Biglietti,[72a] T. R. V. Billoud,[107] M. Bindi,[51] A. Bingul,[12d] C. Bini,[70a,70b] S. Biondi,[23b,23a] M. Birman,[177] T. Bisanz,[51] J. P. Biswal,[158] C. Bittrich,[46] D. M. Bjergaard,[47] J. E. Black,[150] K. M. Black,[25] T. Blazek,[28a] I. Bloch,[44] C. Blocker,[26] A. Blue,[55] U. Blumenschein,[90] S. Blunier,[144a] G. J. Bobbink,[118] V. S. Bobrovnikov,[120b,120a] S. S. Bocchetta,[94] A. Bocci,[47] D. Boerner,[179] D. Bogavac,[112] A. G. Bogdanchikov,[120b,120a] C. Bohm,[43a] V. Boisvert,[91] P. Bokan,[51,169] T. Bold,[81a] A. S. Boldyrev,[111] A. E. Bolz,[59b] M. Bomben,[133] M. Bona,[90] J. S. Bonilla,[128] M. Boonekamp,[142] H. M. Borecka-Bielska,[88] A. Borisov,[121] G. Borissov,[87] J. Bortfeldt,[35] D. Bortoletto,[132] V. Bortolotto,[71a,71b] D. Boscherini,[23b] M. Bosman,[14] J. D. Bossio Sola,[30] K. Bouaouda,[34a] J. Boudreau,[136] E. V. Bouhova-Thacker,[87] D. Boumediene,[37] C. Bourdarios,[129] S. K. Boutle,[55] A. Boveia,[123] J. Boyd,[35] D. Boye,[32b,i] I. R. Boyko,[77] A. J. Bozson,[91] J. Bracinik,[21] N. Brahimi,[99] A. Brandt,[8] G. Brandt,[179] O. Brandt,[59a] F. Braren,[44] U. Bratzler,[161] B. Brau,[100] J. E. Brau,[128] W. D. Breaden Madden,[55] K. Brendlinger,[44] L. Brenner,[44] R. Brenner,[169] S. Bressler,[177] B. Brickwedde,[97] D. L. Briglin,[21] D. Britton,[55] D. Britzger,[113] I. Brock,[24] R. Brock,[104] G. Brooijmans,[38] T. Brooks,[91] W. K. Brooks,[144b] E. Brost,[119] J. H Broughton,[21] P. A. Bruckman de Renstrom,[82] D. Bruncko,[28b] A. Bruni,[23b] G. Bruni,[23b] L. S. Bruni,[118] S. Bruno,[71a,71b] B. H. Brunt,[31] M. Bruschi,[23b] N. Bruscino,[136] P. Bryant,[36] L. Bryngemark,[94] T. Buanes,[17] Q. Buat,[35] P. Buchholz,[148] A. G. Buckley,[55] I. A. Budagov,[77] M. K. Bugge,[131] F. Bührer,[50] O. Bulekov,[110] D. Bullock,[8] T. J. Burch,[119] S. Burdin,[88] C. D. Burgard,[118] A. M. Burger,[5] B. Burghgrave,[8] K. Burka,[82] S. Burke,[141] I. Burmeister,[45] J. T. P. Burr,[132] V. Büscher,[97] E. Buschmann,[51] P. Bussey,[55] J. M. Butler,[25] C. M. Buttar,[55] J. M. Butterworth,[92] P. Butti,[35] W. Buttinger,[35] A. Buzatu,[155] A. R. Buzykaev,[120b,120a] G. Cabras,[23b,23a] S. Cabrera Urbán,[171] D. Caforio,[139] H. Cai,[170] V. M. M. Cairo,[2] O. Cakir,[4a] N. Calace,[35] P. Calafiura,[18] A. Calandri,[99] G. Calderini,[133] P. Calfayan,[63] G. Callea,[55] L. P. Caloba,[78b] S. Calvente Lopez,[96] D. Calvet,[37] S. Calvet,[37] T. P. Calvet,[152] M. Calvetti,[69a,69b] R. Camacho Toro,[133] S. Camarda,[35] D. Camarero Munoz,[96] P. Camarri,[71a,71b] D. Cameron,[131] R. Caminal Armadans,[100] C. Camincher,[35] S. Campana,[35] M. Campanelli,[92] A. Camplani,[39] A. Campoverde,[148] V. Canale,[67a,67b] M. Cano Bret,[58c] J. Cantero,[126] T. Cao,[158] Y. Cao,[170] M. D. M. Capeans Garrido,[35] I. Caprini,[27b] M. Caprini,[27b] M. Capua,[40b,40a] R. M. Carbone,[38] R. Cardarelli,[71a] F. C. Cardillo,[146] I. Carli,[140] T. Carli,[35] G. Carlino,[67a] B. T. Carlson,[136] L. Carminati,[66a,66b] R. M. D. Carney,[43a,43b] S. Caron,[117] E. Carquin,[144b] S. Carrá,[66a,66b] J. W. S. Carter,[164] D. Casadei,[32b] M. P. Casado,[14,j] A. F. Casha,[164] D. W. Casper,[168] R. Castelijn,[118] F. L. Castillo,[171] V. Castillo Gimenez,[171] N. F. Castro,[137a,137e] A. Catinaccio,[35] J. R. Catmore,[131] A. Cattai,[35] J. Caudron,[24] V. Cavaliere,[29] E. Cavallaro,[14] D. Cavalli,[66a] M. Cavalli-Sforza,[14] V. Cavasinni,[69a,69b] E. Celebi,[12b] F. Ceradini,[72a,72b] L. Cerda Alberich,[171] A. S. Cerqueira,[78a] A. Cerri,[153]

L. Cerrito,[71a,71b] F. Cerutti,[18] A. Cervelli,[23b,23a] S. A. Cetin,[12b] A. Chafaq,[34a] D. Chakraborty,[119] S. K. Chan,[57] W. S. Chan,[118] W. Y. Chan,[88] J. D. Chapman,[31] B. Chargeishvili,[156b] D. G. Charlton,[21] C. C. Chau,[33] C. A. Chavez Barajas,[153] S. Che,[123] A. Chegwidden,[104] S. Chekanov,[6] S. V. Chekulaev,[165a] G. A. Chelkov,[77,k] M. A. Chelstowska,[35] B. Chen,[76] C. Chen,[58a] C. H. Chen,[76] H. Chen,[29] J. Chen,[58a] J. Chen,[38] S. Chen,[134] S. J. Chen,[15c] X. Chen,[15b,l] Y. Chen,[80] Y-H. Chen,[44] H. C. Cheng,[61a] H. J. Cheng,[15d] A. Cheplakov,[77] E. Cheremushkina,[121] R. Cherkaoui El Moursli,[34e] E. Cheu,[7] K. Cheung,[62] T. J. A. Chevalérias,[142] L. Chevalier,[142] V. Chiarella,[49] G. Chiarelli,[69a] G. Chiodini,[65a] A. S. Chisholm,[35,21] A. Chitan,[27b] I. Chiu,[160] Y. H. Chiu,[173] M. V. Chizhov,[77] K. Choi,[63] A. R. Chomont,[129] S. Chouridou,[159] Y. S. Chow,[118] V. Christodoulou,[92] M. C. Chu,[61a] J. Chudoba,[138] A. J. Chuinard,[101] J. J. Chwastowski,[82] L. Chytka,[127] D. Cinca,[45] V. Cindro,[89] I. A. Cioară,[24] A. Ciocio,[18] F. Cirotto,[67a,67b] Z. H. Citron,[177] M. Citterio,[66a] A. Clark,[52] M. R. Clark,[38] P. J. Clark,[48] C. Clement,[43a,43b] Y. Coadou,[99] M. Cobal,[64a,64c] A. Coccaro,[53b] J. Cochran,[76] H. Cohen,[158] A. E. C. Coimbra,[177] L. Colasurdo,[117] B. Cole,[38] A. P. Colijn,[118] J. Collot,[56] P. Conde Muiño,[137a,m] E. Coniavitis,[50] S. H. Connell,[32b] I. A. Connelly,[98] S. Constantinescu,[27b] F. Conventi,[67a,n] A. M. Cooper-Sarkar,[132] F. Cormier,[172] K. J. R. Cormier,[164] L. D. Corpe,[92] M. Corradi,[70a,70b] E. E. Corrigan,[94] F. Corriveau,[101,o] A. Cortes-Gonzalez,[35] M. J. Costa,[171] F. Costanza,[5] D. Costanzo,[146] G. Cottin,[31] G. Cowan,[91] J. W. Cowley,[31] B. E. Cox,[98] J. Crane,[98] K. Cranmer,[122] S. J. Crawley,[55] R. A. Creager,[134] G. Cree,[33] S. Crépé-Renaudin,[56] F. Crescioli,[133] M. Cristinziani,[24] V. Croft,[122] G. Crosetti,[40b,40a] A. Cueto,[96] T. Cuhadar Donszelmann,[146] A. R. Cukierman,[150] S. Czekierda,[82] P. Czodrowski,[35] M. J. Da Cunha Sargedas De Sousa,[58b] C. Da Via,[98] W. Dabrowski,[81a] T. Dado,[28a,p] S. Dahbi,[34e] T. Dai,[103] F. Dallaire,[107] C. Dallapiccola,[100] M. Dam,[39] G. D'amen,[23b,23a] J. Damp,[97] J. R. Dandoy,[134] M. F. Daneri,[30] N. P. Dang,[178,g] N. D Dann,[98] M. Danninger,[172] V. Dao,[35] G. Darbo,[53b] S. Darmora,[8] O. Dartsi,[5] A. Dattagupta,[128] T. Daubney,[44] S. D'Auria,[66a,66b] W. Davey,[24] C. David,[44] T. Davidek,[140] D. R. Davis,[47] E. Dawe,[102] I. Dawson,[146] K. De,[8] R. De Asmundis,[67a] A. De Benedetti,[125] M. De Beurs,[118] S. De Castro,[23b,23a] S. De Cecco,[70a,70b] N. De Groot,[117] P. de Jong,[118] H. De la Torre,[104] F. De Lorenzi,[76] A. De Maria,[69a,69b] D. De Pedis,[70a] A. De Salvo,[70a] U. De Sanctis,[71a,71b] M. De Santis,[71a,71b] A. De Santo,[153] K. De Vasconcelos Corga,[99] J. B. De Vivie De Regie,[129] C. Debenedetti,[143] D. V. Dedovich,[77] N. Dehghanian,[3] M. Del Gaudio,[40b,40a] J. Del Peso,[96] Y. Delabat Diaz,[44] D. Delgove,[129] F. Deliot,[142] C. M. Delitzsch,[7] M. Della Pietra,[67a,67b] D. Della Volpe,[52] A. Dell'Acqua,[35] L. Dell'Asta,[25] M. Delmastro,[5] C. Delporte,[129] P. A. Delsart,[56] D. A. DeMarco,[164] S. Demers,[180] M. Demichev,[77] S. P. Denisov,[121] D. Denysiuk,[118] L. D'Eramo,[133] D. Derendarz,[82] J. E. Derkaoui,[34d] F. Derue,[133] P. Dervan,[88] K. Desch,[24] C. Deterre,[44] K. Dette,[164] M. R. Devesa,[30] P. O. Deviveiros,[35] A. Dewhurst,[141] S. Dhaliwal,[26] F. A. Di Bello,[52] A. Di Ciaccio,[71a,71b] L. Di Ciaccio,[5] W. K. Di Clemente,[134] C. Di Donato,[67a,67b] A. Di Girolamo,[35] G. Di Gregorio,[69a,69b] B. Di Micco,[72a,72b] R. Di Nardo,[100] K. F. Di Petrillo,[57] R. Di Sipio,[164] D. Di Valentino,[33] C. Diaconu,[99] M. Diamond,[164] F. A. Dias,[39] T. Dias Do Vale,[137a] M. A. Diaz,[144a] J. Dickinson,[18] E. B. Diehl,[103] J. Dietrich,[19] S. Díez Cornell,[44] A. Dimitrievska,[18] J. Dingfelder,[24] F. Dittus,[35] F. Djama,[99] T. Djobava,[156b] J. I. Djuvsland,[17] M. A. B. Do Vale,[78c] M. Dobre,[27b] D. Dodsworth,[26] C. Doglioni,[94] J. Dolejsi,[140] Z. Dolezal,[140] M. Donadelli,[78d] J. Donini,[37] A. D'onofrio,[90] M. D'Onofrio,[88] J. Dopke,[141] A. Doria,[67a] M. T. Dova,[86] A. T. Doyle,[55] E. Drechsler,[149] E. Dreyer,[149] T. Dreyer,[51] Y. Du,[58b] F. Dubinin,[108] M. Dubovsky,[28a] A. Dubreuil,[52] E. Duchovni,[177] G. Duckeck,[112] A. Ducourthial,[133] O. A. Ducu,[107,q] D. Duda,[113] A. Dudarev,[35] A. C. Dudder,[97] E. M. Duffield,[18] L. Duflot,[129] M. Dührssen,[35] C. Dülsen,[179] M. Dumancic,[177] A. E. Dumitriu,[27b,r] A. K. Duncan,[55] M. Dunford,[59a] A. Duperrin,[99] H. Duran Yildiz,[4a] M. Düren,[54] A. Durglishvili,[156b] D. Duschinger,[46] B. Dutta,[44] D. Duvnjak,[1] G. Dyckes,[134] M. Dyndal,[44] S. Dysch,[98] B. S. Dziedzic,[82] K. M. Ecker,[113] R. C. Edgar,[103] T. Eifert,[35] G. Eigen,[17] K. Einsweiler,[18] T. Ekelof,[169] M. El Kacimi,[34c] R. El Kosseifi,[99] V. Ellajosyula,[99] M. Ellert,[169] F. Ellinghaus,[179] A. A. Elliot,[90] N. Ellis,[35] J. Elmsheuser,[29] M. Elsing,[35] D. Emeliyanov,[141] A. Emerman,[38] Y. Enari,[160] J. S. Ennis,[175] M. B. Epland,[47] J. Erdmann,[45] A. Ereditato,[20] S. Errede,[170] M. Escalier,[129] C. Escobar,[171] O. Estrada Pastor,[171] A. I. Etienvre,[142] E. Etzion,[158] H. Evans,[63] A. Ezhilov,[135] M. Ezzi,[34e] F. Fabbri,[55] L. Fabbri,[23b,23a] V. Fabiani,[117] G. Facini,[92] R. M. Faisca Rodrigues Pereira,[137a] R. M. Fakhrutdinov,[121] S. Falciano,[70a] P. J. Falke,[5] S. Falke,[5] J. Faltova,[140] Y. Fang,[15a] M. Fanti,[66a,66b] A. Farbin,[8] A. Farilla,[72a] E. M. Farina,[68a,68b] T. Farooque,[104] S. Farrell,[18] S. M. Farrington,[175] P. Farthouat,[35] F. Fassi,[34e] P. Fassnacht,[35] D. Fassouliotis,[9] M. Faucci Giannelli,[48] W. J. Fawcett,[31] L. Fayard,[129] O. L. Fedin,[135,s] W. Fedorko,[172] M. Feickert,[41] S. Feigl,[131] L. Feligioni,[99] C. Feng,[58b] E. J. Feng,[35] M. Feng,[47] M. J. Fenton,[55] A. B. Fenyuk,[121] J. Ferrando,[44] A. Ferrari,[169] P. Ferrari,[118] R. Ferrari,[68a] D. E. Ferreira de Lima,[59b] A. Ferrer,[171] D. Ferrere,[52] C. Ferretti,[103] F. Fiedler,[97] A. Filipčič,[89] F. Filthaut,[117] K. D. Finelli,[25] M. C. N. Fiolhais,[137a,137c,t] L. Fiorini,[171] C. Fischer,[14] W. C. Fisher,[104] N. Flaschel,[44] I. Fleck,[148] P. Fleischmann,[103] R. R. M. Fletcher,[134] T. Flick,[179] B. M. Flierl,[112] L. M. Flores,[134] L. R. Flores Castillo,[61a]

F. M. Follega,[73a,73b] N. Fomin,[17] G. T. Forcolin,[73a,73b] A. Formica,[142] F. A. Förster,[14] A. C. Forti,[98] A. G. Foster,[21] D. Fournier,[129] H. Fox,[87] S. Fracchia,[146] P. Francavilla,[69a,69b] M. Franchini,[23b,23a] S. Franchino,[59a] D. Francis,[35] L. Franconi,[143] M. Franklin,[57] M. Frate,[168] A. N. Fray,[90] D. Freeborn,[92] B. Freund,[107] W. S. Freund,[78b] E. M. Freundlich,[45] D. C. Frizzell,[125] D. Froidevaux,[35] J. A. Frost,[132] C. Fukunaga,[161] E. Fullana Torregrosa,[171] E. Fumagalli,[53b,53a] T. Fusayasu,[114] J. Fuster,[171] O. Gabizon,[157] A. Gabrielli,[23b,23a] A. Gabrielli,[18] G. P. Gach,[81a] S. Gadatsch,[52] P. Gadow,[113] G. Gagliardi,[53b,53a] L. G. Gagnon,[107] C. Galea,[27b] B. Galhardo,[137a,137c] E. J. Gallas,[132] B. J. Gallop,[141] P. Gallus,[139] G. Galster,[39] R. Gamboa Goni,[90] K. K. Gan,[123] S. Ganguly,[177] J. Gao,[58a] Y. Gao,[88] Y. S. Gao,[150,u] C. García,[171] J. E. García Navarro,[171] J. A. García Pascual,[15a] C. Garcia-Argos,[50] M. Garcia-Sciveres,[18] R. W. Gardner,[36] N. Garelli,[150] S. Gargiulo,[50] V. Garonne,[131] K. Gasnikova,[44] A. Gaudiello,[53b,53a] G. Gaudio,[68a] I. L. Gavrilenko,[108] A. Gavrilyuk,[109] C. Gay,[172] G. Gaycken,[24] E. N. Gazis,[10] C. N. P. Gee,[141] J. Geisen,[51] M. Geisen,[97] M. P. Geisler,[59a] C. Gemme,[53b] M. H. Genest,[56] C. Geng,[103] S. Gentile,[70a,70b] S. George,[91] D. Gerbaudo,[14] G. Gessner,[45] S. Ghasemi,[148] M. Ghasemi Bostanabad,[173] M. Ghneimat,[24] B. Giacobbe,[23b] S. Giagu,[70a,70b] N. Giangiacomi,[23b,23a] P. Giannetti,[69a] A. Giannini,[67a,67b] S. M. Gibson,[91] M. Gignac,[143] D. Gillberg,[33] G. Gilles,[179] D. M. Gingrich,[3,f] M. P. Giordani,[64a,64c] F. M. Giorgi,[23b] P. F. Giraud,[142] P. Giromini,[57] G. Giugliarelli,[64a,64c] D. Giugni,[66a] F. Giuli,[132] M. Giulini,[59b] S. Gkaitatzis,[159] I. Gkialas,[9,v] E. L. Gkougkousis,[14] P. Gkountoumis,[10] L. K. Gladilin,[111] C. Glasman,[96] J. Glatzer,[14] P. C. F. Glaysher,[44] A. Glazov,[44] M. Goblirsch-Kolb,[26] J. Godlewski,[82] S. Goldfarb,[102] T. Golling,[52] D. Golubkov,[121] A. Gomes,[137a,137b] R. Goncalves Gama,[51] R. Gonçalo,[137a] G. Gonella,[50] L. Gonella,[21] A. Gongadze,[77] F. Gonnella,[21] J. L. Gonski,[57] S. González de la Hoz,[171] S. Gonzalez-Sevilla,[52] L. Goossens,[35] P. A. Gorbounov,[109] H. A. Gordon,[29] B. Gorini,[35] E. Gorini,[65a,65b] A. Gorišek,[89] A. T. Goshaw,[47] C. Gössling,[45] M. I. Gostkin,[77] C. A. Gottardo,[24] C. R. Goudet,[129] D. Goujdami,[34c] A. G. Goussiou,[145] N. Govender,[32b,w] C. Goy,[5] E. Gozani,[157] I. Grabowska-Bold,[81a] P. O. J. Gradin,[169] E. C. Graham,[88] J. Gramling,[168] E. Gramstad,[131] S. Grancagnolo,[19] V. Gratchev,[135] P. M. Gravila,[27f] F. G. Gravili,[65a,65b] C. Gray,[55] H. M. Gray,[18] Z. D. Greenwood,[93,x] C. Grefe,[24] K. Gregersen,[94] I. M. Gregor,[44] P. Grenier,[150] K. Grevtsov,[44] N. A. Grieser,[125] J. Griffiths,[8] A. A. Grillo,[143] K. Grimm,[150,y] S. Grinstein,[14,z] Ph. Gris,[37] J.-F. Grivaz,[129] S. Groh,[97] E. Gross,[177] J. Grosse-Knetter,[51] G. C. Grossi,[93] Z. J. Grout,[92] C. Grud,[103] A. Grummer,[116] L. Guan,[103] W. Guan,[178] J. Guenther,[35] A. Guerguichon,[129] F. Guescini,[165a] D. Guest,[168] R. Gugel,[50] B. Gui,[123] T. Guillemin,[5] S. Guindon,[35] U. Gul,[55] J. Guo,[58c] W. Guo,[103] Y. Guo,[58a,aa] Z. Guo,[99] R. Gupta,[44] S. Gurbuz,[12c] G. Gustavino,[125] P. Gutierrez,[125] C. Gutschow,[92] C. Guyot,[142] M. P. Guzik,[81a] C. Gwenlan,[132] C. B. Gwilliam,[88] A. Haas,[122] C. Haber,[18] H. K. Hadavand,[8] N. Haddad,[34e] A. Hadef,[58a] S. Hageböck,[24] M. Hagihara,[166] M. Haleem,[174] J. Haley,[126] G. Halladjian,[104] G. D. Hallewell,[99] K. Hamacher,[179] P. Hamal,[127] K. Hamano,[173] A. Hamilton,[32a] G. N. Hamity,[146] K. Han,[58a,bb] L. Han,[58a] S. Han,[15d] K. Hanagaki,[79,cc] M. Hance,[143] D. M. Handl,[112] B. Haney,[134] R. Hankache,[133] P. Hanke,[59a] E. Hansen,[94] J. B. Hansen,[39] J. D. Hansen,[39] M. C. Hansen,[24] P. H. Hansen,[39] E. C. Hanson,[98] K. Hara,[166] A. S. Hard,[178] T. Harenberg,[179] S. Harkusha,[105] P. F. Harrison,[175] N. M. Hartmann,[112] Y. Hasegawa,[147] A. Hasib,[48] S. Hassani,[142] S. Haug,[20] R. Hauser,[104] L. Hauswald,[46] L. B. Havener,[38] M. Havranek,[139] C. M. Hawkes,[21] R. J. Hawkings,[35] D. Hayden,[104] C. Hayes,[152] C. P. Hays,[132] J. M. Hays,[90] H. S. Hayward,[88] S. J. Haywood,[141] F. He,[58a] M. P. Heath,[48] V. Hedberg,[94] L. Heelan,[8] S. Heer,[24] K. K. Heidegger,[50] J. Heilman,[33] S. Heim,[44] T. Heim,[18] B. Heinemann,[44,dd] J. J. Heinrich,[112] L. Heinrich,[122] C. Heinz,[54] J. Hejbal,[138] L. Helary,[35] A. Held,[172] S. Hellesund,[131] C. M. Helling,[143] S. Hellman,[43a,43b] C. Helsens,[35] R. C. W. Henderson,[87] Y. Heng,[178] S. Henkelmann,[172] A. M. Henriques Correia,[35] G. H. Herbert,[19] H. Herde,[26] V. Herget,[174] Y. Hernández Jiménez,[32c] H. Herr,[97] M. G. Herrmann,[112] T. Herrmann,[46] G. Herten,[50] R. Hertenberger,[112] L. Hervas,[35] T. C. Herwig,[134] G. G. Hesketh,[92] N. P. Hessey,[165a] A. Higashida,[160] S. Higashino,[79] E. Higón-Rodriguez,[171] K. Hildebrand,[36] E. Hill,[173] J. C. Hill,[31] K. K. Hill,[29] K. H. Hiller,[44] S. J. Hillier,[21] M. Hils,[46] I. Hinchliffe,[18] F. Hinterkeuser,[24] M. Hirose,[130] D. Hirschbuehl,[179] B. Hiti,[89] O. Hladik,[138] D. R. Hlaluku,[32c] X. Hoad,[48] J. Hobbs,[152] N. Hod,[165a] M. C. Hodgkinson,[146] A. Hoecker,[35] M. R. Hoeferkamp,[116] F. Hoenig,[112] D. Hohn,[50] D. Hohov,[129] T. R. Holmes,[36] M. Holzbock,[112] M. Homann,[45] B. H. Hommels,[31] S. Honda,[166] T. Honda,[79] T. M. Hong,[136] A. Hönle,[113] B. H. Hooberman,[170] W. H. Hopkins,[128] Y. Horii,[115] P. Horn,[46] A. J. Horton,[149] L. A. Horyn,[36] J-Y. Hostachy,[56] A. Hostiuc,[145] S. Hou,[155] A. Hoummada,[34a] J. Howarth,[98] J. Hoya,[86] M. Hrabovsky,[127] J. Hrdinka,[35] I. Hristova,[19] J. Hrivnac,[129] A. Hrynevich,[106] T. Hryn'ova,[5] P. J. Hsu,[62] S.-C. Hsu,[145] Q. Hu,[29] S. Hu,[58c] Y. Huang,[15a] Z. Hubacek,[139] F. Hubaut,[99] M. Huebner,[24] F. Huegging,[24] T. B. Huffman,[132] M. Huhtinen,[35] R. F. H. Hunter,[33] P. Huo,[152] A. M. Hupe,[33] N. Huseynov,[77,e] J. Huston,[104] J. Huth,[57] R. Hyneman,[103] G. Iacobucci,[52] G. Iakovidis,[29] I. Ibragimov,[148] L. Iconomidou-Fayard,[129] Z. Idrissi,[34e] P. Iengo,[35] R. Ignazzi,[39] O. Igonkina,[118,ee] R. Iguchi,[160] T. Iizawa,[52] Y. Ikegami,[79]

M. Ikeno,[79] D. Iliadis,[159] N. Ilic,[117] F. Iltzsche,[46] G. Introzzi,[68a,68b] M. Iodice,[72a] K. Iordanidou,[38] V. Ippolito,[70a,70b] M. F. Isacson,[169] N. Ishijima,[130] M. Ishino,[160] M. Ishitsuka,[162] W. Islam,[126] C. Issever,[132] S. Istin,[157] F. Ito,[166] J. M. Iturbe Ponce,[61a] R. Iuppa,[73a,73b] A. Ivina,[177] H. Iwasaki,[79] J. M. Izen,[42] V. Izzo,[67a] P. Jacka,[138] P. Jackson,[1] R. M. Jacobs,[24] V. Jain,[2] G. Jäkel,[179] K. B. Jakobi,[97] K. Jakobs,[50] S. Jakobsen,[74] T. Jakoubek,[138] D. O. Jamin,[126] R. Jansky,[52] J. Janssen,[24] M. Janus,[51] P. A. Janus,[81a] G. Jarlskog,[94] N. Javadov,[77,e] T. Javůrek,[35] M. Javurkova,[50] F. Jeanneau,[142] L. Jeanty,[18] J. Jejelava,[156a,ff] A. Jelinskas,[175] P. Jenni,[50,gg] J. Jeong,[44] N. Jeong,[44] S. Jézéquel,[5] H. Ji,[178] J. Jia,[152] H. Jiang,[76] Y. Jiang,[58a] Z. Jiang,[150,hh] S. Jiggins,[50] F. A. Jimenez Morales,[37] J. Jimenez Pena,[171] S. Jin,[15c] A. Jinaru,[27b] O. Jinnouchi,[162] H. Jivan,[32c] P. Johansson,[146] K. A. Johns,[7] C. A. Johnson,[63] K. Jon-And,[43a,43b] R. W. L. Jones,[87] S. D. Jones,[153] S. Jones,[7] T. J. Jones,[88] J. Jongmanns,[59a] P. M. Jorge,[137a,137b] J. Jovicevic,[165a] X. Ju,[18] J. J. Junggeburth,[113] A. Juste Rozas,[14,z] A. Kaczmarska,[82] M. Kado,[129] H. Kagan,[123] M. Kagan,[150] T. Kaji,[176] E. Kajomovitz,[157] C. W. Kalderon,[94] A. Kaluza,[97] S. Kama,[41] A. Kamenshchikov,[121] L. Kanjir,[89] Y. Kano,[160] V. A. Kantserov,[110] J. Kanzaki,[79] L. S. Kaplan,[178] D. Kar,[32c] M. J. Kareem,[165b] E. Karentzos,[10] S. N. Karpov,[77] Z. M. Karpova,[77] V. Kartvelishvili,[87] A. N. Karyukhin,[121] L. Kashif,[178] R. D. Kass,[123] A. Kastanas,[43a,43b] Y. Kataoka,[160] C. Kato,[58d,58c] J. Katzy,[44] K. Kawade,[80] K. Kawagoe,[85] T. Kawaguchi,[115] T. Kawamoto,[160] G. Kawamura,[51] E. F. Kay,[88] V. F. Kazanin,[120b,120a] R. Keeler,[173] R. Kehoe,[41] J. S. Keller,[33] E. Kellermann,[94] J. J. Kempster,[21] J. Kendrick,[21] O. Kepka,[138] S. Kersten,[179] B. P. Kerševan,[89] S. Ketabchi Haghighat,[164] R. A. Keyes,[101] M. Khader,[170] F. Khalil-Zada,[13] A. Khanov,[126] A. G. Kharlamov,[120b,120a] T. Kharlamova,[120b,120a] E. E. Khoda,[172] A. Khodinov,[163] T. J. Khoo,[52] E. Khramov,[77] J. Khubua,[156b] S. Kido,[80] M. Kiehn,[52] C. R. Kilby,[91] Y. K. Kim,[36] N. Kimura,[64a,64c] O. M. Kind,[19] B. T. King,[88] D. Kirchmeier,[46] J. Kirk,[141] A. E. Kiryunin,[113] T. Kishimoto,[160] D. Kisielewska,[81a] V. Kitali,[44] O. Kivernyk,[5] E. Kladiva,[28b,a] T. Klapdor-Kleingrothaus,[50] M. H. Klein,[103] M. Klein,[88] U. Klein,[88] K. Kleinknecht,[97] P. Klimek,[119] A. Klimentov,[29] T. Klingl,[24] T. Klioutchnikova,[35] F. F. Klitzner,[112] P. Kluit,[118] S. Kluth,[113] E. Kneringer,[74] E. B. F. G. Knoops,[99] A. Knue,[50] A. Kobayashi,[160] D. Kobayashi,[85] T. Kobayashi,[160] M. Kobel,[46] M. Kocian,[150] P. Kodys,[140] P. T. Koenig,[24] T. Koffas,[33] E. Koffeman,[118] N. M. Köhler,[113] T. Koi,[150] M. Kolb,[59b] I. Koletsou,[5] T. Kondo,[79] N. Kondrashova,[58c] K. Köneke,[50] A. C. König,[117] T. Kono,[79] R. Konoplich,[122,ii] V. Konstantinides,[92] N. Konstantinidis,[92] B. Konya,[94] R. Kopeliansky,[63] S. Koperny,[81a] K. Korcyl,[82] K. Kordas,[159] G. Koren,[158] A. Korn,[92] I. Korolkov,[14] E. V. Korolkova,[146] N. Korotkova,[111] O. Kortner,[113] S. Kortner,[113] T. Kosek,[140] V. V. Kostyukhin,[24] A. Kotwal,[47] A. Koulouris,[10] A. Kourkoumeli-Charalampidi,[68a,68b] C. Kourkoumelis,[9] E. Kourlitis,[146] V. Kouskoura,[29] A. B. Kowalewska,[82] R. Kowalewski,[173] T. Z. Kowalski,[81a] C. Kozakai,[160] W. Kozanecki,[142] A. S. Kozhin,[121] V. A. Kramarenko,[111] G. Kramberger,[89] D. Krasnopevtsev,[58a] M. W. Krasny,[133] A. Krasznahorkay,[35] D. Krauss,[113] J. A. Kremer,[81a] J. Kretzschmar,[88] P. Krieger,[164] K. Krizka,[18] K. Kroeninger,[45] H. Kroha,[113] J. Kroll,[138] J. Kroll,[134] J. Krstic,[16] U. Kruchonak,[77] H. Krüger,[24] N. Krumnack,[76] M. C. Kruse,[47] T. Kubota,[102] S. Kuday,[4b] J. T. Kuechler,[179] S. Kuehn,[35] A. Kugel,[59a] T. Kuhl,[44] V. Kukhtin,[77] R. Kukla,[99] Y. Kulchitsky,[105,jj] S. Kuleshov,[144b] Y. P. Kulinich,[170] M. Kuna,[56] T. Kunigo,[83] A. Kupco,[138] T. Kupfer,[45] O. Kuprash,[158] H. Kurashige,[80] L. L. Kurchaninov,[165a] Y. A. Kurochkin,[105] A. Kurova,[110] M. G. Kurth,[15d] E. S. Kuwertz,[35] M. Kuze,[162] J. Kvita,[127] T. Kwan,[101] A. La Rosa,[113] J. L. La Rosa Navarro,[78d] L. La Rotonda,[40b,40a] F. La Ruffa,[40b,40a] C. Lacasta,[171] F. Lacava,[70a,70b] J. Lacey,[44] D. P. J. Lack,[98] H. Lacker,[19] D. Lacour,[133] E. Ladygin,[77] R. Lafaye,[5] B. Laforge,[133] T. Lagouri,[32c] S. Lai,[51] S. Lammers,[63] W. Lampl,[7] E. Lançon,[29] U. Landgraf,[50] M. P. J. Landon,[90] M. C. Lanfermann,[52] V. S. Lang,[44] J. C. Lange,[51] R. J. Langenberg,[35] A. J. Lankford,[168] F. Lanni,[29] K. Lantzsch,[24] A. Lanza,[68a] A. Lapertosa,[53b,53a] S. Laplace,[133] J. F. Laporte,[142] T. Lari,[66a] F. Lasagni Manghi,[23b,23a] M. Lassnig,[35] T. S. Lau,[61a] A. Laudrain,[129] M. Lavorgna,[67a,67b] M. Lazzaroni,[66a,66b] B. Le,[102] O. Le Dortz,[133] E. Le Guirriec,[99] E. P. Le Quilleuc,[142] M. LeBlanc,[7] T. LeCompte,[6] F. Ledroit-Guillon,[56] C. A. Lee,[29] G. R. Lee,[144a] L. Lee,[57] S. C. Lee,[155] B. Lefebvre,[101] M. Lefebvre,[173] F. Legger,[112] C. Leggett,[18] K. Lehmann,[149] N. Lehmann,[179] G. Lehmann Miotto,[35] W. A. Leight,[44] A. Leisos,[159,kk] M. A. L. Leite,[78d] R. Leitner,[140] D. Lellouch,[177] K. J. C. Leney,[92] T. Lenz,[24] B. Lenzi,[35] R. Leone,[7] S. Leone,[69a] C. Leonidopoulos,[48] G. Lerner,[153] C. Leroy,[107] R. Les,[164] A. A. J. Lesage,[142] C. G. Lester,[31] M. Levchenko,[135] J. Levêque,[5] D. Levin,[103] L. J. Levinson,[177] D. Lewis,[90] B. Li,[15b] B. Li,[103] C-Q. Li,[58a,ll] H. Li,[58a] H. Li,[58b] K. Li,[150] L. Li,[58c] M. Li,[15a] Q. Li,[15d] Q. Y. Li,[58a] S. Li,[58d,58c] X. Li,[58c] Y. Li,[148] Z. Liang,[15a] B. Liberti,[71a] A. Liblong,[164] K. Lie,[61c] S. Liem,[118] A. Limosani,[154] C. Y. Lin,[31] K. Lin,[104] T. H. Lin,[97] R. A. Linck,[63] J. H. Lindon,[21] B. E. Lindquist,[152] A. L. Lionti,[52] E. Lipeles,[134] A. Lipniacka,[17] M. Lisovyi,[59b] T. M. Liss,[170,mm] A. Lister,[172] A. M. Litke,[143] J. D. Little,[8] B. Liu,[76] B. L Liu,[6] H. B. Liu,[29] H. Liu,[103] J. B. Liu,[58a] J. K. K. Liu,[132] K. Liu,[133] M. Liu,[58a] P. Liu,[18] Y. Liu,[15a] Y. L. Liu,[58a] Y. W. Liu,[58a] M. Livan,[68a,68b] A. Lleres,[56] J. Llorente Merino,[15a] S. L. Lloyd,[90] C. Y. Lo,[61b] F. Lo Sterzo,[41] E. M. Lobodzinska,[44] P. Loch,[7] T. Lohse,[19]

K. Lohwasser,[146] M. Lokajicek,[138] J. D. Long,[170] R. E. Long,[87] L. Longo,[65a,65b] K. A. Looper,[123] J. A. Lopez,[144b] I. Lopez Paz,[98] A. Lopez Solis,[146] J. Lorenz,[112] N. Lorenzo Martinez,[5] M. Losada,[22] P. J. Lösel,[112] A. Lösle,[50] X. Lou,[44] X. Lou,[15a] A. Lounis,[129] J. Love,[6] P. A. Love,[87] J. J. Lozano Bahilo,[171] H. Lu,[61a] M. Lu,[58a] Y. J. Lu,[62] H. J. Lubatti,[145] C. Luci,[70a,70b] A. Lucotte,[56] C. Luedtke,[50] F. Luehring,[63] I. Luise,[133] L. Luminari,[70a] B. Lund-Jensen,[151] M. S. Lutz,[100] P. M. Luzi,[133] D. Lynn,[29] R. Lysak,[138] E. Lytken,[94] F. Lyu,[15a] V. Lyubushkin,[77] T. Lyubushkina,[77] H. Ma,[29] L. L. Ma,[58b] Y. Ma,[58b] G. Maccarrone,[49] A. Macchiolo,[113] C. M. Macdonald,[146] J. Machado Miguens,[134,137b] D. Madaffari,[171] R. Madar,[37] W. F. Mader,[46] N. Madysa,[46] J. Maeda,[80] K. Maekawa,[160] S. Maeland,[17] T. Maeno,[29] M. Maerker,[46] A. S. Maevskiy,[111] V. Magerl,[50] D. J. Mahon,[38] C. Maidantchik,[78b] T. Maier,[112] A. Maio,[137a,137b,137d] O. Majersky,[28a] S. Majewski,[128] Y. Makida,[79] N. Makovec,[129] B. Malaescu,[133] Pa. Malecki,[82] V. P. Maleev,[135] F. Malek,[56] U. Mallik,[75] D. Malon,[6] C. Malone,[31] S. Maltezos,[10] S. Malyukov,[35] J. Mamuzic,[171] G. Mancini,[49] I. Mandić,[89] J. Maneira,[137a] L. Manhaes de Andrade Filho,[78a] J. Manjarres Ramos,[46] K. H. Mankinen,[94] A. Mann,[112] A. Manousos,[74] B. Mansoulie,[142] S. Manzoni,[66a,66b] A. Marantis,[159] G. Marceca,[30] L. March,[52] L. Marchese,[132] G. Marchiori,[133] M. Marcisovsky,[138] C. Marcon,[94] C. A. Marin Tobon,[35] M. Marjanovic,[37] F. Marroquim,[78b] Z. Marshall,[18] M. U. F Martensson,[169] S. Marti-Garcia,[171] C. B. Martin,[123] T. A. Martin,[175] V. J. Martin,[48] B. Martin dit Latour,[17] M. Martinez,[14,z] V. I. Martinez Outschoorn,[100] S. Martin-Haugh,[141] V. S. Martoiu,[27b] A. C. Martyniuk,[92] A. Marzin,[35] L. Masetti,[97] T. Mashimo,[160] R. Mashinistov,[108] J. Masik,[98] A. L. Maslennikov,[120b,120a] L. H. Mason,[102] L. Massa,[71a,71b] P. Massarotti,[67a,67b] P. Mastrandrea,[152] A. Mastroberardino,[40b,40a] T. Masubuchi,[160] P. Mättig,[24] J. Maurer,[27b] B. Maček,[89] S. J. Maxfield,[88] D. A. Maximov,[120b,120a] R. Mazini,[155] I. Maznas,[159] S. M. Mazza,[143] S. P. Mc Kee,[103] A. McCarn,[41] T. G. McCarthy,[113] L. I. McClymont,[92] W. P. McCormack,[18] E. F. McDonald,[102] J. A. Mcfayden,[35] G. Mchedlidze,[51] M. A. McKay,[41] K. D. McLean,[173] S. J. McMahon,[141] P. C. McNamara,[102] C. J. McNicol,[175] R. A. McPherson,[173,o] J. E. Mdhluli,[32c] Z. A. Meadows,[100] S. Meehan,[145] T. M. Megy,[50] S. Mehlhase,[112] A. Mehta,[88] T. Meideck,[56] B. Meirose,[42] D. Melini,[171,nn] B. R. Mellado Garcia,[32c] J. D. Mellenthin,[51] M. Melo,[28a] F. Meloni,[44] A. Melzer,[24] S. B. Menary,[98] E. D. Mendes Gouveia,[137a] L. Meng,[88] X. T. Meng,[103] S. Menke,[113] E. Meoni,[40b,40a] S. Mergelmeyer,[19] S. A. M. Merkt,[136] C. Merlassino,[20] P. Mermod,[52] L. Merola,[67a,67b] C. Meroni,[66a] F. S. Merritt,[36] A. Messina,[70a,70b] J. Metcalfe,[6] A. S. Mete,[168] C. Meyer,[63] J. Meyer,[157] J-P. Meyer,[142] H. Meyer Zu Theenhausen,[59a] F. Miano,[153] R. P. Middleton,[141] L. Mijović,[48] G. Mikenberg,[177] M. Mikestikova,[138] M. Mikuž,[89] M. Milesi,[102] A. Milic,[164] D. A. Millar,[90] D. W. Miller,[36] A. Milov,[177] D. A. Milstead,[43a,43b] R. A. Mina,[150,hh] A. A. Minaenko,[121] M. Miñano Moya,[171] I. A. Minashvili,[156b] A. I. Mincer,[122] B. Mindur,[81a] M. Mineev,[77] Y. Minegishi,[160] Y. Ming,[178] L. M. Mir,[14] A. Mirto,[65a,65b] K. P. Mistry,[134] T. Mitani,[176] J. Mitrevski,[112] V. A. Mitsou,[171] M. Mittal,[58c] A. Miucci,[20] P. S. Miyagawa,[146] A. Mizukami,[79] J. U. Mjörnmark,[94] T. Mkrtchyan,[181] M. Mlynarikova,[140] T. Moa,[43a,43b] K. Mochizuki,[107] P. Mogg,[50] S. Mohapatra,[38] S. Molander,[43a,43b] R. Moles-Valls,[24] M. C. Mondragon,[104] K. Mönig,[44] J. Monk,[39] E. Monnier,[99] A. Montalbano,[149] J. Montejo Berlingen,[35] F. Monticelli,[86] S. Monzani,[66a] N. Morange,[129] D. Moreno,[22] M. Moreno Llácer,[35] P. Morettini,[53b] M. Morgenstern,[118] S. Morgenstern,[46] D. Mori,[149] M. Morii,[57] M. Morinaga,[176] V. Morisbak,[131] A. K. Morley,[35] G. Mornacchi,[35] A. P. Morris,[92] J. D. Morris,[90] L. Morvaj,[152] P. Moschovakos,[10] M. Mosidze,[156b] H. J. Moss,[146] J. Moss,[150,oo] K. Motohashi,[162] R. Mount,[150] E. Mountricha,[35] E. J. W. Moyse,[100] S. Muanza,[99] F. Mueller,[113] J. Mueller,[136] R. S. P. Mueller,[112] D. Muenstermann,[87] G. A. Mullier,[94] F. J. Munoz Sanchez,[98] P. Murin,[28b] W. J. Murray,[175,141] A. Murrone,[66a,66b] M. Muškinja,[89] C. Mwewa,[32a] A. G. Myagkov,[121,pp] J. Myers,[128] M. Myska,[139] B. P. Nachman,[18] O. Nackenhorst,[45] K. Nagai,[132] K. Nagano,[79] Y. Nagasaka,[60] M. Nagel,[50] E. Nagy,[99] A. M. Nairz,[35] Y. Nakahama,[115] K. Nakamura,[79] T. Nakamura,[160] I. Nakano,[124] H. Nanjo,[130] F. Napolitano,[59a] R. F. Naranjo Garcia,[44] R. Narayan,[11] D. I. Narrias Villar,[59a] I. Naryshkin,[135] T. Naumann,[44] G. Navarro,[22] R. Nayyar,[7] H. A. Neal,[103,a] P. Y. Nechaeva,[108] T. J. Neep,[142] A. Negri,[68a,68b] M. Negrini,[23b] S. Nektarijevic,[117] C. Nellist,[51] M. E. Nelson,[132] S. Nemecek,[138] P. Nemethy,[122] M. Nessi,[35,qq] M. S. Neubauer,[170] M. Neumann,[179] P. R. Newman,[21] T. Y. Ng,[61c] Y. S. Ng,[19] Y. W. Y. Ng,[168] H. D. N. Nguyen,[99] T. Nguyen Manh,[107] E. Nibigira,[37] R. B. Nickerson,[132] R. Nicolaidou,[142] D. S. Nielsen,[39] J. Nielsen,[143] N. Nikiforou,[11] V. Nikolaenko,[121,pp] I. Nikolic-Audit,[133] K. Nikolopoulos,[21] P. Nilsson,[29] H. R. Nindhito,[52] Y. Ninomiya,[79] A. Nisati,[70a] N. Nishu,[58c] R. Nisius,[113] I. Nitsche,[45] T. Nitta,[176] T. Nobe,[160] Y. Noguchi,[83] M. Nomachi,[130] I. Nomidis,[133] M. A. Nomura,[29] T. Nooney,[90] M. Nordberg,[35] N. Norjoharuddeen,[132] T. Novak,[89] O. Novgorodova,[46] R. Novotny,[139] L. Nozka,[127] K. Ntekas,[168] E. Nurse,[92] F. Nuti,[102] F. G. Oakham,[33,f] H. Oberlack,[113] J. Ocariz,[133] A. Ochi,[80] I. Ochoa,[38] J. P. Ochoa-Ricoux,[144a] K. O'Connor,[26] S. Oda,[85] S. Odaka,[79] S. Oerdek,[51] A. Oh,[98] S. H. Oh,[47] C. C. Ohm,[151] H. Oide,[53b,53a] M. L. Ojeda,[164] H. Okawa,[166] Y. Okazaki,[83] Y. Okumura,[160] T. Okuyama,[79] A. Olariu,[27b] L. F. Oleiro Seabra,[137a] S. A. Olivares Pino,[144a] D. Oliveira Damazio,[29]

J. L. Oliver,[1] M. J. R. Olsson,[36] A. Olszewski,[82] J. Olszowska,[82] D. C. O'Neil,[149] A. Onofre,[137a,137e] K. Onogi,[115] P. U. E. Onyisi,[11] H. Oppen,[131] M. J. Oreglia,[36] G. E. Orellana,[86] Y. Oren,[158] D. Orestano,[72a,72b] N. Orlando,[61b] A. A. O'Rourke,[44] R. S. Orr,[164] B. Osculati,[53b,53a,a] V. O'Shea,[55] R. Ospanov,[58a] G. Otero y Garzon,[30] H. Otono,[85] M. Ouchrif,[34d] F. Ould-Saada,[131] A. Ouraou,[142] Q. Ouyang,[15a] M. Owen,[55] R. E. Owen,[21] V. E. Ozcan,[12c] N. Ozturk,[8] J. Pacalt,[127] H. A. Pacey,[31] K. Pachal,[149] A. Pacheco Pages,[14] L. Pacheco Rodriguez,[142] C. Padilla Aranda,[14] S. Pagan Griso,[18] M. Paganini,[180] G. Palacino,[63] S. Palazzo,[48] S. Palestini,[35] M. Palka,[81b] D. Pallin,[37] I. Panagoulias,[10] C. E. Pandini,[35] J. G. Panduro Vazquez,[91] P. Pani,[35] G. Panizzo,[64a,64c] L. Paolozzi,[52] T. D. Papadopoulou,[10] K. Papageorgiou,[9,v] A. Paramonov,[6] D. Paredes Hernandez,[61b] S. R. Paredes Saenz,[132] B. Parida,[163] T. H. Park,[33] A. J. Parker,[87] K. A. Parker,[44] M. A. Parker,[31] F. Parodi,[53b,53a] J. A. Parsons,[38] U. Parzefall,[50] V. R. Pascuzzi,[164] J. M. P. Pasner,[143] E. Pasqualucci,[70a] S. Passaggio,[53b] F. Pastore,[91] P. Pasuwan,[43a,43b] S. Pataraia,[97] J. R. Pater,[98] A. Pathak,[178,g] T. Pauly,[35] B. Pearson,[113] M. Pedersen,[131] L. Pedraza Diaz,[117] R. Pedro,[137a,137b] S. V. Peleganchuk,[120b,120a] O. Penc,[138] C. Peng,[15d] H. Peng,[58a] B. S. Peralva,[78a] M. M. Perego,[129] A. P. Pereira Peixoto,[137a] D. V. Perepelitsa,[29] F. Peri,[19] L. Perini,[66a,66b] H. Pernegger,[35] S. Perrella,[67a,67b] V. D. Peshekhonov,[77,a] K. Peters,[44] R. F. Y. Peters,[98] B. A. Petersen,[35] T. C. Petersen,[39] E. Petit,[56] A. Petridis,[1] C. Petridou,[159] P. Petroff,[129] M. Petrov,[132] F. Petrucci,[72a,72b] M. Pettee,[180] N. E. Pettersson,[100] A. Peyaud,[142] R. Pezoa,[144b] T. Pham,[102] F. H. Phillips,[104] P. W. Phillips,[141] M. W. Phipps,[170] G. Piacquadio,[152] E. Pianori,[18] A. Picazio,[100] R. H. Pickles,[98] R. Piegaia,[30] J. E. Pilcher,[36] A. D. Pilkington,[98] M. Pinamonti,[71a,71b] J. L. Pinfold,[3] M. Pitt,[177] L. Pizzimento,[71a,71b] M.-A. Pleier,[29] V. Pleskot,[140] E. Plotnikova,[77] D. Pluth,[76] P. Podberezko,[120b,120a] R. Poettgen,[94] R. Poggi,[52] L. Poggioli,[129] I. Pogrebnyak,[104] D. Pohl,[24] I. Pokharel,[51] G. Polesello,[68a] A. Poley,[18] A. Policicchio,[70a,70b] R. Polifka,[35] A. Polini,[23b] C. S. Pollard,[44] V. Polychronakos,[29] D. Ponomarenko,[110] L. Pontecorvo,[35] G. A. Popeneciu,[27d] D. M. Portillo Quintero,[133] S. Pospisil,[139] K. Potamianos,[44] I. N. Potrap,[77] C. J. Potter,[31] H. Potti,[11] T. Poulsen,[94] J. Poveda,[35] T. D. Powell,[146] M. E. Pozo Astigarraga,[35] P. Pralavorio,[99] S. Prell,[76] D. Price,[98] M. Primavera,[65a] S. Prince,[101] M. L. Proffitt,[145] N. Proklova,[110] K. Prokofiev,[61c] F. Prokoshin,[144b] S. Protopopescu,[29] J. Proudfoot,[6] M. Przybycien,[81a] A. Puri,[170] P. Puzo,[129] J. Qian,[103] Y. Qin,[98] A. Quadt,[51] M. Queitsch-Maitland,[44] A. Qureshi,[1] P. Rados,[102] F. Ragusa,[66a,66b] G. Rahal,[95] J. A. Raine,[52] S. Rajagopalan,[29] A. Ramirez Morales,[90] K. Ran,[15a] T. Rashid,[129] S. Raspopov,[5] M. G. Ratti,[66a,66b] D. M. Rauch,[44] F. Rauscher,[112] S. Rave,[97] B. Ravina,[146] I. Ravinovich,[177] J. H. Rawling,[98] M. Raymond,[35] A. L. Read,[131] N. P. Readioff,[56] M. Reale,[65a,65b] D. M. Rebuzzi,[68a,68b] A. Redelbach,[174] G. Redlinger,[29] R. Reece,[143] R. G. Reed,[32c] K. Reeves,[42] L. Rehnisch,[19] J. Reichert,[134] D. Reikher,[158] A. Reiss,[97] A. Rej,[148] C. Rembser,[35] H. Ren,[15d] M. Resigno,[70a] S. Resconi,[66a] E. D. Resseguie,[134] S. Rettie,[172] E. Reynolds,[21] O. L. Rezanova,[120b,120a] P. Reznicek,[140] E. Ricci,[73a,73b] R. Richter,[113] S. Richter,[44] E. Richter-Was,[81b] O. Ricken,[24] M. Ridel,[133] P. Rieck,[113] C. J. Riegel,[179] O. Rifki,[44] M. Rijssenbeek,[152] A. Rimoldi,[68a,68b] M. Rimoldi,[20] L. Rinaldi,[23b] G. Ripellino,[151] B. Ristić,[87] E. Ritsch,[35] I. Riu,[14] J. C. Rivera Vergara,[144a] F. Rizatdinova,[126] E. Rizvi,[90] C. Rizzi,[14] R. T. Roberts,[98] S. H. Robertson,[101,o] D. Robinson,[31] J. E. M. Robinson,[44] A. Robson,[55] E. Rocco,[97] C. Roda,[69a,69b] Y. Rodina,[99] S. Rodriguez Bosca,[171] A. Rodriguez Perez,[14] D. Rodriguez Rodriguez,[171] A. M. Rodríguez Vera,[165b] S. Roe,[35] C. S. Rogan,[57] O. Røhne,[131] R. Röhrig,[113] C. P. A. Roland,[63] J. Roloff,[57] A. Romaniouk,[110] M. Romano,[23b,23a] N. Rompotis,[88] M. Ronzani,[122] L. Roos,[133] S. Rosati,[70a] K. Rosbach,[50] N-A. Rosien,[51] B. J. Rosser,[134] E. Rossi,[44] E. Rossi,[72a,72b] E. Rossi,[67a,67b] L. P. Rossi,[53b] L. Rossini,[66a,66b] J. H. N. Rosten,[31] R. Rosten,[14] M. Rotaru,[27b] J. Rothberg,[145] D. Rousseau,[129] D. Roy,[32c] A. Rozanov,[99] Y. Rozen,[157] X. Ruan,[32c] F. Rubbo,[150] F. Rühr,[50] A. Ruiz-Martinez,[171] Z. Rurikova,[50] N. A. Rusakovich,[77] H. L. Russell,[101] J. P. Rutherfoord,[7] E. M. Rüttinger,[44,rr] Y. F. Ryabov,[135] M. Rybar,[38] G. Rybkin,[129] S. Ryu,[6] A. Ryzhov,[121] G. F. Rzehorz,[51] P. Sabatini,[51] G. Sabato,[118] S. Sacerdoti,[129] H. F-W. Sadrozinski,[143] R. Sadykov,[77] F. Safai Tehrani,[70a] P. Saha,[119] M. Sahinsoy,[59a] A. Sahu,[179] M. Saimpert,[44] M. Saito,[160] T. Saito,[160] H. Sakamoto,[160] A. Sakharov,[122,ii] D. Salamani,[52] G. Salamanna,[72a,72b] J. E. Salazar Loyola,[144b] P. H. Sales De Bruin,[169] D. Salihagic,[113,a] A. Salnikov,[150] J. Salt,[171] D. Salvatore,[40b,40a] F. Salvatore,[153] A. Salvucci,[61a,61b,61c] A. Salzburger,[35] J. Samarati,[35] D. Sammel,[50] D. Sampsonidis,[159] D. Sampsonidou,[159] J. Sánchez,[171] A. Sanchez Pineda,[64a,64c] H. Sandaker,[131] C. O. Sander,[44] M. Sandhoff,[179] C. Sandoval,[22] D. P. C. Sankey,[141] M. Sannino,[53b,53a] Y. Sano,[115] A. Sansoni,[49] C. Santoni,[37] H. Santos,[137a] I. Santoyo Castillo,[153] A. Santra,[171] A. Sapronov,[77] J. G. Saraiva,[137a,137d] O. Sasaki,[79] K. Sato,[166] E. Sauvan,[5] P. Savard,[164,f] N. Savic,[113] R. Sawada,[160] C. Sawyer,[141] L. Sawyer,[93,x] C. Sbarra,[23b] A. Sbrizzi,[23a] T. Scanlon,[92] J. Schaarschmidt,[145] P. Schacht,[113] B. M. Schachtner,[112] D. Schaefer,[36] L. Schaefer,[134] J. Schaeffer,[97] S. Schaepe,[35] U. Schäfer,[97] A. C. Schaffer,[129] D. Schaile,[112] R. D. Schamberger,[152] N. Scharmberg,[98] V. A. Schegelsky,[135] D. Scheirich,[140] F. Schenck,[19] M. Schernau,[168]

C. Schiavi,[53b,53a] S. Schier,[143] L. K. Schildgen,[24] Z. M. Schillaci,[26] E. J. Schioppa,[35] M. Schioppa,[40b,40a] K. E. Schleicher,[50] S. Schlenker,[35] K. R. Schmidt-Sommerfeld,[113] K. Schmieden,[35] C. Schmitt,[97] S. Schmitt,[44] S. Schmitz,[97] J. C. Schmoeckel,[44] U. Schnoor,[50] L. Schoeffel,[142] A. Schoening,[59b] E. Schopf,[132] M. Schott,[97] J. F. P. Schouwenberg,[117] J. Schovancova,[35] S. Schramm,[52] A. Schulte,[97] H-C. Schultz-Coulon,[59a] M. Schumacher,[50] B. A. Schumm,[143] Ph. Schune,[142] A. Schwartzman,[150] T. A. Schwarz,[103] Ph. Schwemling,[142] R. Schwienhorst,[104] A. Sciandra,[24] G. Sciolla,[26] M. Scornajenghi,[40b,40a] F. Scuri,[69a] F. Scutti,[102] L. M. Scyboz,[113] C. D. Sebastiani,[70a,70b] P. Seema,[19] S. C. Seidel,[116] A. Seiden,[143] T. Seiss,[36] J. M. Seixas,[78b] G. Sekhniaidze,[67a] K. Sekhon,[103] S. J. Sekula,[41] N. Semprini-Cesari,[23b,23a] S. Sen,[47] S. Senkin,[37] C. Serfon,[131] L. Serin,[129] L. Serkin,[64a,64b] M. Sessa,[58a] H. Severini,[125] F. Sforza,[167] A. Sfyrla,[52] E. Shabalina,[51] J. D. Shahinian,[143] N. W. Shaikh,[43a,43b] D. Shaked Renous,[177] L. Y. Shan,[15a] R. Shang,[170] J. T. Shank,[25] M. Shapiro,[18] A. S. Sharma,[1] A. Sharma,[132] P. B. Shatalov,[109] K. Shaw,[153] S. M. Shaw,[98] A. Shcherbakova,[135] Y. Shen,[125] N. Sherafati,[33] A. D. Sherman,[25] P. Sherwood,[92] L. Shi,[155,ss] S. Shimizu,[79] C. O. Shimmin,[180] Y. Shimogama,[176] M. Shimojima,[114] I. P. J. Shipsey,[132] S. Shirabe,[85] M. Shiyakova,[77] J. Shlomi,[177] A. Shmeleva,[108] D. Shoaleh Saadi,[107] M. J. Shochet,[36] S. Shojaii,[102] D. R. Shope,[125] S. Shrestha,[123] E. Shulga,[110] P. Sicho,[138] A. M. Sickles,[170] P. E. Sidebo,[151] E. Sideras Haddad,[32c] O. Sidiropoulou,[35] A. Sidoti,[23b,23a] F. Siegert,[46] Dj. Sijacki,[16] J. Silva,[137a] M. Silva Jr.,[178] M. V. Silva Oliveira,[78a] S. B. Silverstein,[43a] S. Simion,[129] E. Simioni,[97] M. Simon,[97] R. Simoniello,[97] P. Sinervo,[164] N. B. Sinev,[128] M. Sioli,[23b,23a] I. Siral,[103] S. Yu. Sivoklokov,[111] J. Sjölin,[43a,43b] P. Skubic,[125] M. Slater,[21] T. Slavicek,[139] M. Slawinska,[82] K. Sliwa,[167] R. Slovak,[140] V. Smakhtin,[177] B. H. Smart,[5] J. Smiesko,[28a] N. Smirnov,[110] S. Yu. Smirnov,[110] Y. Smirnov,[110] L. N. Smirnova,[111] O. Smirnova,[94] J. W. Smith,[51] M. Smizanska,[87] K. Smolek,[139] A. Smykiewicz,[82] A. A. Snesarev,[108] I. M. Snyder,[128] S. Snyder,[29] R. Sobie,[173,o] A. M. Soffa,[168] A. Soffer,[158] A. Søgaard,[48] F. Sohns,[51] G. Sokhrannyi,[89] C. A. Solans Sanchez,[35] M. Solar,[139] E. Yu. Soldatov,[110] U. Soldevila,[171] A. A. Solodkov,[121] A. Soloshenko,[77] O. V. Solovyanov,[121] V. Solovyev,[135] P. Sommer,[146] H. Son,[167] W. Song,[141] W. Y. Song,[165b] A. Sopczak,[139] F. Sopkova,[28b] C. L. Sotiropoulou,[69a,69b] S. Sottocornola,[68a,68b] R. Soualah,[64a,64c,tt] A. M. Soukharev,[120b,120a] D. South,[44] S. Spagnolo,[65a,65b] M. Spalla,[113] M. Spangenberg,[175] F. Spanò,[91] D. Sperlich,[19] T. M. Spieker,[59a] R. Spighi,[23b] G. Spigo,[35] L. A. Spiller,[102] D. P. Spiteri,[55] M. Spousta,[140] A. Stabile,[66a,66b] R. Stamen,[59a] S. Stamm,[19] E. Stanecka,[82] R. W. Stanek,[6] C. Stanescu,[72a] B. Stanislaus,[132] M. M. Stanitzki,[44] B. Stapf,[118] E. A. Starchenko,[121] G. H. Stark,[143] J. Stark,[56] S. H Stark,[39] P. Staroba,[138] P. Starovoitov,[59a] S. Stärz,[101] R. Staszewski,[82] M. Stegler,[44] P. Steinberg,[29] B. Stelzer,[149] H. J. Stelzer,[35] O. Stelzer-Chilton,[165a] H. Stenzel,[54] T. J. Stevenson,[153] G. A. Stewart,[35] M. C. Stockton,[35] G. Stoicea,[27b] P. Stolte,[51] S. Stonjek,[113] A. Straessner,[46] J. Strandberg,[151] S. Strandberg,[43a,43b] M. Strauss,[125] P. Strizenec,[28b] R. Ströhmer,[174] D. M. Strom,[128] R. Stroynowski,[41] A. Strubig,[48] S. A. Stucci,[29] B. Stugu,[17] J. Stupak,[125] N. A. Styles,[44] D. Su,[150] J. Su,[136] S. Suchek,[59a] Y. Sugaya,[130] M. Suk,[139] V. V. Sulin,[108] M. J. Sullivan,[88] D. M. S. Sultan,[52] S. Sultansoy,[4c] T. Sumida,[83] S. Sun,[103] X. Sun,[3] K. Suruliz,[153] C. J. E. Suster,[154] M. R. Sutton,[153] S. Suzuki,[79] M. Svatos,[138] M. Swiatlowski,[36] S. P. Swift,[2] A. Sydorenko,[97] I. Sykora,[28a] M. Sykora,[140] T. Sykora,[140] D. Ta,[97] K. Tackmann,[44,uu] J. Taenzer,[158] A. Taffard,[168] R. Tafirout,[165a] E. Tahirovic,[90] N. Taiblum,[158] H. Takai,[29] R. Takashima,[84] E. H. Takasugi,[113] K. Takeda,[80] T. Takeshita,[147] Y. Takubo,[79] M. Talby,[99] A. A. Talyshev,[120b,120a] J. Tanaka,[160] M. Tanaka,[162] R. Tanaka,[129] B. B. Tannenwald,[123] S. Tapia Araya,[144b] S. Tapprogge,[97] A. Tarek Abouelfadl Mohamed,[133] S. Tarem,[157] G. Tarna,[27b,r] G. F. Tartarelli,[66a] P. Tas,[140] M. Tasevsky,[138] T. Tashiro,[83] E. Tassi,[40b,40a] A. Tavares Delgado,[137a,137b] Y. Tayalati,[34e] A. J. Taylor,[48] G. N. Taylor,[102] P. T. E. Taylor,[102] W. Taylor,[165b] A. S. Tee,[87] R. Teixeira De Lima,[150] P. Teixeira-Dias,[91] H. Ten Kate,[35] J. J. Teoh,[118] S. Terada,[79] K. Terashi,[160] J. Terron,[96] S. Terzo,[14] M. Testa,[49] R. J. Teuscher,[164,o] S. J. Thais,[180] T. Theveneaux-Pelzer,[44] F. Thiele,[39] D. W. Thomas,[91] J. P. Thomas,[21] A. S. Thompson,[55] P. D. Thompson,[21] L. A. Thomsen,[180] E. Thomson,[134] Y. Tian,[38] R. E. Ticse Torres,[51] V. O. Tikhomirov,[108,vv] Yu. A. Tikhonov,[120b,120a] S. Timoshenko,[110] P. Tipton,[180] S. Tisserant,[99] K. Todome,[162] S. Todorova-Nova,[5] S. Todt,[46] J. Tojo,[85] S. Tokár,[28a] K. Tokushuku,[79] E. Tolley,[123] K. G. Tomiwa,[32c] M. Tomoto,[115] L. Tompkins,[150,hh] K. Toms,[116] B. Tong,[57] P. Tornambe,[50] E. Torrence,[128] H. Torres,[46] E. Torró Pastor,[145] C. Tosciri,[132] J. Toth,[99,ww] F. Touchard,[99] D. R. Tovey,[146] C. J. Treado,[122] T. Trefzger,[174] F. Tresoldi,[153] A. Tricoli,[29] I. M. Trigger,[165a] S. Trincaz-Duvoid,[133] W. Trischuk,[164] B. Trocmé,[56] A. Trofymov,[129] C. Troncon,[66a] M. Trovatelli,[173] F. Trovato,[153] L. Truong,[32b] M. Trzebinski,[82] A. Trzupek,[82] F. Tsai,[44] J. C-L. Tseng,[132] P. V. Tsiareshka,[105,jj] A. Tsirigotis,[159] N. Tsirintanis,[9] V. Tsiskaridze,[152] E. G. Tskhadadze,[156a] I. I. Tsukerman,[109] V. Tsulaia,[18] S. Tsuno,[79] D. Tsybychev,[152,163] Y. Tu,[61b] A. Tudorache,[27b] V. Tudorache,[27b] T. T. Tulbure,[27a] A. N. Tuna,[57] S. Turchikhin,[77] D. Turgeman,[177] I. Turk Cakir,[4b,xx] R. J. Turner,[21] R. T. Turra,[66a] P. M. Tuts,[38] S. Tzamarias,[159] E. Tzovara,[97] G. Ucchielli,[45] I. Ueda,[79] M. Ughetto,[43a,43b] F. Ukegawa,[166] G. Unal,[35] A. Undrus,[29]

G. Unel,[168] F. C. Ungaro,[102] Y. Unno,[79] K. Uno,[160] J. Urban,[28b] P. Urquijo,[102] G. Usai,[8] J. Usui,[79] L. Vacavant,[99] V. Vacek,[139] B. Vachon,[101] K. O. H. Vadla,[131] A. Vaidya,[92] C. Valderanis,[112] E. Valdes Santurio,[43a,43b] M. Valente,[52] S. Valentinetti,[23b,23a] A. Valero,[171] L. Valéry,[44] R. A. Vallance,[21] A. Vallier,[5] J. A. Valls Ferrer,[171] T. R. Van Daalen,[14] H. Van der Graaf,[118] P. Van Gemmeren,[6] I. Van Vulpen,[118] M. Vanadia,[71a,71b] W. Vandelli,[35] A. Vaniachine,[163] P. Vankov,[118] R. Vari,[70a] E. W. Varnes,[7] C. Varni,[53b,53a] T. Varol,[41] D. Varouchas,[129] K. E. Varvell,[154] G. A. Vasquez,[144b] J. G. Vasquez,[180] F. Vazeille,[37] D. Vazquez Furelos,[14] T. Vazquez Schroeder,[35] J. Veatch,[51] V. Vecchio,[72a,72b] L. M. Veloce,[164] F. Veloso,[137a,137c] S. Veneziano,[70a] A. Ventura,[65a,65b] N. Venturi,[35] V. Vercesi,[68a] M. Verducci,[72a,72b] C. M. Vergel Infante,[76] C. Vergis,[24] W. Verkerke,[118] A. T. Vermeulen,[118] J. C. Vermeulen,[118] M. C. Vetterli,[149,f] N. Viaux Maira,[144b] M. Vicente Barreto Pinto,[52] I. Vichou,[170,a] T. Vickey,[146] O. E. Vickey Boeriu,[146] G. H. A. Viehhauser,[132] S. Viel,[18] L. Vigani,[132] M. Villa,[23b,23a] M. Villaplana Perez,[66a,66b] E. Vilucchi,[49] M. G. Vincter,[33] V. B. Vinogradov,[77] A. Vishwakarma,[44] C. Vittori,[23b,23a] I. Vivarelli,[153] S. Vlachos,[10] M. Vogel,[179] P. Vokac,[139] G. Volpi,[14] S. E. von Buddenbrock,[32c] E. Von Toerne,[24] V. Vorobel,[140] K. Vorobev,[110] M. Vos,[171] J. H. Vossebeld,[88] N. Vranjes,[16] M. Vranjes Milosavljevic,[16] V. Vrba,[139] M. Vreeswijk,[118] T. Šfiligoj,[89] R. Vuillermet,[35] I. Vukotic,[36] T. Ženiš,[28a] L. Živković,[16] P. Wagner,[24] W. Wagner,[179] J. Wagner-Kuhr,[112] H. Wahlberg,[86] S. Wahrmund,[46] K. Wakamiya,[80] V. M. Walbrecht,[113] J. Walder,[87] R. Walker,[112] S. D. Walker,[91] W. Walkowiak,[148] V. Wallangen,[43a,43b] A. M. Wang,[57] C. Wang,[58b] F. Wang,[178] H. Wang,[18] H. Wang,[3] J. Wang,[154] J. Wang,[59b] P. Wang,[41] Q. Wang,[125] R.-J. Wang,[133] R. Wang,[58a] R. Wang,[6] S. M. Wang,[155] W. T. Wang,[58a] W. Wang,[15c,yy] W. X. Wang,[58a,yy] Y. Wang,[58a,ll] Z. Wang,[58c] C. Wanotayaroj,[44] A. Warburton,[101] C. P. Ward,[31] D. R. Wardrope,[92] A. Washbrook,[48] P. M. Watkins,[21] A. T. Watson,[21] M. F. Watson,[21] G. Watts,[145] S. Watts,[98] B. M. Waugh,[92] A. F. Webb,[11] S. Webb,[97] C. Weber,[180] M. S. Weber,[20] S. A. Weber,[33] S. M. Weber,[59a] A. R. Weidberg,[132] J. Weingarten,[45] M. Weirich,[97] C. Weiser,[50] P. S. Wells,[35] T. Wenaus,[29] T. Wengler,[35] S. Wenig,[35] N. Wermes,[24] M. D. Werner,[76] P. Werner,[35] M. Wessels,[59a] T. D. Weston,[20] K. Whalen,[128] N. L. Whallon,[145] A. M. Wharton,[87] A. S. White,[103] A. White,[8] M. J. White,[1] R. White,[144b] D. Whiteson,[168] B. W. Whitmore,[87] F. J. Wickens,[141] W. Wiedenmann,[178] M. Wielers,[141] C. Wiglesworth,[39] L. A. M. Wiik-Fuchs,[50] F. Wilk,[98] H. G. Wilkens,[35] L. J. Wilkins,[91] H. H. Williams,[134] S. Williams,[31] C. Willis,[104] S. Willocq,[100] J. A. Wilson,[21] I. Wingerter-Seez,[5] E. Winkels,[153] F. Winklmeier,[128] O. J. Winston,[153] B. T. Winter,[50] M. Wittgen,[150] M. Wobisch,[93] A. Wolf,[97] T. M. H. Wolf,[118] R. Wolff,[99] J. Wollrath,[50] M. W. Wolter,[82] H. Wolters,[137a,137c] V. W. S. Wong,[172] N. L. Woods,[143] S. D. Worm,[21] B. K. Wosiek,[82] K. W. Woźniak,[82] K. Wraight,[55] M. Wu,[36] S. L. Wu,[178] X. Wu,[52] Y. Wu,[58a] T. R. Wyatt,[98] B. M. Wynne,[48] S. Xella,[39] Z. Xi,[103] L. Xia,[175] D. Xu,[15a] H. Xu,[58a,r] L. Xu,[29] T. Xu,[142] W. Xu,[103] Z. Xu,[150] B. Yabsley,[154] S. Yacoob,[32a] K. Yajima,[130] D. P. Yallup,[92] D. Yamaguchi,[162] Y. Yamaguchi,[162] A. Yamamoto,[79] T. Yamanaka,[160] F. Yamane,[80] M. Yamatani,[160] T. Yamazaki,[160] Y. Yamazaki,[80] Z. Yan,[25] H. J. Yang,[58c,58d] H. T. Yang,[18] S. Yang,[75] Y. Yang,[160] Z. Yang,[17] W-M. Yao,[18] Y. C. Yap,[44] Y. Yasu,[79] E. Yatsenko,[58c,58d] J. Ye,[41] S. Ye,[29] I. Yeletskikh,[77] E. Yigitbasi,[25] E. Yildirim,[97] K. Yorita,[176] K. Yoshihara,[134] C. J. S. Young,[35] C. Young,[150] J. Yu,[8] J. Yu,[76] X. Yue,[59a] S. P. Y. Yuen,[24] B. Zabinski,[82] G. Zacharis,[10] E. Zaffaroni,[52] R. Zaidan,[14] A. M. Zaitsev,[121,pp] T. Zakareishvili,[156b] N. Zakharchuk,[33] S. Zambito,[57] D. Zanzi,[35] D. R. Zaripovas,[55] S. V. Zeißner,[45] C. Zeitnitz,[179] G. Zemaityte,[132] J. C. Zeng,[170] Q. Zeng,[150] O. Zenin,[121] D. Zerwas,[129] M. Zgubič,[132] D. F. Zhang,[58b] D. Zhang,[103] F. Zhang,[178] G. Zhang,[58a] G. Zhang,[15b] H. Zhang,[15c] J. Zhang,[6] L. Zhang,[15c] L. Zhang,[58a] M. Zhang,[170] P. Zhang,[15c] R. Zhang,[58a] R. Zhang,[24] X. Zhang,[58b] Y. Zhang,[15d] Z. Zhang,[129] P. Zhao,[47] Y. Zhao,[58b,129,bb] Z. Zhao,[58a] A. Zhemchugov,[77] Z. Zheng,[103] D. Zhong,[170] B. Zhou,[103] C. Zhou,[178] M. S. Zhou,[15d] M. Zhou,[152] N. Zhou,[58c] Y. Zhou,[7] C. G. Zhu,[58b] H. L. Zhu,[58a] H. Zhu,[15a] J. Zhu,[103] Y. Zhu,[58a] X. Zhuang,[15a] K. Zhukov,[108] V. Zhulanov,[120b,120a] A. Zibell,[174] D. Zieminska,[63] N. I. Zimine,[77] S. Zimmermann,[50] Z. Zinonos,[113] M. Ziolkowski,[148] G. Zobernig,[178] A. Zoccoli,[23b,23a] K. Zoch,[51] T. G. Zorbas,[146] R. Zou,[36] M. Zur Nedden,[19] and L. Zwalinski[35]

(ATLAS Collaboration)

[1]*Department of Physics, University of Adelaide, Adelaide, Australia*
[2]*Physics Department, SUNY Albany, Albany, New York, USA*
[3]*Department of Physics, University of Alberta, Edmonton, Alberta, Canada*
[4a]*Department of Physics, Ankara University, Ankara, Turkey*
[4b]*Istanbul Aydin University, Istanbul, Turkey*
[4c]*Division of Physics, TOBB University of Economics and Technology, Ankara, Turkey*
[5]*LAPP, Université Grenoble Alpes, Université Savoie Mont Blanc, CNRS/IN2P3, Annecy, France*

[6]High Energy Physics Division, Argonne National Laboratory, Argonne, Illinois, USA
[7]Department of Physics, University of Arizona, Tucson, Arizona, USA
[8]Department of Physics, University of Texas at Arlington, Arlington, Texas, USA
[9]Physics Department, National and Kapodistrian University of Athens, Athens, Greece
[10]Physics Department, National Technical University of Athens, Zografou, Greece
[11]Department of Physics, University of Texas at Austin, Austin, Texas, USA
[12a]Bahcesehir University, Faculty of Engineering and Natural Sciences, Istanbul, Turkey
[12b]Istanbul Bilgi University, Faculty of Engineering and Natural Sciences, Istanbul, Turkey
[12c]Department of Physics, Bogazici University, Istanbul, Turkey
[12d]Department of Physics Engineering, Gaziantep University, Gaziantep, Turkey
[13]Institute of Physics, Azerbaijan Academy of Sciences, Baku, Azerbaijan
[14]Institut de Física d'Altes Energies (IFAE), Barcelona Institute of Science and Technology, Barcelona, Spain
[15a]Institute of High Energy Physics, Chinese Academy of Sciences, Beijing, China
[15b]Physics Department, Tsinghua University, Beijing, China
[15c]Department of Physics, Nanjing University, Nanjing, China
[15d]University of Chinese Academy of Science (UCAS), Beijing, China
[16]Institute of Physics, University of Belgrade, Belgrade, Serbia
[17]Department for Physics and Technology, University of Bergen, Bergen, Norway
[18]Physics Division, Lawrence Berkeley National Laboratory and University of California, Berkeley, California, USA
[19]Institut für Physik, Humboldt Universität zu Berlin, Berlin, Germany
[20]Albert Einstein Center for Fundamental Physics and Laboratory for High Energy Physics, University of Bern, Bern, Switzerland
[21]School of Physics and Astronomy, University of Birmingham, Birmingham, United Kingdom
[22]Centro de Investigaciónes, Universidad Antonio Nariño, Bogota, Colombia
[23a]Dipartimento di Fisica e Astronomia, Università di Bologna, Bologna, Italy
[23b]INFN Sezione di Bologna, Bologna, Italy
[24]Physikalisches Institut, Universität Bonn, Bonn, Germany
[25]Department of Physics, Boston University, Boston, Massachusetts, USA
[26]Department of Physics, Brandeis University, Waltham, Massachusetts, USA
[27a]Transilvania University of Brasov, Brasov, Romania
[27b]Horia Hulubei National Institute of Physics and Nuclear Engineering, Bucharest, Romania
[27c]Department of Physics, Alexandru Ioan Cuza University of Iasi, Iasi, Romania
[27d]National Institute for Research and Development of Isotopic and Molecular Technologies, Physics Department, Cluj-Napoca, Romania
[27e]University Politehnica Bucharest, Bucharest, Romania
[27f]West University in Timisoara, Timisoara, Romania
[28a]Faculty of Mathematics, Physics and Informatics, Comenius University, Bratislava, Slovak Republic
[28b]Department of Subnuclear Physics, Institute of Experimental Physics of the Slovak Academy of Sciences, Kosice, Slovak Republic
[29]Physics Department, Brookhaven National Laboratory, Upton, New York, USA
[30]Departamento de Física, Universidad de Buenos Aires, Buenos Aires, Argentina
[31]Cavendish Laboratory, University of Cambridge, Cambridge, United Kingdom
[32a]Department of Physics, University of Cape Town, Cape Town, South Africa
[32b]Department of Mechanical Engineering Science, University of Johannesburg, Johannesburg, South Africa
[32c]School of Physics, University of the Witwatersrand, Johannesburg, South Africa
[33]Department of Physics, Carleton University, Ottawa, Ontario, Canada
[34a]Faculté des Sciences Ain Chock, Réseau Universitaire de Physique des Hautes Energies—Université Hassan II, Casablanca, Morocco
[34b]Centre National de l'Energie des Sciences Techniques Nucleaires (CNESTEN), Rabat, Morocco
[34c]Faculté des Sciences Semlalia, Université Cadi Ayyad, LPHEA-Marrakech, Morocco
[34d]Faculté des Sciences, Université Mohamed Premier and LPTPM, Oujda, Morocco
[34e]Faculté des sciences, Université Mohammed V, Rabat, Morocco
[35]CERN, Geneva, Switzerland
[36]Enrico Fermi Institute, University of Chicago, Chicago, Illinois, USA
[37]LPC, Université Clermont Auvergne, CNRS/IN2P3, Clermont-Ferrand, France
[38]Nevis Laboratory, Columbia University, Irvington, New York, USA
[39]Niels Bohr Institute, University of Copenhagen, Copenhagen, Denmark

[40a]*Dipartimento di Fisica, Università della Calabria, Rende, Italy*
[40b]*INFN Gruppo Collegato di Cosenza, Laboratori Nazionali di Frascati, Italy*
[41]*Physics Department, Southern Methodist University, Dallas, Texas, USA*
[42]*Physics Department, University of Texas at Dallas, Richardson, Texas, USA*
[43a]*Department of Physics, Stockholm University, Sweden*
[43b]*Oskar Klein Centre, Stockholm, Sweden*
[44]*Deutsches Elektronen-Synchrotron DESY, Hamburg and Zeuthen, Germany*
[45]*Lehrstuhl für Experimentelle Physik IV, Technische Universität Dortmund, Dortmund, Germany*
[46]*Institut für Kern- und Teilchenphysik, Technische Universität Dresden, Dresden, Germany*
[47]*Department of Physics, Duke University, Durham, North Carolina, USA*
[48]*SUPA—School of Physics and Astronomy, University of Edinburgh, Edinburgh, United Kingdom*
[49]*INFN e Laboratori Nazionali di Frascati, Frascati, Italy*
[50]*Physikalisches Institut, Albert-Ludwigs-Universität Freiburg, Freiburg, Germany*
[51]*II. Physikalisches Institut, Georg-August-Universität Göttingen, Göttingen, Germany*
[52]*Département de Physique Nucléaire et Corpusculaire, Université de Genève, Genève, Switzerland*
[53a]*Dipartimento di Fisica, Università di Genova, Genova, Italy*
[53b]*INFN Sezione di Genova, Genova, Italy*
[54]*II. Physikalisches Institut, Justus-Liebig-Universität Giessen, Giessen, Germany*
[55]*SUPA—School of Physics and Astronomy, University of Glasgow, Glasgow, United Kingdom*
[56]*LPSC, Université Grenoble Alpes, CNRS/IN2P3, Grenoble INP, Grenoble, France*
[57]*Laboratory for Particle Physics and Cosmology, Harvard University, Cambridge, Massachusetts, USA*
[58a]*Department of Modern Physics and State Key Laboratory of Particle Detection and Electronics, University of Science and Technology of China, Hefei, China*
[58b]*Institute of Frontier and Interdisciplinary Science and Key Laboratory of Particle Physics and Particle Irradiation (MOE), Shandong University, Qingdao, China*
[58c]*School of Physics and Astronomy, Shanghai Jiao Tong University, KLPPAC-MoE, SKLPPC, Shanghai, China*
[58d]*Tsung-Dao Lee Institute, Shanghai, China*
[59a]*Kirchhoff-Institut für Physik, Ruprecht-Karls-Universität Heidelberg, Heidelberg, Germany*
[59b]*Physikalisches Institut, Ruprecht-Karls-Universität Heidelberg, Heidelberg, Germany*
[60]*Faculty of Applied Information Science, Hiroshima Institute of Technology, Hiroshima, Japan*
[61a]*Department of Physics, Chinese University of Hong Kong, Shatin, N.T., Hong Kong, China*
[61b]*Department of Physics, University of Hong Kong, Hong Kong, China*
[61c]*Department of Physics and Institute for Advanced Study, Hong Kong University of Science and Technology, Clear Water Bay, Kowloon, Hong Kong, China*
[62]*Department of Physics, National Tsing Hua University, Hsinchu, Taiwan*
[63]*Department of Physics, Indiana University, Bloomington, Indiana, USA*
[64a]*INFN Gruppo Collegato di Udine, Sezione di Trieste, Udine, Italy*
[64b]*ICTP, Trieste, Italy*
[64c]*Dipartimento Politecnico di Ingegneria e Architettura, Università di Udine, Udine, Italy*
[65a]*INFN Sezione di Lecce, Lecce, Italy*
[65b]*Dipartimento di Matematica e Fisica, Università del Salento, Lecce, Italy*
[66a]*INFN Sezione di Milano, Milano, Italy*
[66b]*Dipartimento di Fisica, Università di Milano, Milano, Italy*
[67a]*INFN Sezione di Napoli, Napoli, Italy*
[67b]*Dipartimento di Fisica, Università di Napoli, Napoli, Italy*
[68a]*INFN Sezione di Pavia, Pavia, Italy*
[68b]*Dipartimento di Fisica, Università di Pavia, Pavia, Italy*
[69a]*INFN Sezione di Pisa, Pisa, Italy*
[69b]*Dipartimento di Fisica E. Fermi, Università di Pisa, Pisa, Italy*
[70a]*INFN Sezione di Roma, Roma, Italy*
[70b]*Dipartimento di Fisica, Sapienza Università di Roma, Roma, Italy*
[71a]*INFN Sezione di Roma Tor Vergata, Roma, Italy*
[71b]*Dipartimento di Fisica, Università di Roma Tor Vergata, Roma, Italy*
[72a]*INFN Sezione di Roma Tre, Roma, Italy*
[72b]*Dipartimento di Matematica e Fisica, Università Roma Tre, Roma, Italy*
[73a]*INFN-TIFPA, Trento, Italy*
[73b]*Università degli Studi di Trento, Trento, Italy*
[74]*Institut für Astro- und Teilchenphysik, Leopold-Franzens-Universität, Innsbruck, Austria*
[75]*University of Iowa, Iowa City, Iowa, USA*

[76]Department of Physics and Astronomy, Iowa State University, Ames, Iowa, USA
[77]Joint Institute for Nuclear Research, Dubna, Russia
[78a]Departamento de Engenharia Elétrica, Universidade Federal de Juiz de Fora (UFJF), Juiz de Fora, Brazil
[78b]Universidade Federal do Rio De Janeiro COPPE/EE/IF, Rio de Janeiro, Brazil
[78c]Universidade Federal de São João del Rei (UFSJ), São João del Rei, Brazil
[78d]Instituto de Física, Universidade de São Paulo, São Paulo, Brazil
[79]KEK, High Energy Accelerator Research Organization, Tsukuba, Japan
[80]Graduate School of Science, Kobe University, Kobe, Japan
[81a]AGH University of Science and Technology, Faculty of Physics and Applied Computer Science, Krakow, Poland
[81b]Marian Smoluchowski Institute of Physics, Jagiellonian University, Krakow, Poland
[82]Institute of Nuclear Physics Polish Academy of Sciences, Krakow, Poland
[83]Faculty of Science, Kyoto University, Kyoto, Japan
[84]Kyoto University of Education, Kyoto, Japan
[85]Research Center for Advanced Particle Physics and Department of Physics, Kyushu University, Fukuoka, Japan
[86]Instituto de Física La Plata, Universidad Nacional de La Plata and CONICET, La Plata, Argentina
[87]Physics Department, Lancaster University, Lancaster, United Kingdom
[88]Oliver Lodge Laboratory, University of Liverpool, Liverpool, United Kingdom
[89]Department of Experimental Particle Physics, Jožef Stefan Institute and Department of Physics, University of Ljubljana, Ljubljana, Slovenia
[90]School of Physics and Astronomy, Queen Mary University of London, London, United Kingdom
[91]Department of Physics, Royal Holloway University of London, Egham, United Kingdom
[92]Department of Physics and Astronomy, University College London, London, United Kingdom
[93]Louisiana Tech University, Ruston, Louisiana, USA
[94]Fysiska institutionen, Lunds universitet, Lund, Sweden
[95]Centre de Calcul de l'Institut National de Physique Nucléaire et de Physique des Particules (IN2P3), Villeurbanne, France
[96]Departamento de Física Teorica C-15 and CIAFF, Universidad Autónoma de Madrid, Madrid, Spain
[97]Institut für Physik, Universität Mainz, Mainz, Germany
[98]School of Physics and Astronomy, University of Manchester, Manchester, United Kingdom
[99]CPPM, Aix-Marseille Université, CNRS/IN2P3, Marseille, France
[100]Department of Physics, University of Massachusetts, Amherst, Massachusetts, USA
[101]Department of Physics, McGill University, Montreal, Québec, Canada
[102]School of Physics, University of Melbourne, Victoria, Australia
[103]Department of Physics, University of Michigan, Ann Arbor, Michigan, USA
[104]Department of Physics and Astronomy, Michigan State University, East Lansing, Michigan, USA
[105]B.I. Stepanov Institute of Physics, National Academy of Sciences of Belarus, Minsk, Belarus
[106]Research Institute for Nuclear Problems of Byelorussian State University, Minsk, Belarus
[107]Group of Particle Physics, University of Montreal, Montreal, Québec, Canada
[108]P.N. Lebedev Physical Institute of the Russian Academy of Sciences, Moscow, Russia
[109]Institute for Theoretical and Experimental Physics of the National Research Centre Kurchatov Institute, Moscow, Russia
[110]National Research Nuclear University MEPhI, Moscow, Russia
[111]D.V. Skobeltsyn Institute of Nuclear Physics, M.V. Lomonosov Moscow State University, Moscow, Russia
[112]Fakultät für Physik, Ludwig-Maximilians-Universität München, München, Germany
[113]Max-Planck-Institut für Physik (Werner-Heisenberg-Institut), München, Germany
[114]Nagasaki Institute of Applied Science, Nagasaki, Japan
[115]Graduate School of Science and Kobayashi-Maskawa Institute, Nagoya University, Nagoya, Japan
[116]Department of Physics and Astronomy, University of New Mexico, Albuquerque, New Mexico, USA
[117]Institute for Mathematics, Astrophysics and Particle Physics, Radboud University Nijmegen/Nikhef, Nijmegen, Netherlands
[118]Nikhef National Institute for Subatomic Physics and University of Amsterdam, Amsterdam, Netherlands
[119]Department of Physics, Northern Illinois University, DeKalb, Illinois, USA
[120a]Budker Institute of Nuclear Physics and NSU, SB RAS, Novosibirsk, Russia
[120b]Novosibirsk State University Novosibirsk, Novosibirsk, Russia
[121]Institute for High Energy Physics of the National Research Centre Kurchatov Institute, Protvino, Russia
[122]Department of Physics, New York University, New York, New York, USA

[123]*The Ohio State University, Columbus, Ohio, USA*
[124]*Faculty of Science, Okayama University, Okayama, Japan*
[125]*Homer L. Dodge Department of Physics and Astronomy, University of Oklahoma, Norman, Oklahoma, USA*
[126]*Department of Physics, Oklahoma State University, Stillwater, Oklahoma, USA*
[127]*Palacký University, RCPTM, Joint Laboratory of Optics, Olomouc, Czech Republic*
[128]*Center for High Energy Physics, University of Oregon, Eugene, Oregon, USA*
[129]*LAL, Université Paris-Sud, CNRS/IN2P3, Université Paris-Saclay, Orsay, France*
[130]*Graduate School of Science, Osaka University, Osaka, Japan*
[131]*Department of Physics, University of Oslo, Oslo, Norway*
[132]*Department of Physics, Oxford University, Oxford, United Kingdom*
[133]*LPNHE, Sorbonne Université, Paris Diderot Sorbonne Paris Cité, CNRS/IN2P3, Paris, France*
[134]*Department of Physics, University of Pennsylvania, Philadelphia, Pennsylvania, USA*
[135]*Konstantinov Nuclear Physics Institute of National Research Centre "Kurchatov Institute", PNPI, St. Petersburg, Russia*
[136]*Department of Physics and Astronomy, University of Pittsburgh, Pittsburgh, Pennsylvania, USA*
[137a]*Laboratório de Instrumentação e Física Experimental de Partículas—LIP, Portugal*
[137b]*Departamento de Física, Faculdade de Ciências, Universidade de Lisboa, Lisboa, Portugal*
[137c]*Departamento de Física, Universidade de Coimbra, Coimbra, Portugal*
[137d]*Centro de Física Nuclear da Universidade de Lisboa, Lisboa, Portugal*
[137e]*Departamento de Física, Universidade do Minho, Braga, Portugal*
[137f]*Departamento de Física Teorica y del Cosmos, Universidad de Granada, Granada (Spain), Spain*
[137g]*Dep Física and CEFITEC of Faculdade de Ciências e Tecnologia, Universidade Nova de Lisboa, Caparica, Portugal*
[138]*Institute of Physics of the Czech Academy of Sciences, Prague, Czech Republic*
[139]*Czech Technical University in Prague, Prague, Czech Republic*
[140]*Charles University, Faculty of Mathematics and Physics, Prague, Czech Republic*
[141]*Particle Physics Department, Rutherford Appleton Laboratory, Didcot, United Kingdom*
[142]*IRFU, CEA, Université Paris-Saclay, Gif-sur-Yvette, France*
[143]*Santa Cruz Institute for Particle Physics, University of California Santa Cruz, Santa Cruz, California, USA*
[144a]*Departamento de Física, Pontificia Universidad Católica de Chile, Santiago, Chile*
[144b]*Departamento de Física, Universidad Técnica Federico Santa María, Valparaíso, Chile*
[145]*Department of Physics, University of Washington, Seattle, Washington, USA*
[146]*Department of Physics and Astronomy, University of Sheffield, Sheffield, United Kingdom*
[147]*Department of Physics, Shinshu University, Nagano, Japan*
[148]*Department Physik, Universität Siegen, Siegen, Germany*
[149]*Department of Physics, Simon Fraser University, Burnaby, British Columbia, Canada*
[150]*SLAC National Accelerator Laboratory, Stanford, California, USA*
[151]*Physics Department, Royal Institute of Technology, Stockholm, Sweden*
[152]*Departments of Physics and Astronomy, Stony Brook University, Stony Brook, New York, USA*
[153]*Department of Physics and Astronomy, University of Sussex, Brighton, United Kingdom*
[154]*School of Physics, University of Sydney, Sydney, Australia*
[155]*Institute of Physics, Academia Sinica, Taipei, Taiwan*
[156a]*E. Andronikashvili Institute of Physics, Iv. Javakhishvili Tbilisi State University, Tbilisi, Georgia*
[156b]*High Energy Physics Institute, Tbilisi State University, Tbilisi, Georgia*
[157]*Department of Physics, Technion, Israel Institute of Technology, Haifa, Israel*
[158]*Raymond and Beverly Sackler School of Physics and Astronomy, Tel Aviv University, Tel Aviv, Israel*
[159]*Department of Physics, Aristotle University of Thessaloniki, Thessaloniki, Greece*
[160]*International Center for Elementary Particle Physics and Department of Physics, University of Tokyo, Tokyo, Japan*
[161]*Graduate School of Science and Technology, Tokyo Metropolitan University, Tokyo, Japan*
[162]*Department of Physics, Tokyo Institute of Technology, Tokyo, Japan*
[163]*Tomsk State University, Tomsk, Russia*
[164]*Department of Physics, University of Toronto, Toronto, Ontario, Canada*
[165a]*TRIUMF, Vancouver, British Columbia, Canada*
[165b]*Department of Physics and Astronomy, York University, Toronto, Ontario, Canada*
[166]*Division of Physics and Tomonaga Center for the History of the Universe, Faculty of Pure and Applied Sciences, University of Tsukuba, Tsukuba, Japan*
[167]*Department of Physics and Astronomy, Tufts University, Medford, Massachusetts, USA*

[168]*Department of Physics and Astronomy, University of California Irvine, Irvine, California, USA*
[169]*Department of Physics and Astronomy, University of Uppsala, Uppsala, Sweden*
[170]*Department of Physics, University of Illinois, Urbana, Illinois, USA*
[171]*Instituto de Física Corpuscular (IFIC), Centro Mixto Universidad de Valencia—CSIC, Valencia, Spain*
[172]*Department of Physics, University of British Columbia, Vancouver, British Columbia, Canada*
[173]*Department of Physics and Astronomy, University of Victoria, Victoria, British Columbia, Canada*
[174]*Fakultät für Physik und Astronomie, Julius-Maximilians-Universität Würzburg, Würzburg, Germany*
[175]*Department of Physics, University of Warwick, Coventry, United Kingdom*
[176]*Waseda University, Tokyo, Japan*
[177]*Department of Particle Physics, Weizmann Institute of Science, Rehovot, Israel*
[178]*Department of Physics, University of Wisconsin, Madison, Wisconsin, USA*
[179]*Fakultät für Mathematik und Naturwissenschaften, Fachgruppe Physik, Bergische Universität Wuppertal, Wuppertal, Germany*
[180]*Department of Physics, Yale University, New Haven, Connecticut, USA*
[181]*Yerevan Physics Institute, Yerevan, Armenia*

[a]Deceased.
[b]Also at Department of Physics, King's College London, London, United Kingdom.
[c]Also at Istanbul University, Department of Physics, Istanbul, Turkey.
[d]Also at Instituto de Física Teórica de la Universidad Autónoma de Madrid, Spain.
[e]Also at Institute of Physics, Azerbaijan Academy of Sciences, Baku, Azerbaijan.
[f]Also at TRIUMF, Vancouver, British Columbia, Canada.
[g]Also at Department of Physics and Astronomy, University of Louisville, Louisville, Kentucky, USA.
[h]Also at Department of Physics, University of Fribourg, Fribourg, Switzerland.
[i]Also at Physics Department, University of South Africa, Pretoria, South Africa.
[j]Also at Departament de Fisica de la Universitat Autonoma de Barcelona, Barcelona, Spain.
[k]Also at Tomsk State University, Tomsk, and Moscow Institute of Physics and Technology State University, Dolgoprudny, Russia.
[l]Also at The Collaborative Innovation Center of Quantum Matter (CICQM), Beijing, China.
[m]Also at Departamento de Física, Instituto Superior Técnico, Universidade de Lisboa, Lisboa, Portugal.
[n]Also at Universita di Napoli Parthenope, Napoli, Italy.
[o]Also at Institute of Particle Physics (IPP), Canada.
[p]Also at II. Physikalisches Institut, Georg-August-Universität Göttingen, Göttingen, Germany.
[q]Also at Horia Hulubei National Institute of Physics and Nuclear Engineering, Bucharest, Romania.
[r]Also at CPPM, Aix-Marseille Université, CNRS/IN2P3, Marseille, France.
[s]Also at Department of Physics, St. Petersburg State Polytechnical University, St. Petersburg, Russia.
[t]Also at Borough of Manhattan Community College, City University of New York, New York, USA.
[u]Also at Department of Physics, California State University, Fresno, California, USA.
[v]Also at Department of Financial and Management Engineering, University of the Aegean, Chios, Greece.
[w]Also at Centre for High Performance Computing, CSIR Campus, Rosebank, Cape Town, South Africa.
[x]Also at Louisiana Tech University, Ruston, Louisiana, USA.
[y]Also at California State University, East Bay, Hayward, California, USA.
[z]Also at Institucio Catalana de Recerca i Estudis Avancats, ICREA, Barcelona, Spain.
[aa]Also at Department of Physics, University of Michigan, Ann Arbor, Michigan, USA.
[bb]Also at LAL, Université Paris-Sud, CNRS/IN2P3, Université Paris-Saclay, Orsay, France.
[cc]Also at Graduate School of Science, Osaka University, Osaka, Japan.
[dd]Also at Physikalisches Institut, Albert-Ludwigs-Universität Freiburg, Freiburg, Germany.
[ee]Also at Institute for Mathematics, Astrophysics and Particle Physics, Radboud University Nijmegen/Nikhef, Nijmegen, Netherlands.
[ff]Also at Institute of Theoretical Physics, Ilia State University, Tbilisi, Georgia.
[gg]Also at CERN, Geneva, Switzerland.
[hh]Also at Department of Physics, Stanford University, Stanford, California, USA.
[ii]Also at Manhattan College, New York, New York, USA.
[jj]Also at Joint Institute for Nuclear Research, Dubna, Russia.
[kk]Also at Hellenic Open University, Patras, Greece.
[ll]Also at LPNHE, Sorbonne Université, Paris Diderot Sorbonne Paris Cité, CNRS/IN2P3, Paris, France.
[mm]Also at The City College of New York, New York, New York, USA.
[nn]Also at Departamento de Física Teorica y del Cosmos, Universidad de Granada, Granada (Spain), Spain.
[oo]Also at Department of Physics, California State University, Sacramento, California, USA.
[pp]Also at Moscow Institute of Physics and Technology State University, Dolgoprudny, Russia.
[qq]Also at Département de Physique Nucléaire et Corpusculaire, Université de Genève, Genève, Switzerland.

[rr]Also at Department of Physics and Astronomy, University of Sheffield, Sheffield, United Kingdom.
[ss]Also at School of Physics, Sun Yat-sen University, Guangzhou, China.
[tt]Also at Department of Applied Physics and Astronomy, University of Sharjah, Sharjah, United Arab Emirates.
[uu]Also at Institut für Experimentalphysik, Universität Hamburg, Hamburg, Germany.
[vv]Also at National Research Nuclear University MEPhI, Moscow, Russia.
[ww]Also at Institute for Particle and Nuclear Physics, Wigner Research Centre for Physics, Budapest, Hungary.
[xx]Also at Giresun University, Faculty of Engineering, Giresun, Turkey.
[yy]Also at Institute of Physics, Academia Sinica, Taipei, Taiwan.